TUDelft

M.Sc. Thesis

Stability of rock on slopes under wave attack

Comparison and analysis of datasets

VAN DER MEER [1988] and VAN GENT ET AL. [2003]

Marcel Mertens

Delft University of Technology

Faculty of Civil Engineering

Department of Hydraulic Engineering

M.Sc. Thesis

Stability of rock on slopes under wave attack

Comparison and analysis of datasets
VAN DER MEER [1988] and VAN GENT ET AL. [2003]

April 2007

Graduation Committee:

Prof. Dr. Ir. M.J.F. Stive

Ir. H.J. Verhagen

Dr. Ir. J.W. Van der Meer

Drs. R. Booij

Graduation Student:

Ing. M. Mertens

PREFACE

This document contains the final report of my M.Sc. Thesis at Delft University of Technology, faculty of Civil Engineering, department of Hydraulic Engineering. This report can be used as a starting point to further research on this topic. During the work on this M.Sc. Thesis and because of the great amount of data sometimes it was really difficult not to make the same mistakes which formed the basis of this report. Also for me it became clear how difficult it is to prove empirical relations in processes that are not yet fully understood. This M.Sc. Thesis is another step closer to a clear solution on this topic.

This M.Sc. Thesis would not have succeeded without the great help and patience of Mr. Verhagen who really was of great support for me. Also I would like to thank the other members of the graduation committee Mr. Stive, Mr. Van der Meer and Mr. Booij for their support and guidance and Mr. Van Gent for providing his graphs. Last but not least I would like to thank my parents and my girlfriend for their great support and patience during my whole study.

Marcel Mertens
Delft, April 2007

ABSTRACT

On the stability of rock in the twentieth century a lot of research has been done. In VAN DER MEER [1988] two stability formulae were presented for breakwater design that were later generally accepted in the engineering practice. Most of the tests of VAN DER MEER [1988] were done with foreshore deep water conditions. In practice however structures with shallow foreshores showed more damage than average. This was a starting point for the work of VAN GENT ET AL. [2003], who did most of the tests with shallow water conditions.

In VAN GENT [2004] graphs were presented in which the datasets of VAN DER MEER [1988] and VAN GENT ET AL. [2003] were compared. These graphs are presented in Figure 0.1.
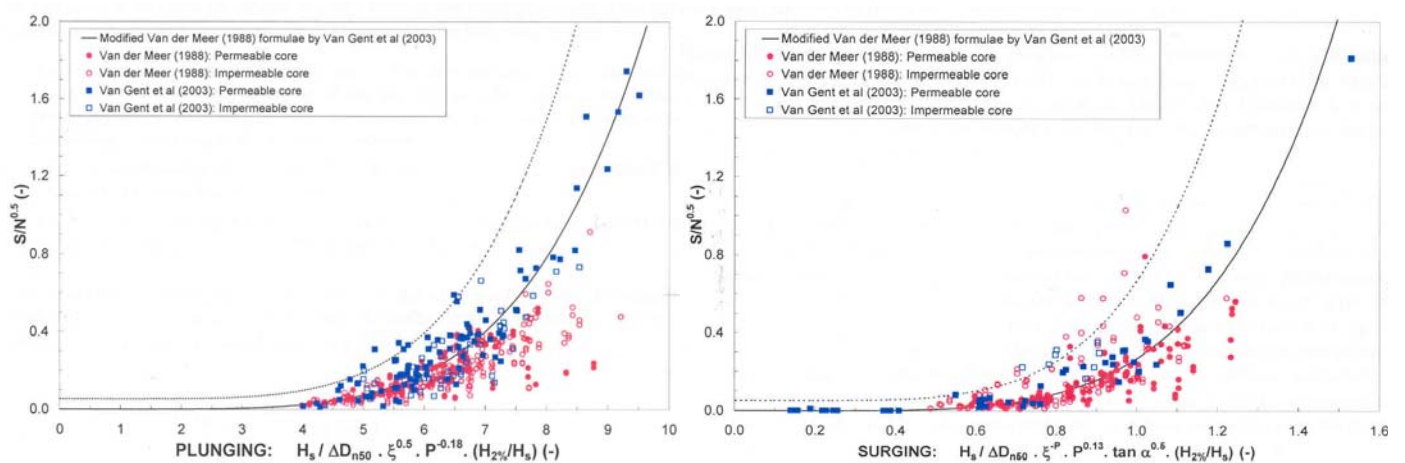
Figure 0.1: Data VAN GENT ET AL. [2003] (blue) compared with data VAN DER MEER [1988] (red) for plunging (left) and surging waves (right)

There has been a lot of discussion about the graphs as presented in Figure 0.1. It can be seen that differences occur between the two datasets. However one problem was that the two datasets were not compared in a proper way because a number of parameters were not correctly transformed in a comparable format. Therefore in this M.Sc. Thesis the datasets were analysed and all parameters were individually transformed in a proper way so that a good comparison can be made. After that possible explanations for the differences were discussed.

For the dataset of VAN DER MEER [1988] differences occurred between the original graphs for plunging and surging waves and the reconstructed graphs which could not be explained by errors in the spreadsheet. After a thorough investigation of these differences it could be seen that mistakes were made in the original graphs of VAN DER MEER [1988]. Some points which did not appear in the graph for plunging waves appeared in the graph for surging waves and vice versa. A probable reason for this is that mistakes were made with the use of the boundary between plunging and surging waves. In the development of the formulae of VAN DER MEER [1988] different values of P were used in order to describe the permeability of the structures. In this way the boundary between plunging and surging waves, which depends on the permeability, also varied during experiments, which probably caused the mistakes. Also it must be mentioned that at the time the PhD thesis was written less sophisticated computer programmes were used.

The dataset of VAN GENT ET AL. [2003] was not available for this M.Sc. Thesis. Data could only be read of from the graphs presented in VAN GENT ET AL. [2003]. To be able to make a good comparison the data coordinates from the original graphs were entered in the spreadsheet. Because of the unavailability of the data of VAN GENT ET AL. [2003] no changes to this dataset can be made. The dataset of THOMPSON & SHUTTLER [1975] which was a starting point for the work of VAN DER MEER [1988] was also entered in the spreadsheet.

After this in the digitalised datasets parameters had to be transformed. In the dataset of THOMPSON & SHUTTLER [1975] the damage level was indicated with the parameter N_Δ, which had to be transformed to the damage parameter S, that was used by VAN DER MEER [1988] and VAN GENT ET AL. [2003]. Also for the stone diameter THOMPSON & SHUTTLER [1975] used a different parameter. In VAN DER MEER [1988] and THOMPSON & SHUTTLER [1975] for the wave height the significant wave height, H_s, has been used, while in VAN GENT ET AL. [2003] the wave height exceeded by 2% of the waves, $H_{2\%}$, was used.

Using the approach of BATTJES & GROENENDIJK [2000] the wave height was transformed for each point individually. For the wave period VAN DER MEER [1988] and THOMPSON & SHUTTLER [1975] used the mean period, T_m. VAN GENT ET AL. [2003] however showed that it is better to use the spectral period, $T_{m-1,0}$, for stability calculations. The transformation from the mean period, T_m, to the spectral period, $T_{m-1,0}$, depends on the spectral shape. For the dataset of VAN DER MEER [1988] the spectra that were used were indicated as PM (Pierson Moskowitz) spectra, narrow- and wide spectra. A close inspection of these spectra showed that all these spectra are quite a lot narrower than they should be. Therefore for each spectrum that was used the transformation to the spectral wave period was done for each point individually using the correct spectrum.

In VAN DER MEER [1988] it was already mentioned that data with different spectra showed more damage than average especially for surging waves. These differences could not be caused by the difference in spectra, but a possible explanation was the effect of rounding due to frequent handling and the painting process. LATHAM ET AL. [1988] did some research to the effects of roundness on stability with stones of different roundness, where also subsamples from the stones used by VAN DER MEER [1988] were tested. In LATHAM ET AL. [1988] correction factors for the stability formulae were presented to include the effects of roundness Including these factors in the formulae for the dataset of VAN DER MEER [1988] gives remarkable effects, which are visualized in Figure 0.2.
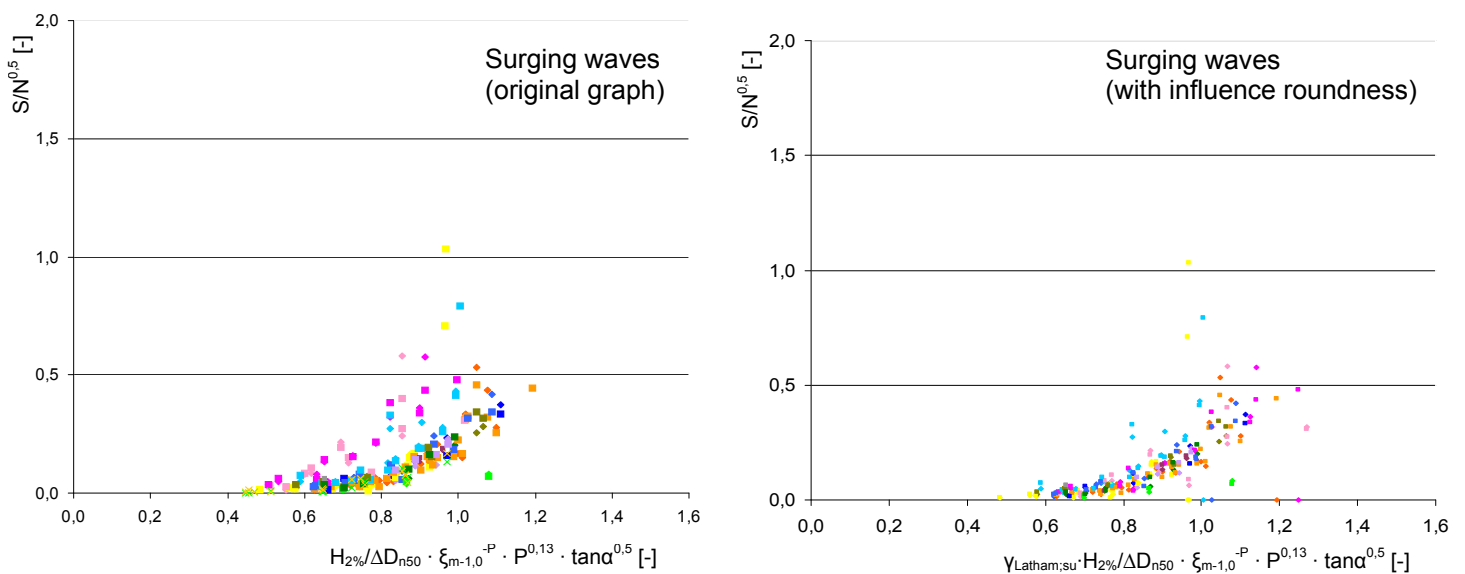
Figure 0.2: The effects of including the roundness parameter, γ_{Latham}, on the graphs of the dataset for surging waves of VAN DER MEER [1988]

After transforming all parameters of the datasets of THOMPSON & SHUTTLER [1975] and VAN DER MEER [1988] into the same format as the parameters from the dataset of VAN GENT ET AL. [2003] the datasets have been compared with graphs like presented in Figure 0.3.
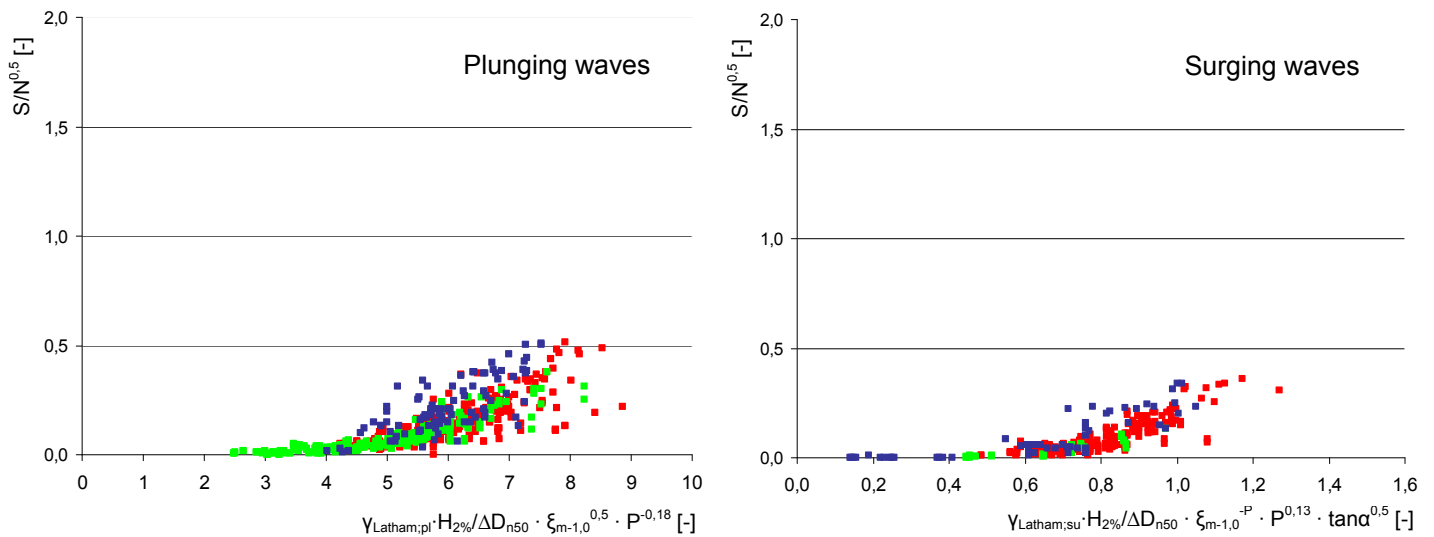
Figure 0.3: The datasets of VAN DER MEER [1988] (red), THOMPSON & SHUTTLER [1975] (green) and VAN GENT ET AL. [2003] (blue) for plunging waves (left) and surging waves (right)

Using the statistical T-test the differences between the datasets of VAN DER MEER [1988] and THOMPSON & SHUTTLER [1975] and the dataset of VAN GENT ET AL. [2003] are approved with a probability of 95%. The results of the T-test for the datasets of THOMPSON & SHUTTLER [1975] and VAN DER MEER [1988] indicate that these datasets are not significantly different on most points.

Explanations for the differences found between the datasets of VAN DER MEER [1988] and VAN GENT ET AL. [2003] can be found in the fact that most of the tests of VAN GENT ET AL. [2003] were done with shallow foreshores where VAN DER MEER [1988] did the majority of tests with deep water conditions. Tests by a number of M.Sc. students at Delft University of Technology already showed that tests with identical spectra at the toe of the structure, but with different foreshore slope angles show different damage patterns. In the dataset of VAN GENT [2003] also the 1:30 foreshore slopes on average show more damage than the 1:100 foreshore slopes. In further research to this topic the influence of the foreshore should be incorporated in the modified formulae of VAN DER MEER [1988] for example by an Iribarren parameter, ξ_β, for the foreshore. Also a detailed investigation to the effects of wave breaking on shallow foreshores has to be done. For this of course the complete dataset of VAN GENT ET AL. [2003] needs to be available and accessible.

CONTENTS

LIST OF FIGURES

LIST OF TABLES

NOTATIONS

a	=	Amplitude	[m]
A_i	=	erosion area in a cross-section (indices 1, 2, 3)	[m²]
A_1	=	accretion area in beach crest area	[m²]
A_2	=	erosion area	[m²]
A_3	=	accretion area below the water surface	[m²]
A_n	=	phase angle in Fourier series	[-]
$c_{plunging}, c_{pl}$	=	regression coefficient in formula of VAN DER MEER [1988] for plunging waves	[-]
$c_{plunging}, c_{su}$	=	regression coefficient in formula of VAN DER MEER [1988] for plunging waves	[-]
C_n	=	amplitude coefficient of the nth harmonic in Fourier series	[-]
d	=	water depth	[m]
$d_{foreshore}$	=	water depth on foreshore	[m]
dof	=	degrees of freedom in T-test	[-]
D	=	Duration of a wave record	[s]
D	=	Diameter	[m]
D_{15}	=	Sieve diameter exceeded by 15% of the stones	[m]
D_{50}	=	Sieve diameter exceeded by 50% of the stones	[m]
D_{85}	=	Sieve diameter exceeded by 85% of the stones	[m]

D_n	=	nominal diameter $(W/\rho_a)^{1/3}$	[m]
D_{n50}	=	nominal diameter exceeded by 50% of the stones	[m]
f	=	Frequency	[Hz]
g	=	gravitational acceleration	[m/s^2]
H	=	Wave height	[m]
H_1, H_2	=	Scale parameters in Composite Weibull distribution	[-]
H_s	=	(incoming) significant wave height	[m]
$H_{2\%}$	=	Wave height exceeded by 2% of the waves	[m]
$H_{1/3}$	=	average of the highest 1/3 of the wave heights in a wave record	[m]
H_{m0}	=	4 times the standard deviation of the surface elevation	[m]
H_{rms}	=	root mean square wave height	[m]
H_{tr}	=	transitional wave height in Composite Weibull distribution	[m]
k_1,k_2	=	shape parameters of the distribution determining the curvature in Composite Weibull distribution	[-]
L	=	Wave length	[m]
L_0	=	Deep water wave length ($=gT^2/2\pi$)	[m]
m_0	=	zero-th order spectral moment	[-]
m_{-1}	=	first order negative spectral moment	[-]
n	=	number of tests	[-]
$N_{Iribarren}$	=	dustbin factor in stability formula of IRIBARREN [1938]	[-]
N_Δ	=	damage parameter defined in THOMPSON & SHUTTLER [1975]	[-]
N	=	number of waves	[-]
P	=	permeability coefficient defined in VAN DER MEER [1988]	[-]
P_f	=	fictitious porosity $=100(1-(\rho_a/\rho_b))$	[%]
P_n	=	Fourier noncircularity, based on harmonic amplitudes from 1 to ∞	[-]
P_C	=	Fourier shape contribution factor ($=10P_n$) (LATHAM ET AL. [1988])	[-]
P_R	=	Fourier asperity roughness based on the 11th to 20th harmonic amplitudes as defined in LATHAM ET AL. [1988]	[-]
P_S	=	Fourier shape factor based on the 1th to 10th harmonic amplitudes as defined in LATHAM ET AL. [1988]	[-]
PM	=	Pierson Moskowitz	
sd	=	standard deviation	
S	=	damage level as defined in VAN DER MEER [1988] ($=A_i/D_{n50}^2$)	[-]
t	=	Time	[s]

t_{armour}	=	thickness armour layer	[m]
t_{filter}	=	thickness filter layer	[m]
t_{obs}	=	ratio between difference and variability of two groups (T-test)	[-]
T	=	Wave period	[s]
T_m	=	Mean wave period	[s]
$T_{m-1,0}$	=	spectral wave period m_{-1}/m_0	[s]
$T_{m-1,0;a}$		spectral wave period $T_{m-1,0}$ using a cut-off frequency for the lower frequencies	[s]
T_p	=	Peak wave period	[s]
$T_{p;a}$		the peak period using a cut off frequency for the higher frequencies.	[s]
$T_{p;b}$		The peak period $T_{m-1,0}$ from the part of the spectrum for which the energy is more than 40% of the maximum value	[s]
$T_{p;d}$		The peak period $T_{m-1,0}$ from the part of the spectrum for which the energy is more than 80% of the maximum value	[s]
W	=	weight of stone/block	[N]
$\overline{X}$	=	group mean of group X (x_1, x_2, ……..x_n)	
$\overline{Y}$	=	group mean of group Y (y_1, y_2, ……..y_n)	
α	=	Slope angle of construction	[-]
β	=	Slope angle of foreshore	[-]
β_{tr}	=	Slope-dependent coefficient in calculation of H_{tr}	[-]
γ_{Latham}	=	correction factor for the influence of stone roundness according to LATHAM ET AL. [1988])	[-]
Δ	=	relative density: $(\rho_{r} - \rho_w)/\rho_w$	[-]
$\eta(t)$	=	the surface elevation in a time record reproduced as the sum of a large number of harmonic wave components (Fourier series)	[m]
θ	=	Polar angle measured from an arbitrary reference line	[-]
μ	=	friction coefficient	[-]
ξ_{β}	=	Iribarren parameter for the foreshore $\xi_{\beta}=\tan\beta/\sqrt{(H/L)}$	[-]
ξ_c	=	Critical Iribarren parameter indicating transition between plunging and surging waves	[-]
ξ_m	=	Iribarren parameter calculated with T_m	[-]
$\xi_{m-1,0}$	=	Iribarren parameter calculated with $T_{m-1,0}$	[-]

ξ_p	=	Iribarren parameter calculated with T_p	[-]
ρ_a	=	Mass density of stone	[kg/m³]
ρ_b	=	bulk density of material as laid on the slope	[kg/m³]
ρ_w	=	density of water	[kg/m³]
ρ_r	=	density of stone/block (rock)	[kg/m³]

Chapter 1

INTRODUCTION

1.1 Background

A lot of research has been done to the stability of stones or sediments. In this we can distinguish stability due currents, waves or a combination of the two. This M.Sc. Thesis deals with the stability of rock on a slope, attacked by waves. Practical applications of rock on a slope are breakwaters and sea– or inland water defences.

1.1.1 Breakwaters and sea defences

Breakwaters are generally shore-parallel structures that reduce the amount of wave energy (wave height) reaching the protected area. They are similar to natural bars, reefs or near shore islands and are designed to dissipate wave energy. In high wave energy environments breakwaters are usually constructed using large armour stone, or pre-cast concrete units or blocks. Where stone weight and interlocking are important stability mechanisms. In lower wave-energy environments, grout-filled fabric bags, gabions and other proprietary units are common used. Typical rubble mound breakwater design is similar to that of a revetment, with a core or filter layer of smaller stone, overlain by the armouring layer of armour stone or pre-cast concrete units. Special types of breakwaters are caisson breakwaters and floating breakwaters, which will not be discussed in this M.Sc. Thesis.

1.1.2 Stability of rock

Movement of stones and sediments due to currents or waves does only occur when the acting forces out of the water motion, like drag and lift forces, exceed friction and weight forces. Whether a particle is moving or not is described in so-called threshold conditions. Because of the complex water movement of waves breaking on a slope fully theoretical expressions for the forces and the stability of the stones are very hard to derive. Therefore a number of empirical formulae have been developed, all based on results of small-scale experiments. In these formulae stability of an individual stone is often defined by a ratio of the unit size (weight/length scale) and the wave height. Movement of stones does not automatically mean failure. As long as the armour layer is able to protect the underlying filter layer (existing out of smaller stones which will easily be moved) the structure has not failed. Depending on the amount of damage a construction needs to be repaired after a severe storm.

In stability formulae sometimes a distinction is made between plunging and surging waves. The difference between these two types of wave breaking is shown in Figure 1.1.
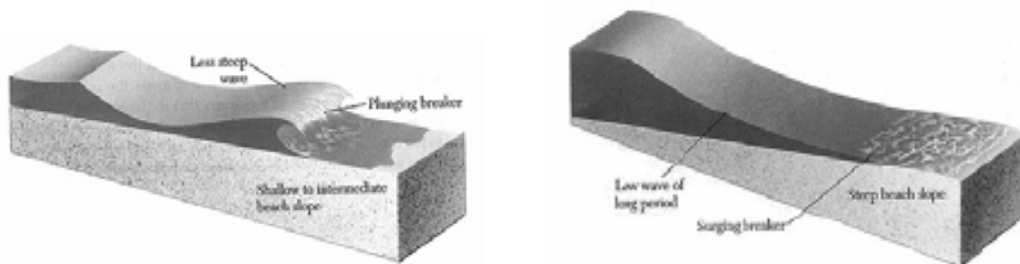
Figure 1.1: Plunging breaker (left) and surging breaker (right)

Plunging breakers overall are the result of steeper waves over moderate slopes, where wave energy is released suddenly as the crest curls and then descends violently. This is a typical "surfer" wave, it breaks very quickly and with substantial force. Surging breakers mostly occur when the beach slope exceeds wave steepness and are usually found on very steep slopes. The wave does not really curl and break in the traditional way but runs up against the shore while producing foam and large surges of water. A surging wave often starts as a plunging wave, then the wave catches up with the crest, and the breaker surges up slope as a wall of water, with the wave crest and base travelling at the same speed. This results in a quickly rising and falling water level on the shore face.

1.1.3 Iribarren/Hudson

For many years breakwater design was a question of trial and error. In 1938 in IRIBARREN
[1938] a theoretical model for the stability of stone on a slope under wave attack was
developed. IRIBARREN [1938] concentrated on a theoretical approach, assisted by some
experiments.

According to IRIBARREN [1938] the forces acting on a stone placed at an angle α are:

- Weight of the stone (acting in vertical downward direction)
- Buoyancy of the stone (acting in vertical upward direction)
- Wave force (acting parallel to the slope, upwards or downwards)
- Frictional resistance (acting parallel to the slope, upwards or downwards, opposite
  direction to the wave force)

The design formula of IRIBARREN [1938] distinguishes downrush and uprush along the slope.
According to IRIBARREN [1938] the required block weight is given by:

$$W \geq \frac{N \cdot \rho_r \cdot g \cdot H^3}{\Delta^3 \cdot (\mu \cdot \cos\alpha \pm \sin\alpha)}$$

In which:

W	=	weight of stone/block	[N]
N	=	dustbin factor	[-]
ρ_r	=	density of stone/block (rock)	[kg/m³]
g	=	gravitational acceleration	[m/s²]
H	=	wave height	[m]
Δ	=	relative density: $(\rho_r - \rho_w)/ \rho_w$	[-]
ρ_w	=	density of water	[kg/m³]
μ	=	friction coefficient	[-]
α	=	slope angle	[-]

In the formulae of IRIBARREN [1938] and HUDSON [1953] a kind of "dustbin"-factors are
included to reckon all the unknown variables and unaccounted irregularities in the model
investigations. Variables in this "dustbin"-factors are:

- Shape of the blocks

- Layer thickness of the outer layer

- Manner of placing the blocks

- Roughness and interlocking of the blocks

- Type of wave attack

- Head or trunk section of the breakwater

- Angle of incidence of wave attack

- Size and porosity of the underlying material

- Crest level (overtopping)

- Crest type

- Wave period

- Shape of the foreshore

- Accuracy of wave height measurement (reflection)

- Scale effects

1.1.4 THOMPSON & SHUTTLER [1975]

An extensive investigation on stability of riprap under irregular wave attack was done by THOMPSON & SHUTTLER [1975]. In THOMPSON & SHUTTLER [1975] the damage was defined by the parameter N_Δ, which can best be described as the theoretical number of round stones removed from an area with a width of 9 diameters. The damage profile was measured with 10 sounding rods, placed one D_{50} apart from each other. This results in the total width of $9D_{50}$. N_Δ can be described as:

$$N_\Delta = \frac{A \cdot \rho_b \cdot 9D_{50}}{\rho_a \cdot D_{50}{}^3 \cdot \pi/6}$$

where:

N_Δ = damage parameter

A = erosion area in a cross-section

ρ_b = bulk density of material as laid on the slope

D_{50} = diameter of stone which exceeds the 50% value of the sieve curve

ρ_a = mass density of stone

Start of damage was at N_Δ=20. The filter layer was on average visible at N_Δ=80. The damage was measured after N=1000 and N=3000 waves. Further boundary conditions were:

- Core: Impermeable
- Slope angle: $\cot\alpha$=2 - 6
- Stone diameter: D_{50} = 20 - 40 mm
- Wave period: T_z = 0,92 - 1,30 s
- Stability parameter: $H_s/\Delta D_{n50}$: 0,5 – 3,0
- Armour gradation: D_{85} / D_{15} = 2,25

THOMPSON & SHUTTLER [1975] concluded that there was no influence of the period on stability, however a recalculation of this dataset in VAN DER MEER [1988] to ξ-values shows very clear the influence of the wave period. In THOMPSON & SHUTTLER [1975] only short wave periods were investigated which makes it difficult to see relations between the wave period and stability. For this a complementary study with longer wave periods was needed to complete the research to the static stability of riprap slopes for irregular waves.

1.1.5 *VAN DER MEER [1988]*

With THOMPSON & SHUTTLER [1975] as a starting point in his PhD thesis at Delft University, VAN DER MEER [1988] presented an approach based on irregular waves that has been gradually accepted in the engineering community. New variables that were included in the approach of VAN DER MEER [1988] are:

- a clear and measurable definition of damage, S
- the mean wave period, T_m, via the Iribarren breaker index ξ_m,
- a certain influence of the permeability or the porosity of the breakwater structure as a whole, the notional permeability, P

In Figure 1.2 the model set up used in VAN DER MEER [1988] is shown.
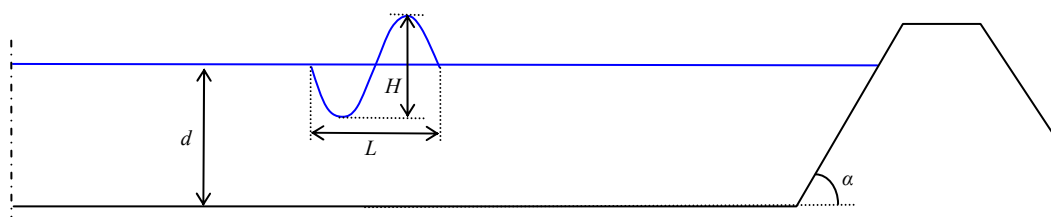
Figure 1.2: Model set up of VAN DER MEER [1988]

The original equations of VAN DER MEER [1988] are:

Plunging waves:
$$\frac{S}{\sqrt{N}} = \left(\frac{1}{c_{plunging}} \frac{H_s}{\Delta D_{n50}} \xi_m^{\,0.5} P^{-0.18} \right)^5$$

Surging waves:
$$\frac{S}{\sqrt{N}} = \left(\frac{1}{c_{surging}} \frac{H_s}{\Delta D_{n50}} \xi_m^{\,-P} P^{0.13} \tan \alpha^{0.5} \right)^5$$

The damage level S in these formulae can be defined as:

$$S_i = \frac{A_i}{D_{n50}^2}$$

The damage is measured with 9 piling rods. The eroded area, A_i, can be divided in 3 parts:

A_1 : the beach crest area, above the water surface (normally an accretion area)

A_2 : the erosion area around the water surface, area of interest for this research

A_3 : accretion area below the water surface

By dividing the eroded area by the square of the nominal stone diameter this area is normalized. In this way S represents the number of squares (width D_{n50}) fitting in the eroded area. More physically S represents the number of removed stones in a row with a width of 1 diameter. S=8 means that 8 stones have moved from a row with a width of 1 diameter.

The values for $c_{plunging}$ and $c_{surging}$ were found by calibrating the formula to model tests. The ranges of the parameters used in VAN DER MEER [1988] are listed below.

- Slope angle: $\cot\alpha = 1,5 - 6$
- Relative density: $\Delta = 1 - 2,1$
- Number of waves: $N < 7500$
- Surf similarity parameter: $\xi_m = 0,7 - 7$
- Permeability: $P = 0,1 - 0,6$
- Armour grading: $D_{n85}/D_{n15} < 2,5$
- Stability parameter: $H_s/\Delta D_{n50} = 1 - 4$
- Damage level: $S = <30$

With these tests VAN DER MEER [1988] found for plunging waves $c_{plunging}$ = 6.2 and for surging waves $c_{surging}$ = 1.0.

1.1.6 *VAN GENT Et Al. [2003]*

In the stability formulae of VAN DER MEER [1988] shallow water and steep foreshores are not considered extensively. An example of the increase of damage caused by a steep foreshore is the Scarborough sea defence where after a storm only the part of the structure with a steep foreshore showed severe damage, while the rest of the structure was hardly damaged.

In shallow water the waves break and deform on the foreshore before they reach the structure which might cause different damage patterns. Therefore VAN GENT ET AL. [2003] did a series of experiments with waves on shallow foreshores. Test have been done with foreshore slopes 1 : 100 and 1 : 30. The ranges of the parameters used in VAN GENT ET AL. [2003] are listed below.

- Slope angle: $\cot\alpha$ = 2 - 4
- Relative density: Δ = 1,65 – 1,75
- Number of waves: N <3000
- Surf similarity parameter: ξ_m = 1 – 5 ($\xi_{m-1,0}$ = 1,3 – 15)
- Wave height ratio: $H_{2\%}/H_s$ = 1,2 – 1,4
- Armour grading: D_{n85}/D_{n15} = 1,4 – 2,0
- Stability parameter: $H_s/\Delta D_{n50}$ = 0,5 – 4,5
- Damage level: S = < 62

The model set-up used by VAN GENT ET AL. [2003] is shown in Figure 1.3.
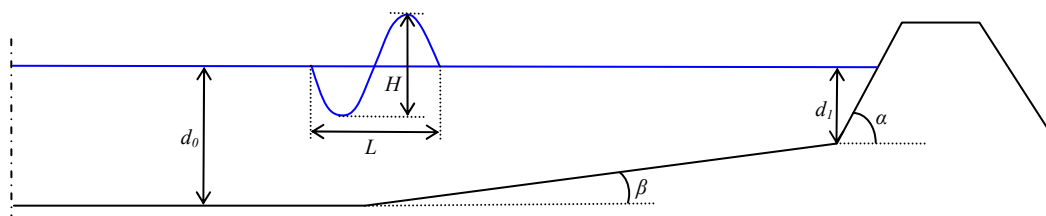
Figure 1.3: Model set up VAN GENT ET AL. [2003]

One adaptation made by VAN GENT ET AL. [2003] was to use the spectral period instead of the peak period or the mean period. In case of shallow water conditions (strongly deformed

waves and double peaked spectra) it is better to base the formulae on the spectral period, $T_{m-1,0}$. This gives more weight to lower wave frequencies, because long periods (low frequencies) are more relevant than short periods (high frequencies). Using the $T_{m-1,0}$ value for the wave period instead of the peak period, T_p, or the significant (spectral) wave period, T_{m0}, gives more reliable results for both run-up an overtopping formulae as well as stability formulae and is nowadays frequently used. For this reason only the $c_{plunging}$ and $c_{surging}$ factors in the original Van der Meer formulae have to be adapted, so no major adjustments have to be made. When replacing the period with several other periods the spectral period gave the smallest standard deviation (o) for the difference between measured values for $S/\sqrt{N}$ and predicted values for $S/\sqrt{N}$.

As recommended by VAN DER MEER [1988], VAN GENT ET AL. [2003] also used the 2% wave height, $H_{2\%}$, instead of the significant wave height, H_s, for shallow water conditions. This is because wave heights in shallow waters are distributed in a different way, because of wave breaking. This conversion also needs an adaptation of the $c_{plunging}$ and $c_{surging}$ factors.

This leads to the following equations for shallow water conditions:

Plunging waves:
$$\frac{S}{\sqrt{N}} = \left(\frac{1}{c_{plunging}} \frac{H_s}{\Delta D_{n50}} \xi_{m-1,0}^{0.5} P^{-0.18} \frac{H_{2\%}}{H_s} \right)^5$$

Surging waves:
$$\frac{S}{\sqrt{N}} = \left(\frac{1}{c_{surging}} \frac{H_s}{\Delta D_{n50}} \xi_{m-1,0}^{-P} P^{0.13} \tan\alpha^{0.5} \frac{H_{2\%}}{H_s} \right)^5$$

The only difference between these equations is the use of the spectral period in the Iribarren parameter and the use of $H_{2\%}$ in the formula. For Rayleigh distributed (deep water) waves the ratio $H_{2\%}/H_s$ is 1.4. This constant factor was also used in the modified Van der Meer equations in VAN GENT ET AL. [2003] in which the values for the factors $c_{plunging}$ and $c_{surging}$ were adapted to include the effects of the use of $H_{2\%}$.

The value for the $c_{plunging}$ factor was found by calibration with the dataset of VAN GENT ET AL. [2003]. He found $c_{plunging}$= 8,4 and $c_{surging}$ = 1,3. The analysis of VAN GENT ET AL. [2003] is based on tests in shallow water conditions (H_s/d = 0,23 to 0,78) and a slopes of the foreshore of 1 : 30 and 1 : 100.

1.2 Problem description

In Figure 1.4 a graph from VAN GENT [2004] is shown. In this graph the datasets for plunging waves of VAN DER MEER [1988] and VAN GENT ET AL. [2003] have been compared. It can be seen from Figure 1.4 that there is a clear difference between the dataset of VAN DER MEER [1988] (red) and VAN GENT ET AL. [2003] (blue). Thorough investigation of both Van der Meer and Van Gent indicate that there are no systematic differences in the modelling approach. A difference of 5 to 10 % can be seen between the datasets even when the data is corrected.
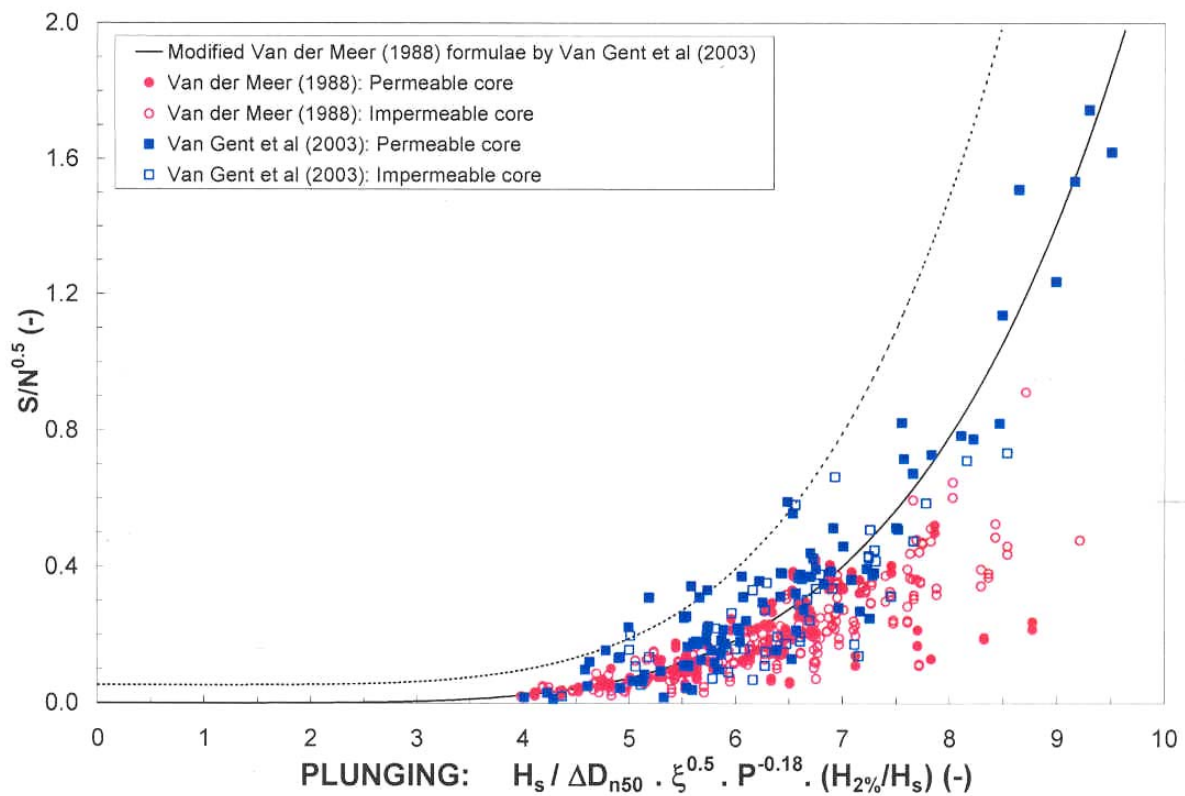
Figure 1.4: Data of VAN GENT ET AL. [2003] and VAN DER MEER [1988]

A certain part of the experiential results of VAN GENT ET AL. [2003] should be the same as the results found by VAN DER MEER [1988]. For relatively deep water conditions VAN GENT ET AL. [2003] and VAN DER MEER [1988] find the same results. In (very) shallow waters with steep foreshores differences in the results can be found. The damage levels in the dataset of VAN GENT ET AL. [2003] are on average 5 to 10% higher than the damage levels in dataset of VAN DER MEER [1988].

Tests from a number of M.Sc. students in the Laboratory of Fluid Mechanics of Delft University of Technology have indicated that identical spectra at the toe of a breakwater can have a different damage to the construction because of differences in the foreshore (TROMP[2004], TERILLE [2004, HOVESTAD [2005], OORTMAN [2006]).

Because in the experiments the spectra are identical, but the damage is clearly not identical this implies that the damage to the breakwater is also dependent of a wave parameter that is not represented by the shallow water wave spectrum as described in VERHAGEN [2005]. This parameter is different for waves on different foreshore slopes. From this it might be possible to add an extra parameter to the equations of VAN DER MEER [1988] to deal with the effects of accelerating flow and decreasing phase difference due to shoaling waves. In deep water and horizontal foreshores this parameter is equal to 1.0, because in deep water there is no increase of the acceleration. Entering shallow water this parameter will increase.

To be able to make a proper comparison between the datasets it must be made sure that all parameters are in the correct form. In VAN DER MEER [1988] for the wave height the significant wave height was used. For the wave period VAN DER MEER [1988] used the mean period, T_m. VAN GENT ET AL. [2003] used for the wave height the wave height exceeded by 2% of the waves, $H_{2\%}$. For the wave period VAN GENT ET AL. [2003] used the spectral period, $T_{m-1,0}$. General transformation ratios exist to recalculate these values, but these ratios are not generally applicable. Therefore it is expected that the graphs, like in Figure 1.4, in which the datasets of VAN GENT ET AL. [2003] and VAN DER MEER [1988] are not always correct, because parameters were not transformed in a proper way. Also it must be checked whether the test conditions are similar for both datasets. The aim of this M.Sc. Thesis is to produce the correct and comparable datasets of VAN DER MEER [1988] and VAN GENT ET AL. [2003]. Also the dataset of THOMPSON & SHUTTLER [1975], which formed the basis of the work of VAN DER MEER [1988] will be investigated. After this further research can be done to the differences between the datasets for which this work will form a basis.

1.3   Problem definition

To be able to couple the datasets of VAN DER MEER [1988] and VAN GENT ET AL. [2003] into one general formula for rock stability on slopes under wave attack, for example by adding an extra parameter to the original formulae of VAN DER MEER [1988], the datasets need to be

made comparable. This includes the transformation of all parameters into one format in which each data point is treated individually. After this with statistical tests the transformed datasets of VAN DER MEER [1988], THOMPSON & SHUTTLER [1975] and VAN GENT ET AL. [2003] will be compared. To this aim a spreadsheet will be produced consisting all 3 datasets, which will be a basis for further investigations.

1.4   Report outline

In Chapter 2, Chapter 3 and Chapter 4 successively the datasets of VAN DER MEER [1988], THOMPSON & SHUTTLER [1975] and VAN GENT ET AL. [2003] will be entered in a spreadsheet, analysed and transformed into a comparable format. After this in Chapter 5 the datasets will be compared in a proper way. In Chapter 6 the datasets will be compared by means of statistical tests. In Chapter 7 suggestions are made for the use of the damage graphs in design practice and again the datasets have been compared with switched axes. In Chapter 8 possible explanations for the differences found will be discussed and starting point for further research is given. Finally in Chapter 9 conclusions and recommendations of this M.Sc. Thesis are given.

Chapter 2

VAN DER MEER

2.1   Introduction

Within the framework of this M.Sc. Thesis with the objective to compare the datasets of VAN DER MEER [1988] and VAN GENT ET AL. [2003] at first the dataset of VAN DER MEER [1988] was investigated. To this aim the dataset of VAN DER MEER [1988] was entered in an Excel spreadsheet. After this the graphs 3.27 and 3.28 out of VAN DER MEER [1988] were redrawn to check the correctness of the spreadsheet. In this again a distinction was made between plunging and surging waves. After this the spreadsheet the dataset was transformed into a dataset which can be compared with the dataset of VAN GENT ET AL. [2003].

2.2   Graph for plunging waves

In Figure 2.1 the graph for plunging waves is given. The coloured points show the recomputed test results. Each category is indicated with a different colour (permeable structure, impermeable structure, homogenous structure, density of stones, water depth, large scale tests and different spectra). A complete legend is given in Appendix D. Also a difference is made between tests with N=1000 waves (squared points) and tests with N=3000

waves (rhomboidal points). In the background in black the original graph from VAN DER MEER [1988] for plunging waves is shown. Test results for low crested structures are not shown in this graph.
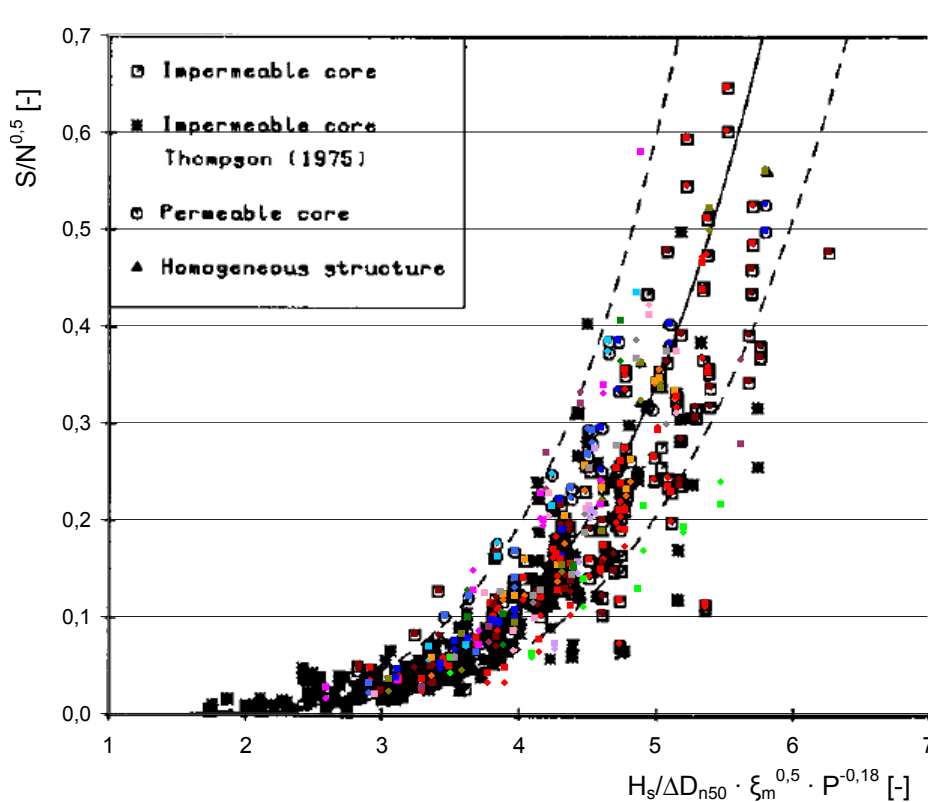
Figure 2.1: Plunging waves (VAN DER MEER [1988])

At first sight it can be seen that is not much difference between the original graph and the new graph. Small deviations might be possible because of round off errors in the gravitational acceleration, g, and the number π. Also small differences can have occurred because of scaling errors in the document scanning. In the lower part of the graph especially the light-green coloured points are conspicuous. These are the test results with low-density stones (quarry run) ($\Delta=0,92$). Also the points which describe the influence of different spectra (pink coloured) are obviously not in the original graph from VAN DER MEER [1988].

It can be concluded that in VAN DER MEER [1988] only the categories permeable, impermeable and homogenous have been plot. Therefore in Figure 2.2 the results are plotted with only the categories permeable, impermeable and homogenous.
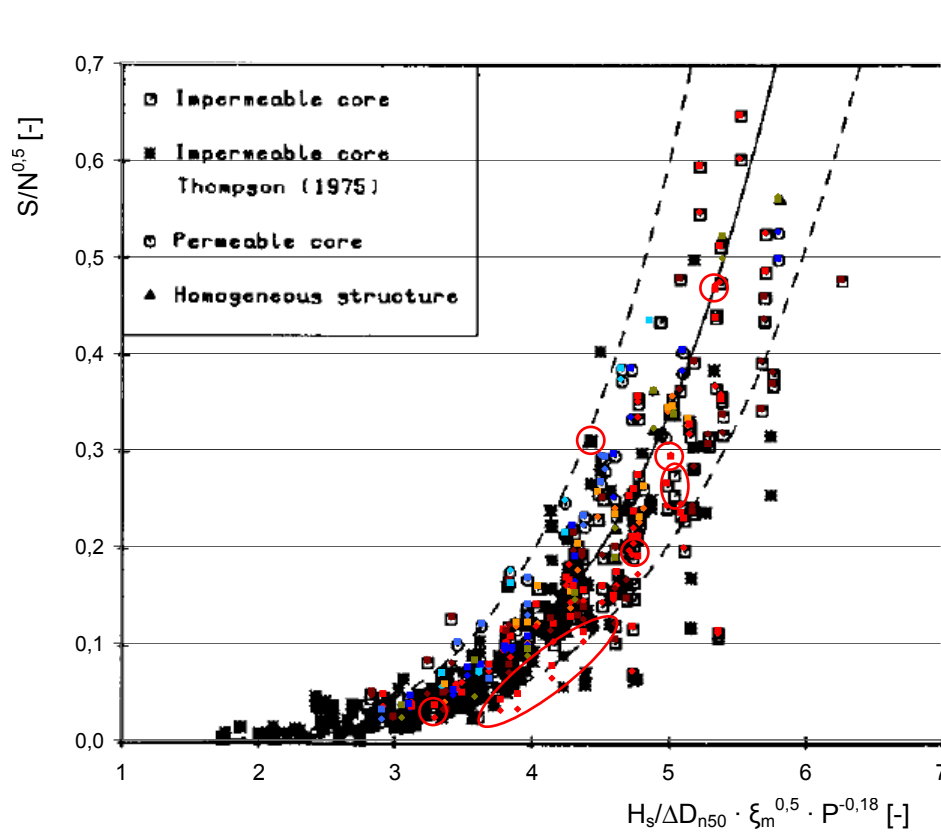
Figure 2.2: Plunging waves VAN DER MEER [1988] (permeable, impermeable, homogenous)

In the graph in Figure 2.2 some deviations are visible between the original graph and the new graph. Some points which appear in the new graph do not appear in the original graph and vice versa. These points have been marked with a red circle. An explanation for this is will be given in paragraph 2.4

Another difference is the absence of the dataset of THOMPSON & SHUTTLER [1975] which is indicated in Figure 2.1 by black crosses. This dataset is investigated and added to the graph in Chapter 3.

2.3 Graph for surging waves

Subsequently in Figure 2.3 the graph for surging waves is drawn, also with the original graph of VAN DER MEER [1988] in the background again.
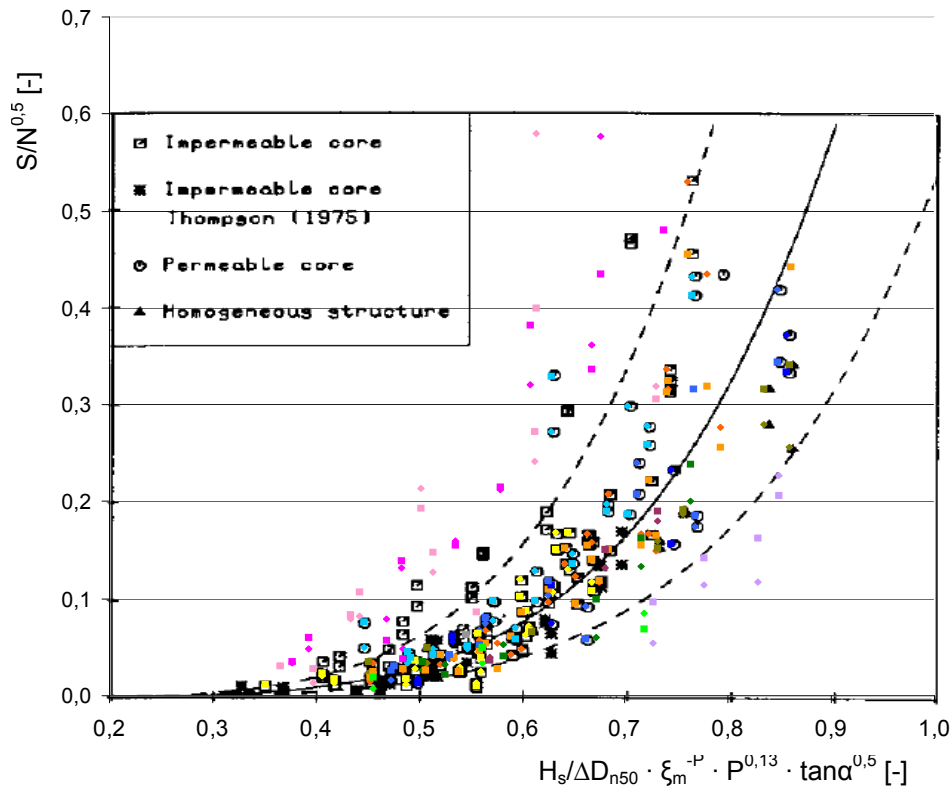
Figure 2.3: Surging waves (VAN DER MEER [1988])

In the graph with surging waves again deviations can be seen in the test results with different spectra (the pink coloured points) and the test results with different densities (in green). Again also a number of points in the categories impermeable and permeable (orange and blue) show deviations.

To make clear that most of the differences occur in the test categories with different spectra density, depth and the large scale tests again in Figure 2.4 the graph is plotted with only the categories permeable, impermeable and homogenous.

In Figure 2.4 the points that differ from the original graph and vice versa have been marked with red circles. For these differences an explanation will also be given later on in this section.
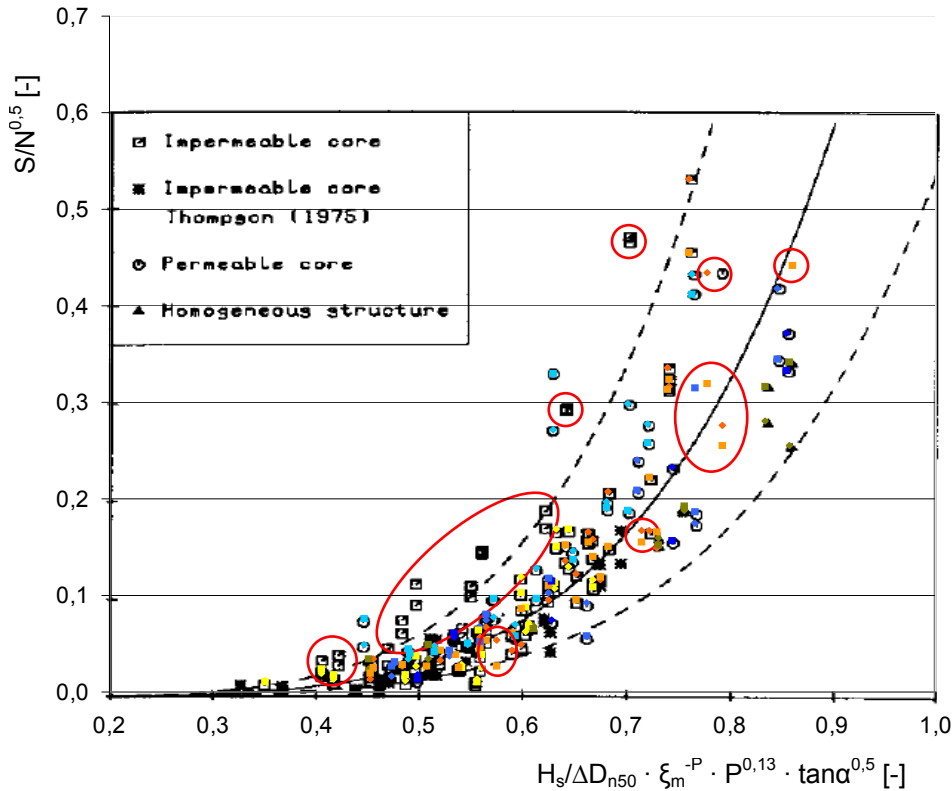
Figure 2.4: Surging waves VAN DER MEER [1988] (only permeable, impermeable and homogenous)

2.4 Explanation differences

In the previous sections it has become clear that the new graphs for plunging and surging waves do not completely match with the original graphs of VAN DER MEER [1988]. In this only the categories Impermeable, Permeable and Homogenous are considered. Some points in the new graphs cannot be found in the original graphs and vice versa. A very close look to the graphs for plunging waves shows that the missing points in the original graph for surging waves do appear in the original graph for plunging waves and vice versa. The reason for this is that the distinction between surging and plunging waves is not correctly dealt with. The boundary between plunging and surging waves is given by the boundary (critical) Iribarren parameter, ξ_c .

$$\xi_c = \left(\frac{c_{plunging}}{c_{surging}} \cdot P^{0,31} \cdot \sqrt{\tan \alpha} \right)^{\frac{1}{P+0,5}}$$ in which $c_{plunging}$ = 6,2 and $c_{surging}$ = 1,0

The probable reason why mistakes were made with the critical Iribarren parameter is that in the development of the equations of VAN DER MEER [1988] the value of the parameter P,

which describes the permeability, has changed a number of times before the final values were reached. The permeability coefficient affects the critical Iribarren parameter what has probably caused some points to be switched from the graph for plunging waves to the graph for surging waves. From this it can be concluded that in VAN DER MEER [1988] some mistakes were made with the distinction between plunging and surging waves. Also it must be mentioned that less sophisticated computer programmes were used in the time the Ph.D. Thesis was written.

In Table 2.1 the deviating points are listed:

Test nr.	Construction type	$\cot\alpha$	Plunging factor	Surging factor	$\dfrac{S_{1000}}{\sqrt{N}}$	$\dfrac{S_{3000}}{\sqrt{N}}$	ξ_m	ξ_{crit}	Breaker type
102	Impermeable	4	5,34	1,12	0,44	0,37	1,29	2,01	Plunging
76	Impermeable	4	5,35	0,70	0,47	0,47	2,83	2,01	Plunging
69	Impermeable	4	3,80	0,50	0,11	0,09	2,84	2,01	Plunging
90	Impermeable	4	4,78	0,62	0,19	0,17	2,87	2,01	Plunging
72	Impermeable	4	5,02	0,64	0,29	0,30	2,96	2,01	Plunging
91	Impermeable	4	4,38	0,55	0,11	0,10	3,04	2,01	Plunging
70	Impermeable	4	3,29	0,41	0,04	0,02	3,13	2,01	Plunging
75	Impermeable	4	4,60	0,56	0,15	0,15	3,19	2,01	Plunging
89	Impermeable	4	3,90	0,47	0,05	0,03	3,25	2,01	Plunging
73	Impermeable	4	4,15	0,48	0,08	0,06	3,45	2,01	Plunging
74	Impermeable	4	3,78	0,42	0,04	0,03	3,69	2,01	Plunging
245	Permeable	1,5	4,86	0,79	0,43	-0,02	4,05	4,08	Plunging
40	Impermeable	3	5,35	0,86	0,44	-0,02	2,56	2,55	Surging
59	Impermeable	3	3,61	0,58	0,03	0,05	2,60	2,55	Surging
43	Impermeable	3	3,36	0,53	0,04	0,04	2,61	2,55	Surging
21	Impermeable	3	4,94	0,78	0,32	0,43	2,65	2,55	Surging
39	Impermeable	3	5,04	0,79	0,26	0,28	2,66	2,55	Surging
35	Impermeable	3	4,75	0,73	0,17	0,15	2,77	2,55	Surging
24	Impermeable	3	4,66	0,71	0,15	0,17	2,77	2,55	Surging
217	Permeable	2	3,29	0,53	0,04	0,04	3,55	3,54	Surging
226	Permeable	2	4,98	0,77	0,32	-0,02	3,70	3,54	Surging

Table 2.1: Deviating points in graphs for plunging and surging waves

In VAN DER MEER [1988] all these points were mistakenly switched from the graph for plunging waves to the graph of surging waves and vice versa. It might be possible that more points were wrongly plotted in the dense area near the curves, where points are hard to distinguish.

For the formulae of VAN DER MEER [1988] adapting the graphs has positive effects for the categories Impermeable, Permeable and Homogenous, because most of the wrongly placed points are mostly outside the 90%-confidence interval. Missing points are mostly inside this interval. Differences occurring in other categories will be considered later on this chapter.

2.5 Test results with different spectra

It could be seen that the points which indicate the test results of the tests with different spectra, especially in the graph for surging waves, are not always within the 90%-confidence interval of the formula of VAN DER MEER [1988]. From this a possible conclusion is that in waves with different spectra other mechanisms might influence the stability. To get a better view on this the results for different spectra are plotted separately for plunging and surging waves.
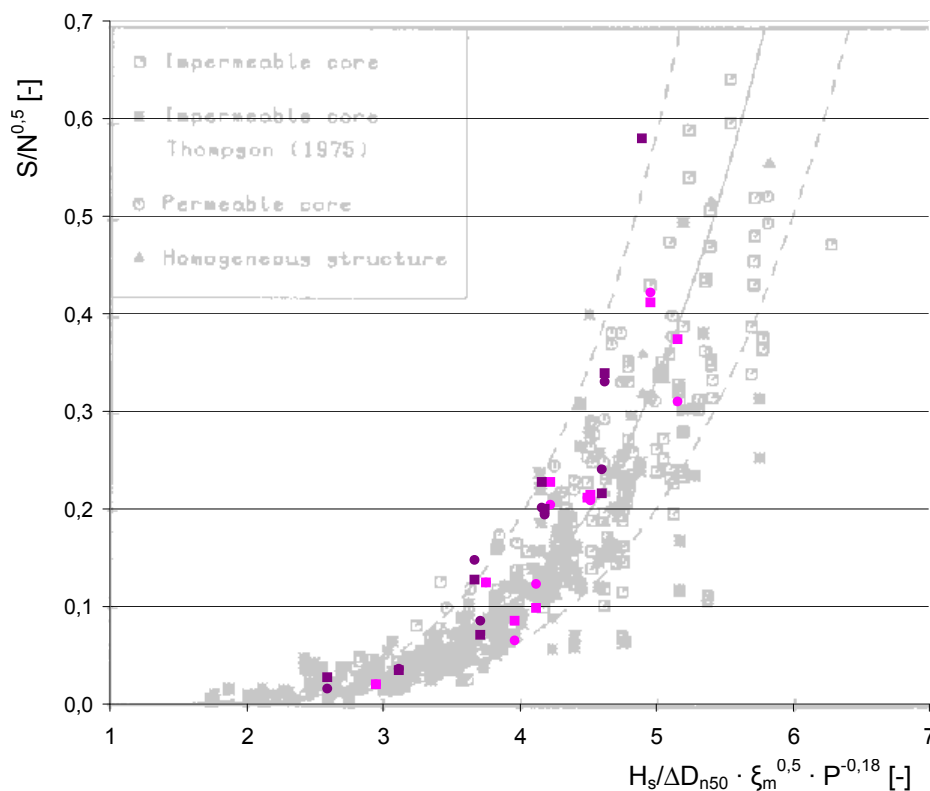
Figure 2.5: Plunging waves VAN DER MEER [1988] (only different spectra)

According to VAN DER MEER [1988] the purple (dark) coloured points in this graph indicate wide spectra and the pink (light) coloured points indicate narrow spectra. In the graph for plunging waves in Figure 2.5 it can be seen that the test results for different spectra mostly fit within the 90%-confidence interval of the formula for plunging waves.
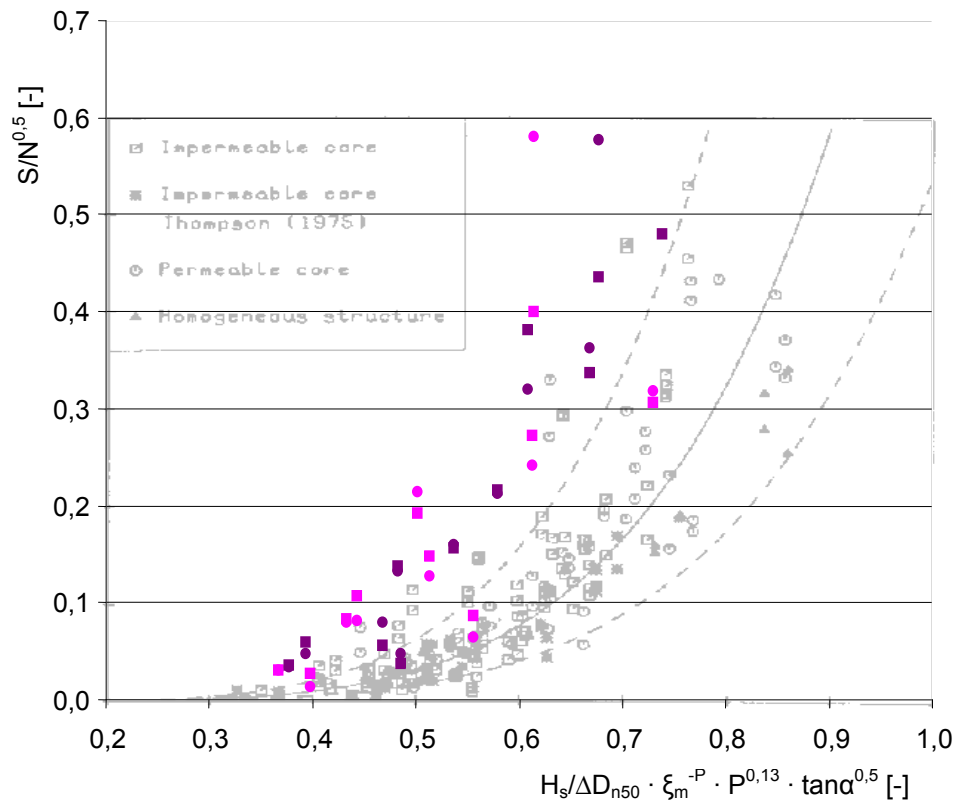
Figure 2.6: Surging waves VAN DER MEER [1988] (only different spectra)

In the graph for surging waves in Figure 2.6 it can be seen that the test results for different spectra do not fit within the 90%-confidence interval. In fact the occurring damage is worse in almost every case in comparison with the rest of the test results. This could mean that the formula of VAN DER MEER [1988] is only applicable for the spectra used in most of the tests of VAN DER MEER [1988] and that for different spectra other mechanisms affect the stability of rock.

To find out what can cause these differences in VAN DER MEER [1988] test 32 was repeated. This repeated test (nr. 189) gives a damage that is about 2,5 times bigger than the original test (nr. 32) while the wave characteristics, slope angle and stone dimensions are equal for both tests. The damage levels of test 32 are $S_{1000} = 4,43$ and $S_{3000} = 8,70$, while the damages of test 189 are $S_{1000} = 11,43$ and $S_{3000} = 20,65$. This is in accordance with the tests with different

spectra (tests 158 to 197), which also show damage levels that are about 2,5 times bigger than the average damage level of the other tests.

According to VAN DER MEER [1988] the differences in damage can be caused by the painting process. After test 151, just before the tests with different spectra, the stones that were used in the previous tests were painted by rolling the stones together with paint in a concrete mill. During this painting process the stones got rounder and less sharp edged because of the intensive rolling in the concrete mill. It must be mentioned that stones got rounder because of the painting process and not by the paint itself. Stones also got a bit rounder and less sharp edged by rolling during the tests and because of frequent handling in between the tests. After test 197 a new made stone class was used which was not painted, which explains why no problems occurred during later tests.

In the graphs it can also be seen that the differences only occur in tests with surging waves. This can be explained because in surging waves rundown is decisive for stability, while in plunging waves wave run up has more influence on the stability. Wave rundown has more effect on stones because stones will easier roll in a downward direction with help of gravity. Smoother stones will easier be picked up by flowing water. With this information according to VAN DER MEER [1988] it can be concluded that the spectral shape does not influence stability. More on the influence of stone roundness will be discussed in paragraph 2.8.

In VAN DER MEER [1988] three types of spectra are used, indicated as PM-, narrow an wide spectra. In DELFT HYDRAULICS, M1983 PART I [1988],in which the experiments of VAN DER MEER [1988] are described in a very detailed way, for only 15 tests the spectrum is given. In Figure 2.7 the spectral shapes of test 25 (PM-spectrum), 195 (narrow spectrum) and 171 (wide spectrum) from of VAN DER MEER [1988] are shown. On the background in red a standard PM-spectrum is drawn with the same peak frequency as the original test. In Appendix B all 15 spectra from DELFT HYDRAULICS, M1983 PART I [1988] are shown with a standard PM-spectrum in red on the background.
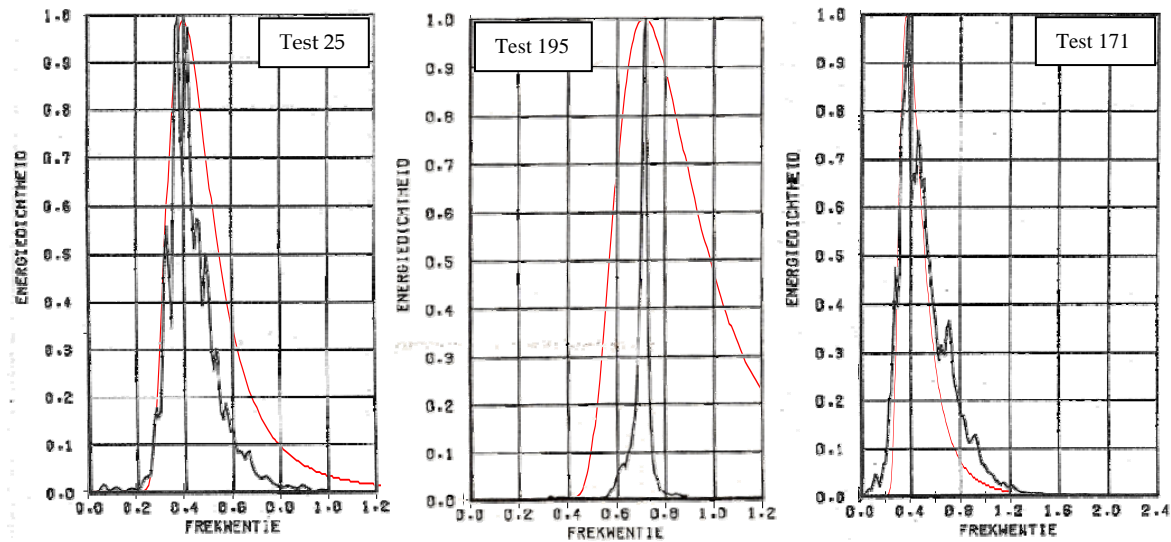
Figure 2.7: Spectra used in VAN DER MEER [1988]

According to VAN DER MEER [1988] the spectrum used in test 25 is a PM-spectrum. For test 25 it can be seen that especially on the right tail of the spectrum a lot of weight is missing. This is in accordance with all 7 PM-spectra of VAN DER MEER [1988]. The question arises whether these spectra used in VAN DER MEER [1988] really are PM-spectra.

Test 195 should be a narrow spectrum according to VAN DER MEER [1988]. For this test it can be seen that this spectrum is al lot narrower than the standard PM-spectrum, which makes it indeed a very narrow spectrum, if not too narrow. This is in accordance with all other tests with narrow spectra.

Subsequently test 171 should be a test with a wide spectrum according to VAN DER MEER [1988]. For test 171 it can be seen that the spectrum is a bit wider than the standard PM-spectrum. Again this is in accordance with the other tests with a so called wide spectrum. The question arises whether one can really speak of a wide spectrum in this case.

Because of this the spectral shape can be somewhat confusing, in this M.Sc. Thesis the different spectra will be indicated as spectrum I, II and III. Spectrum I contains all tests that where indicated in VAN DER MEER [1988] as PM-spectra, but apparently not really are. Spectrum II contains all tests indicated in VAN DER MEER [1988] as narrow spectra (tests 158 to 167, 183 to 186 and 193 to 197). Spectrum III contains all tests indicated by VAN DER MEER [1988] as wide spectra (tests 168 to 182, 187, 188 and 190 to 192).

Although there are differences in the spectral shapes it must be mentioned that at least 3 studies, THOMPSON & SHUTTLER [1975], VAN DER MEER [1988] and VAN GENT ET AL. [2003], showed that the spectral shape does not affect stability.

2.6   Conversion dataset to $T_{m-1,0}$ and $H_{2\%}$ values

Because VAN GENT ET AL. [2003] concluded that the wave characteristics in the stability formulae can better be described by $T_{m-1,0}$ and $H_{2\%}$ instead of T_m and H_s, the original dataset of VAN DER MEER [1988] needs to be converted. By doing this the datasets of VAN GENT ET AL. [2003] and VAN DER MEER [1988] can be compared in a proper way.

2.6.1 Wave height

The conversion from H_s to $H_{2\%}$ can be done using the point model of BATTJES & GROENENDIJK [2000] as described in Appendix A1. To do this first the zero-th order spectral moment, m_0, of each test needs to be calculated.

In DELFT HYDRAULICS, M1983 PART I [1988] only for only 15 tests out of the dataset of VAN DER MEER [1988] the exact value of m_0 has been calculated from the original tapes. To find, read and calculate m_0 for all tests out of the original data tapes used in the research of VAN DER MEER [1988] would be very time-consuming. Therefore this is not done in this M.Sc. Thesis. For the tests in which m_0 is not known it is calculated.

For Rayleigh distributed waves the significant wave height estimated from the wave spectrum, H_{m0}, can be calculated with the following approximation.

$$H_{m0} = 4,005... \cdot \sqrt{m_0}$$

Real time wave observations by LONGUET & HIGGINS [1980] and numerical simulations by GODA [1988] show that the significant wave height measured from a zero crossing analysis, $H_{1/3}$, may be 5% to 10% lower than the significant wave height as estimated from the spectrum. GODA [1988] suggests $H_{1/3} = 0,95 H_{m0}$, which results in:

$$H_{1/3} = 3,804 \cdot \sqrt{m_0}$$

Test nr.	Spectrum	H_s	$m_{0;exact}$	$m_{0;appr}$	$H_s / \sqrt{m_0}$	$m_{0;average}$
	[-]	[m]	[m²]	[m²]		[m²]
21	I	0,1177	1,05E-03	0,87E-03	3,641	1,04E-03
22	I	0,0995	0,75E-03	0,62E-03	3,638	0,74E-03
23	I	0,0858	0,55E-03	0,46E-03	3,662	0,55E-03
24	I	0,1085	0,87E-03	0,74E-03	3,683	0,88E-03
25	I	0,0705	0,37E-03	0,31E-03	3,675	0,37E-03
26	I	0,1173	1,09E-03	0,86E-03	3,553	1,03E-03
60	I	0,1159	0,97E-03	0,84E-03	3,723	1,01E-03
161	II	0,1108	0,80E-03	0,77E-03	3,910	0,86E-03
164	II	0,1193	0,96E-03	0,89E-03	3,850	1,00E-03
186	II	0,0970	0,85E-03	0,59E-03	3,325	0,66E-03
195	II	0,1240	0,95E-03	0,96E-03	4,029	1,08E-03
171	III	0,1221	1,03E-03	0,93E-03	3,804	1,16E-03
175	III	0,1056	1,01E-03	0,70E-03	3,323	0,87E-03
182	III	0,1117	1,05E-03	0,78E-03	3,447	0,97E-03
188	III	0,1253	1,12E-03	0,98E-03	3,744	1,23E-03

Table 2.2: Values of m_0 for the 15 tests of DELFT HYDRAULICS, M1983 PART I

In VAN DER MEER [1988] the wave height is measured by wave gauges, which means the approach of GODA [1988] has to used to calculate the significant wave height from the spectrum. Therefore for the 15 test of which the exact value of $m_{0;exact}$ is known from DELFT HYDRAULICS, M1983 PART I [1988] in Table 2.2 this value is compared with the calculated value of $m_{0;appr}$, which was calculated with the approximation of GODA [1988]. In the table it can be seen that the calculated $m_{0;appr}$ in most tests lower than the exact value from DELFT HYDRAULICS, M1983 PART I [1988], which makes this approach not very accurate.

Therefore in Table 2.2 for each of the 15 tests for which the spectrum is known the ratio $H_s/\sqrt{m_{0;exact}}$ is calculated. From these values averages of $H_s/\sqrt{m_{0;exact}}$ have been calculated for the three spectra used. For spectrum I the average value of $H_s/\sqrt{m_{0;exact}}$ is 3,654, for spectrum II this average is 3,779 and for spectrum III the average value is 3,580. Using these average ratios the value of $m_{0;average}$ is calculated for all 15 tests. These values do better correspond to

the exact values of m_0. In Figure 2.8 the calculated values of $m_{0;average}$ are compared with the exact values of $m_{0;exact}$.
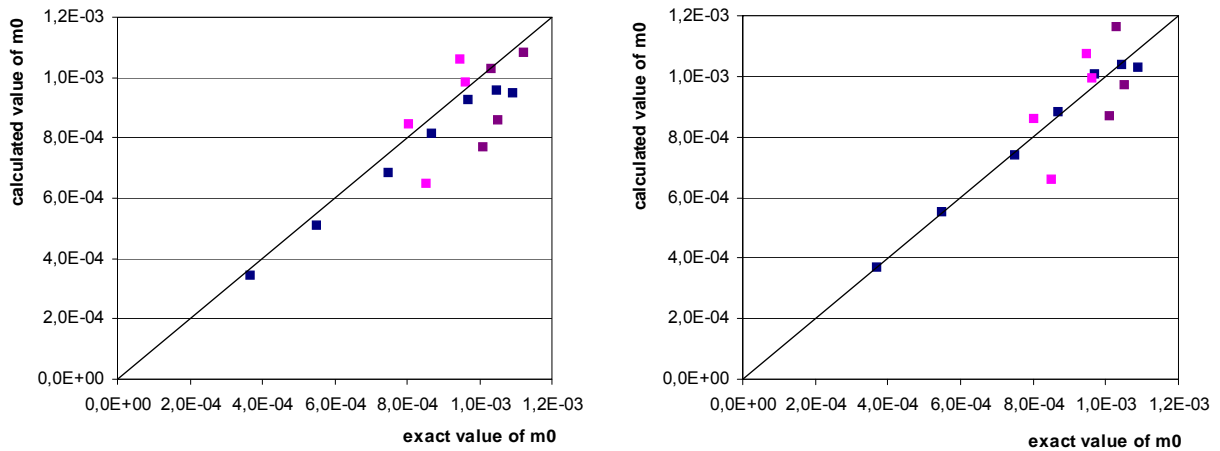
Figure 2.8: Calculated m_0 compared with exact m_0 (left : GODA [1988] ; right : average ratios)

From Figure 2.8 it can be concluded that it is better to use the averaged values of $H_s/\sqrt{m_0}$ to calculate m_0 for the tests for which this value is unknown. Therefore in the spreadsheet the average values of $Hs/\sqrt{m_0}$ are used according to Table 2.3. For the tests for which m_0 was exactly measured in VAN DER MEER [1988] the exact value is used.

Spectrum	Average $H_s/\sqrt{m_0}$
I	3,654
II	3,779
III	3,580

Table 2.3: Average values of $H_s/\sqrt{m_0}$ for 3 different spectra

When the zero-th order spectral moment is known the root-mean-square wave height, H_{rms}, of each test can be calculated. With this H_{rms} the transitional wave height, H_{tr}, is normalised to the normalised transitional wave height as described in Appendix A1.

In table 2 of BATTJES & GROENENDIJK [2000] the characteristic normalised wave heights are given as a function of the normalised transitional wave height, $\tilde{H}_{tr}$. Out of this table the ratio $H_{2\%}/H_{1/3}$ can be calculated. The ratio $H_{2\%}/H_{1/3}$ varies between 1,21 and 1,40. For $\tilde{H}_{tr} \geq 2$ the ratio $H_{2\%}/H_{1/3}$ remains constant at 1,4. For $\tilde{H}_{tr} \leq 1,2$ the ratio $H_{2\%}/H_{1/3}$ remains constant at

1,21. For $1,2 \leq \tilde{H}_{tr} \leq 2$ the ratio $H_{2\%}/H_{1/3}$ increases. In the spreadsheet for all tests the value of $\tilde{H}_{tr}$ is calculated. When this value is known the ratio $H_{2\%}/H_{1/3}$ can be read in table 2 of BATTJES & GROENENDIJK [2000].

In most of the tests of VAN DER MEER [1988] it can be seen that $H_{2\%} = 1,4H_s$. Only for the tests with smaller depth (0,20 and 0,40 m) and for the large scale tests a lower $H_{2\%}/H_s$ ratio occurs. Using this ratio the $H_{2\%}$ values are calculated in the spreadsheet.

2.6.2 Wave period

The conversion from T_m to $T_{m-1,0}$ can be done by using known ratios. In INFRAM I489 [2001] the ratio $T_p/T_{m-1,0}$ was calculated for the tests from VAN DER MEER [1988]. This ratio was based on the peak period, T_p.

In DELFT HYDRAULICS, M1983 PART I [1988] it is mentioned that $T_p = 1,15T_m$ for all PM spectra. However, when this ratio is calculated from the measured values for T_m and T_p in VAN DER MEER [1988] for many tests different ratios are found. In Figure 2.9 the calculated value of T_p (=1,15T_m) is compared with the measured value of T_p.
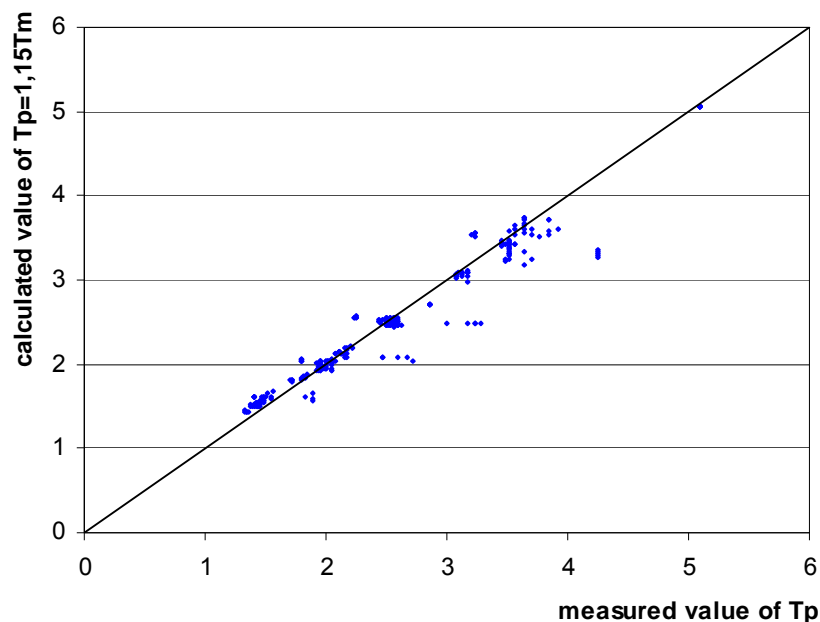
Figure 2.9: Differences due calculated or measured value of T_p

From this it can be seen that the most accurate approach to calculate the spectral period, $T_{m-1,0}$, is to calculate it from the measured values of T_p. This approach is used in this M. Sc. Thesis.

In INFRAM I489 [2001] the ratio $T_{pb}/T_{m-1,0a}$ has been calculated for the spectra used in VAN DER MEER [1988], see also Appendix A3. T_{pb} has been used instead of T_p because T_p depends strongly on the 'smoothness' of the spectrum. The T_{pb} value gives a better fixed value. T_{pb} represents the spectral period $T_{m-1,0}$ of the part of the spectrum where the energy is above 40% of the energy of the maximum. The ratios and corresponding standard deviations were presented in Table 2.4, where also the ratio $T_p/T_{m-1,0}$ is calculated.

	$T_{pb}/T_{m-1,0a}$	Standard Deviation	$T_p/T_{m-1,0}$	Standard Deviation
Spectrum I	1,042	0,013	1,031	0,047
Spectrum II	0,985	0,018	0,933	0,038
Spectrum III	1,061	0,023	1,094	0,052

Table 2.4: Ratios peak period / spectral period and corresponding standard deviations

From Table 2.4 it can be seen that the ratios $T_p/T_{m-1,0}$ for spectrum I are quite low. According to VAN DER MEER [1988] spectrum I is a PM-spectrum, for which normal values of the ratio $T_p/T_{m-1,0}$ are about 1,1 to 1,15. In paragraph 2.5 it was already discussed that spectrum I, II and III really were not really PM-, narrow and wide spectra. This results in these somewhat strange values for the ratio $T_p/T_{m-1,0}$. In this M.Sc. Thesis the ratios $T_{pb}/T_{m-1,0a}$ calculated in Table 2.4 are used for the calculation of $T_{m-1,0}$.

2.7   Graphs with $H_{2\%}$ and $T_{m-1,0}$

In Figure 2.10 and Figure 2.11 the dataset of VAN DER MEER [1988] is plotted with the adaptations in wave height and wave period as described in paragraph 2.6. In the graph for plunging waves it can be seen that the test results with low density material (light green) on average show less damage and that test results from the large scale tests on average show more damage. Furthermore a distinction occurs between permeable (blue) and impermeable (red, orange, yellow) structures.
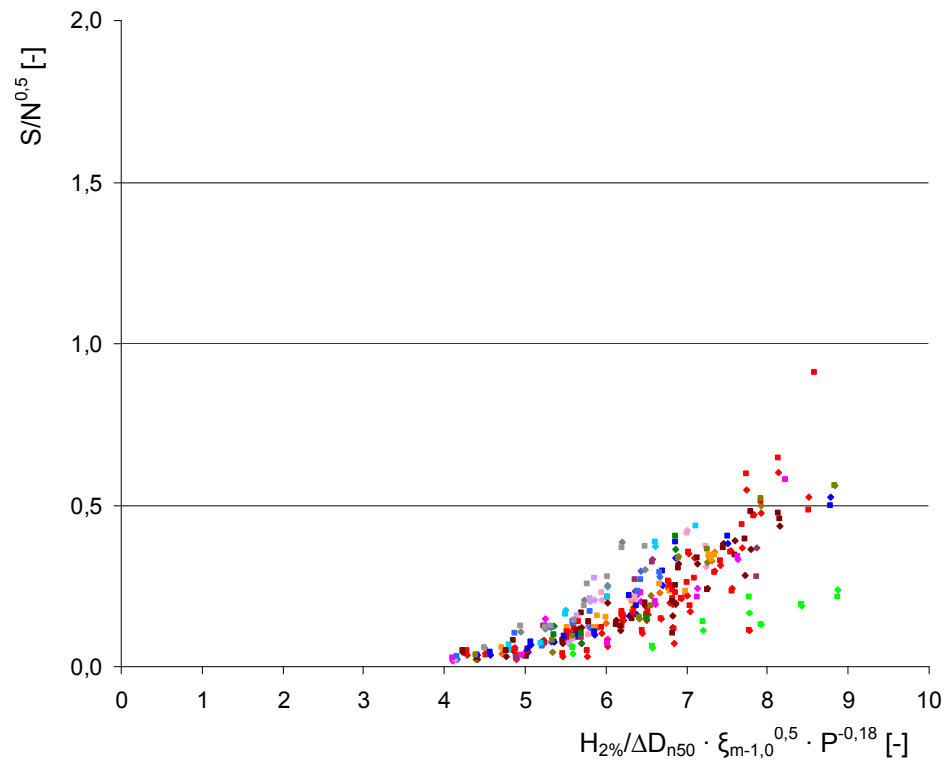
Figure 2.10: Plunging waves with H$_{2\%}$ and T$_{m-1,0}$ from dataset VAN DER MEER [1988]
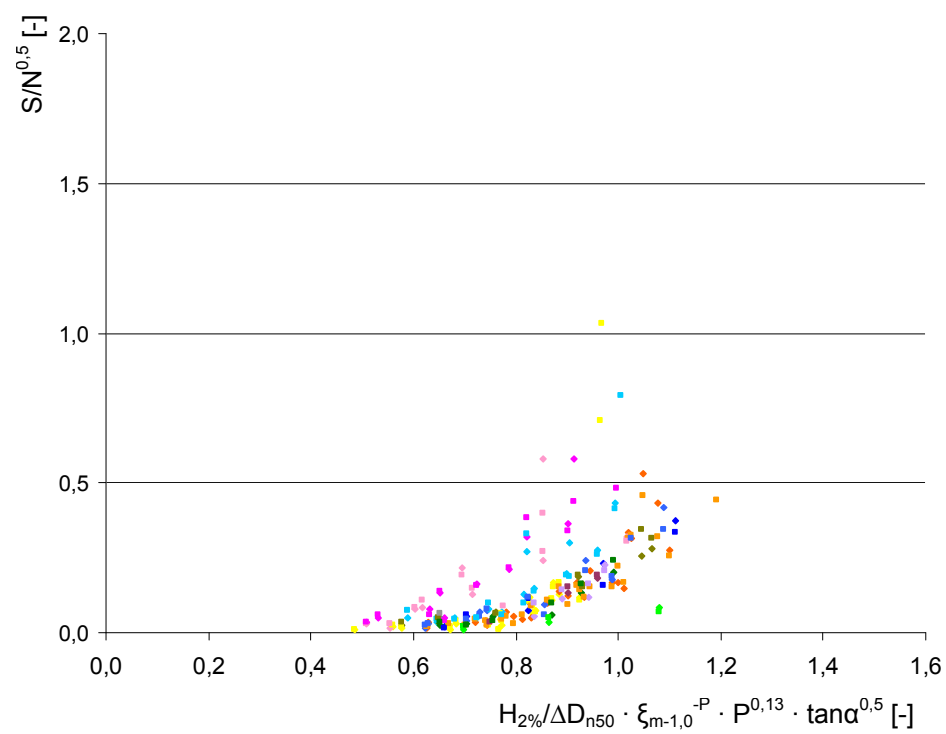
Figure 2.11: Surging waves with H$_{2\%}$ and T$_{m-1,0}$ from dataset VAN DER MEER [1988]

In the graph for surging waves it can be seen that again the test results of the tests with different spectra (pink) show significantly more damage than average. According to VAN DER MEER [1988] this is caused by the influence of stone roundness.

2.8   Influence of stone roundness

In paragraph 2.5 it was already mentioned that a possible explanation for the deviations of tests with different spectra is the difference in stone roundness. Also HUDSON [1953, 1959] had already indicated that angularity of quarry stone has influence on stability. In VAN DER MEER [1988] five types of stone have been used, for which the roundness has been measured according to the definition of roundness given by ALLSOP [1985].

$$roundness = \frac{average\ radius\ of\ 4\ corners}{radius\ of\ internal\ circle}$$

In Table 2.5 the stone types used by VAN DER MEER [1988] are shown.

	Painted	Nr of tests	Roundness	Surface
Riprap	2x	151	$0,50 \pm 0,10$	Smooth
Uniform stone	1x	106	$0,41 \pm 0,10$	Smooth
Uniform stone	Not	41	$0,52 \pm 0,14$	Irregular
Quarry run	Not	10	$0,43 \pm 0,13$	Coarse and irregular
Basalt	Not	10	$0,33 \pm 0,13$	Smooth and irregular

Table 2.5: Stone types used in VAN DER MEER [1988]

In Figure 2.12 to Figure 2.16 photographs of all stone types used by VAN DER MEER [1988] are shown (see also Appendix C).

Figure 2.12: Riprap after 134 tests, 2x painted

Figure 2.13: Uniform stone after 106 tests, 1x painted

Figure 2.14: Uniform stone after 41 tests, not painted

Figure 2.15: Quarry run after 10 tests, not painted

Figure 2.16: Basalt after 10 tests, not painted

In these figures it can be seen that there is quite some difference in stone shapes and roundness. However the definition for stone roundness according to ALLSOP [1985] makes no difference between smooth and irregular surfaces, while in general irregular surfaces show more stability than smooth surfaces. Therefore LATHAM ET AL. [1988] investigated the effects of armour stone shape and roundness on stability. In this approach the stone shape is entered in Fourier components of the form:

$$C_n \cos(n\theta - A_n)$$

Where:

C_n = amplitude coefficient of the nth harmonic

n = harmonic order

θ = polar angle measured from an arbitrary reference line

A_n = phase angle

The first Fourier component is a circle, the second Fourier component is a oval and the n-th component is a n-leafed cloverleaf. In this way the first 10 harmonics form a shape factor, P_S, describing the shape of a rather smooth surface. The higher harmonics describe increasingly fine scale surface texture and in this way the roughness factor, P_R, is represented by the 10th to 20th harmonics. P_n represents the Fourier noncircularity and is calculated from harmonics 1 to ∞, but in reality an upper boundary of n=30 was set. In this way P_C (=10P_n) also forms a shape contribution factor. P_C carries practically the same information as P_S, but is scaled with a factor 10 for better compatibility. In the tables from LATHAM ET AL. the roughness is given in P_R and P_C. P_C was introduced because P_R and P_S did not distinguish well between smooth and jagged squares, rectangles and polygons. [1988].

LATHAM ET AL. [1988] investigated a number of stone types. These are:

Tabular: Max./min. dimension > 2, flat and elongate was included. Selection by eye.

Equant: Max./min. dimension < 2, at least two parallel faces. Selection by eye.

Fresh: Angular material left over after removing tabular and equant rock.

Semi round: Fresh material rounded with 5 to 10% weight loss

Very round: Fresh material rounded with 20 to 25% weight loss

For these stone types LATHAM ET AL. [1988] calculated the values of the shape factor, P_C, and the roughness factor, P_R, as presented in Table 2.6. For each stone type the Fourier components where derived from photos using special imaging techniques.

Stone type	Shape factor				Roughness factor			
	Mean	$P_{C;50\%}$	$P_{C;85\%}$	$P_{C;15\%}$	$P_R{}^*$	$P_{R;50\%}$	$P_{R;85\%}$	$P_{R;15\%}$
Tabular	2,67	3,03	1,82	4,65	0,0165	0,0180	0,0125	0,0325
Equant	1,43	1,52	1,00	2,21	0,0117	0,0124	0,0095	0,0166
Fresh	1,88	2,08	1,38	3,06	0,0138	0,0150	0,0107	0,0216
Semi round	1,89	2,13	1,22	3,19	0,0097	0,0121	0,0080	0,0153
Very round	1,55	1,80	1,05	2,64	0,0046	0,0053	0,0035	0,0092

Table 2.6: Shape and roughness factors for stones from LATHAM ET AL. [1988]

In Figure 2.17 to Figure 2.21 the photos are shown of the stones tested by LATHAM ET AL. [1988].

Figure 2.17: Tabular stones, LATHAM ET AL. [1988]

Figure 2.18: Equant stones, LATHAM ET AL. [1988]

Figure 2.19: Fresh stones, LATHAM ET AL. [1988]

Figure 2.20: Semi round stones, LATHAM ET AL. [1988]

Figure 2.21: Very round stones, LATHAM ET AL.1988]

LATHAM ET AL. [1988] also investigated the shape and roughness of 4 subsamples from the model materials used by VAN DER MEER [1988]. For these subsamples in Table 2.7 the values of the shape and roughness factor have been given. A sub sample of broken basalt was not available for this research. Photos of the stone types used by VAN DER MEER [1988] were given in Figure 2.12 to Figure 2.16.

Stone type	Shape factor				Roughness factor			
	Mean	$P_{C;50\%}$	$P_{C;85\%}$	$P_{C;15\%}$	P_R^*	$P_{R;50\%}$	$P_{R;85\%}$	$P_{R;15\%}$
Quarry run (DH1)	1,51	1,59	1,12	2,24	0,0115	0,0123	0,0092	0,0163
Uniform stone 0x painted (DH2)	1,52	1,77	1,12	2,25	0,0107	0,0114	0,0081	0,0167
Uniform stone 1x painted (DH3)	1,43	1,45	1,05	2,14	0,0093	0,0103	0,0075	0,0142
Riprap 2x painted (DH4)	1,46	1,55	1,08	2,30	0,0085	0,0101	0,0063	0,0132

Table 2.7: Shape and roughness factors for subsamples from VAN DER MEER [1988]

From these tables it can be seen that the P_C values of all subsamples of VAN DER MEER [1988] strongly correspond to the values of equant stones from LATHAM ET AL. [1988]. Looking at the roughness factor sub sample DH1 is almost similar to the equant stones of LATHAM ET AL. [1988]. The roughness of DH2 is somewhere between equant and semi round. DH3 is most similar to semi round and DH4 is in terms of roughness factor somewhere between semi round and very round. These findings can be approved by comparing the photos, however according to the photos sub sample DH4 tends to be much closer to very round than to semi round.

After deriving shape and roughness parameters LATHAM ET AL. [1988] tested the influence of these factors on stability. Therefore a model setup was used comparable with the model setup of VAN DER MEER [1988]. In these tests the damage was measured at N=1000 and N=3000 waves, while wave height and wave period were varied. To get a clear view on the influence of roundness and also because of limited flume time a number of parameters were not varied. Differences between the test conditions of VAN DER MEER [1988] and LATHAM ET AL. [1988] are mainly based on the fact that it is inappropriate to use sieve sizes in an investigation to shape effects. Important differences are:

- Armour thickness: LATHAM ET AL. [1988] used a double layer ($t_{armour} \approx 1,3D_{50}$), while VAN DER MEER [1988] and THOMPSON & SHUTTLER [1975] used $t_{armour} = 2D_{50}$. Another aspect is that for all stone types the armour thickness was calculated using the D_{50} of equant stones to avoid different armour thicknesses for each stone type, because of the varying D_{50}.
- Filter size and thickness: LATHAM ET AL. [1988] used a filter thickness of $t_{filter} \approx 0,43D_{50}$ instead of $t_{filter} = 0,5D_{50}$. Because of this also the filter size ratio changed was $D_{50;armour}/D_{50;filter} = 5,4$ instead of 4,5.
- Placement technique: In LATHAM ET AL. [1988] the stones were placed individually by hand.

From this the main problem is the validity of the permeability coefficient P, because of the differences in armour thickness and filter thickness. At first LATHAM ET AL. [1988] used P = 0.1, but during the research it was concluded that a better estimate is P=0.05 to 0.07. Another problem was that the approach used in LATHAM ET AL. [1988] was based on the assumption that shape and texture of the stones is independent of all parameters appearing in the

formulae of VAN DER MEER [1988]. Unfortunately the permeability depends to some extend on the shape of the armour stone. This could be seen in the differences in fictitious porosity (void space expressed as a percentage of the armour layer volume). For the very round rock the fictitious porosity was 28%, while for the other four stone type values were about 37%. Also because no tests were done with permeable constructions it could not be proved that for both permeable (P=0.5) and impermeable (P=0.1) the same effects occur. Therefore the conclusions from LATHAM ET AL. [1988] can only be applied on impermeable structures (P=0.1).
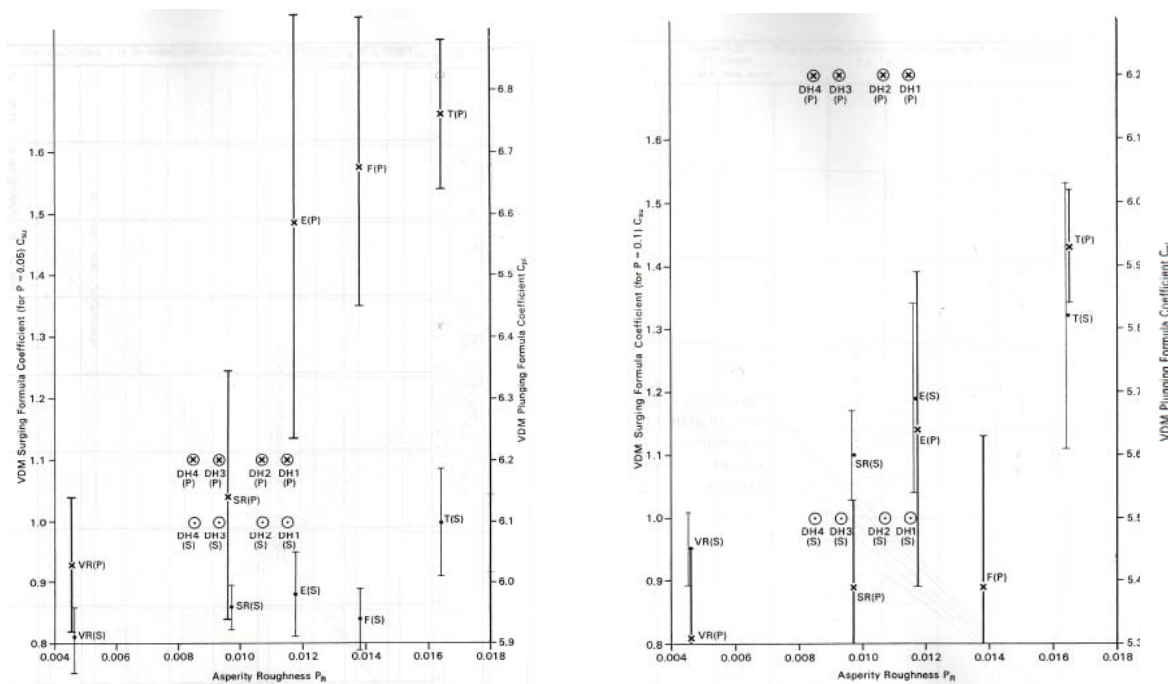
Figure 2.22: P_r - c_{pl} and P_r - c_{su} plots from LATHAM ET AL. [1988]: Left P=0,05; right P=0,1

To include the effects of stone shape and roundness LATHAM ET AL. [1988] suggested to change the values for $c_{surging}$ and $c_{plunging}$, which makes this effects independent of the other parameters. To do this in LATHAM ET AL. [1988] 2 plots were made showing the influence of the asperity roughness P_R on $c_{plunging}$ and $c_{surging}$ for P=0.1 and P=0.05 as shown in Figure 2.22. From these figures a more or less linear relationship can be seen in (averages of) $c_{plunging}/P_R$ and $c_{surging}/P_R$. In the graph with P=0.1 the data points which indicate the subsamples from VAN DER MEER [1988] are far above the point indicating the test results from LATHAM ET AL. [1988]. In the graph with P=0.05 the test results from LATHAM ET AL. [1988] for plunging waves show on average higher values of $c_{plunging}$. However the test results from LATHAM ET AL. [1988] for surging waves on average show lower values of $c_{surging}$ than VAN DER MEER [1988].

Assuming a linear relationship from both graphs an average slope for the ratio $c_{plunging}/P_R$ and $c_{surging}/P_R$ is derived. After this the lines are extrapolated in such a way that they intercept the data points of VAN DER MEER [1988]. In this way the effects of stone roundness can be interpreted on a very simple way by changing the coefficients $c_{plunging}$ and $c_{surging}$. It must be mentioned that this analysis is not very accurate because of the low number of tests and the scattered data.

As compared with standard quarry stone the coefficients in the original formulae of VAN DER MEER [1988] are changed according to Table 2.8 to include the effects of roundness on stability. In this table also γ-values are presented which can be used as a multiplier for the whole equations of VAN DER MEER [1988]. In Table 2.6 only the ratios are given for stones rounder than the stones used by VAN DER MEER [1988], because for more blockied stones also the effects of packing has an important role on the stability, which was not investigated by LATHAM ET AL. [1988].

	$c_{plunging}$	$γ_{Lath;pl}$	$c_{surging}$	$γ_{Lath;su}$
Standard Van der Meer	6,20	1,00	1,00	1,00
Semi round (0,009<P_R<0,011)	5,89	0,95	1,00	1,00
Very round (P_R<0,009)	5,89	0,95	0,80	0,80

Table 2.8: Influence stone roundness on coefficients Van der Meer formulae

With this information the graphs of VAN DER MEER [1988] are redrawn. The stones used in the tests with different spectra (sub sample DH4 according to LATHAM ET AL. [1988]) with P_R = 0,0087 are indicated as 'Very Round', with a factor 0.95 for plunging waves and a factor 0.80 for surging waves.

In Figure 2.23 the influence of including the roundness parameter into is shown by comparing each graph with the original graph without influence of roundness. It can be seen that especially for surging waves the impact of including the roundness parameter is huge. All points that were originally far outside the normal range are nice inside the normal range in the modified graph. It can be concluded that a rather small deviation in stone roundness can have large effects on stability.
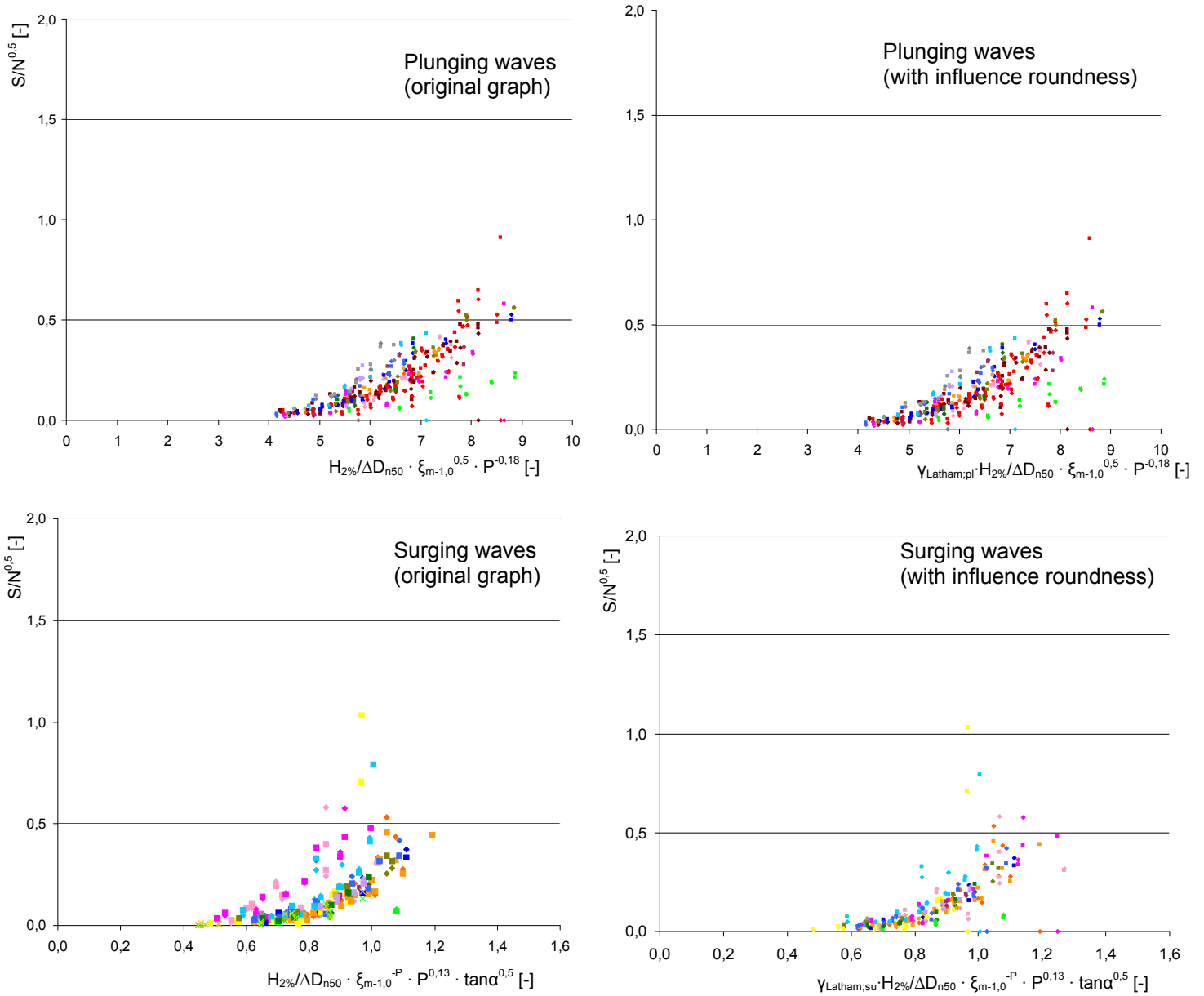
Figure 2.23: Effects of influence stone-roundness on graphs of VAN DER MEER [1988]

2.9 New graphs of VAN DER MEER [1988]

With all the adaptations described in the previous sections the graphs are drawn again in Figure 2.24 and Figure 2.25. In these graphs the correct value of $T_{m-1,0}$ and $H_{2\%}$ is used and also the effect of stone roundness is incorporated.
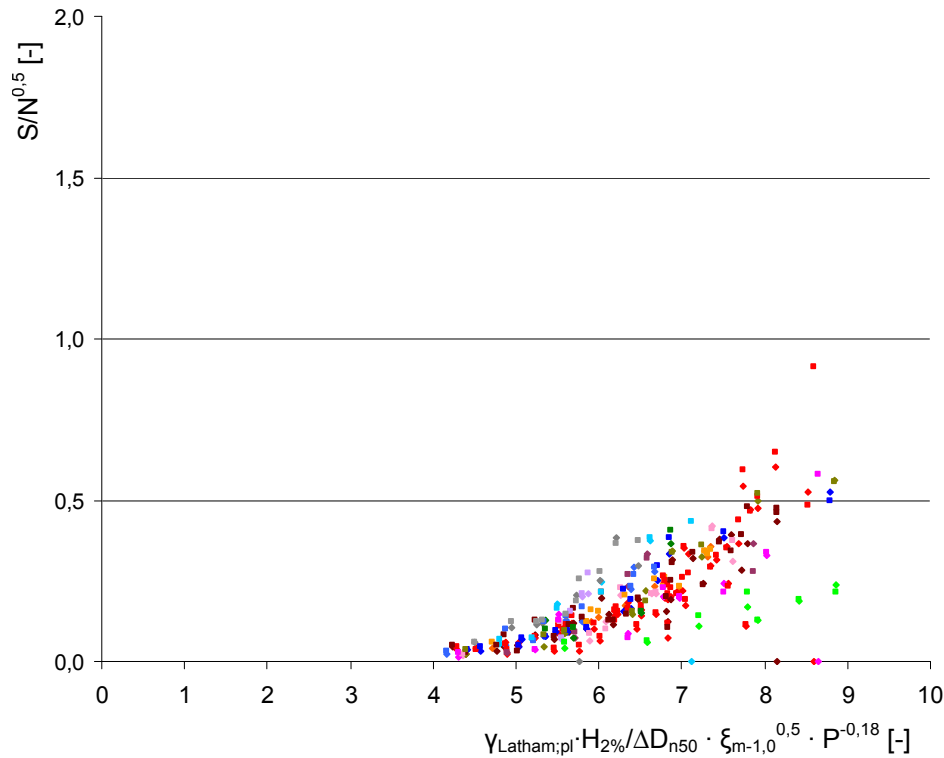
Figure 2.24: New graph for Plunging waves of VAN DER MEER [1988]

In the graph for plunging waves it can be seen that the tests with lower density ($\Delta=0,92$ (light green) still don't really correspond to the average test results. They show less damage with equal wave characteristics than the rest of the tests. On the other hand the large scale tests (grey) show more damage than the (average) rest of the test results. Also a distinction occurs between test results with a permeable construction (blue) and test results with an impermeable construction (yellow, orange and red). It looks like that the test results with permeable structures (blue) show on average more damage than tests with impermeable structures.

In the graph for surging waves after correcting for the stone roundness the test results with narrow and wide spectra (pink) now fit. But strangely some test results in the upper part don't really fit. These are test results with permeable structures (blue) and impermeable structures (yellow).
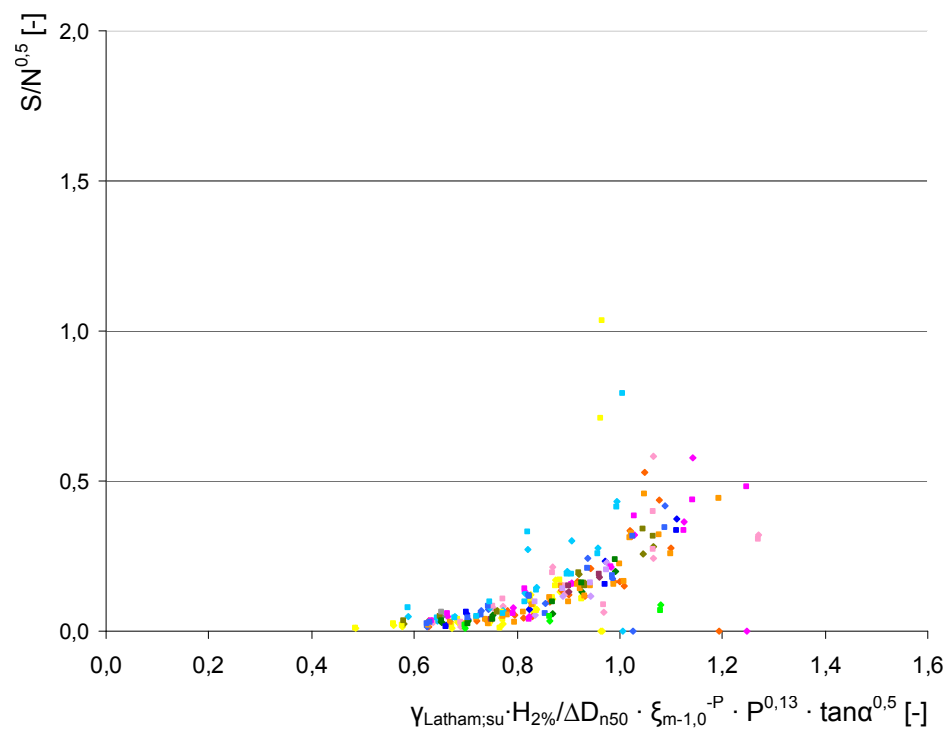
Figure 2.25: New graph for surging waves of VAN DER MEER [1988]

With these graphs further on in this M.Sc. Thesis the dataset of VAN DER MEER [1988] will be compared with the datasets of THOMPSON & SHUTTLER [1975] and VAN GENT ET AL. [2003].

Chapter 3

THOMPSON & SHUTTLER

3.1   Introduction

The research of THOMPSON & SHUTTLER [1975] was used as a starting point for the work of VAN DER MEER [1988]. Therefore in this M.Sc. Thesis this dataset will also be analysed and compared with the datasets of VAN DER MEER [1988] and VAN GENT ET AL. [2003]. To do this first the data from THOMPSON & SHUTTLER [1975] had to be entered in the spreadsheet, because no digital data was available.

3.2   Damage level

The damage level in the dataset of THOMPSON & SHUTTLER [1975] is written as N_Δ. This parameter has to be rewritten to the damage level, S, used in the dataset of VAN DER MEER [1988]. For the dataset of THOMPSON & SHUTTLER [1975] the ratio D_{n50}/D_{50} is 0,82 according to VAN DER MEER [1988]. In Table 3.1 the conversion is made from N_Δ to S using the following formula.

$$N_\Delta = \frac{A \cdot \rho_b \cdot 9 D_{50}}{\rho_a \cdot D_{50}{}^3 \cdot \pi/6} = \frac{9}{\pi/6} \cdot \frac{\rho_b}{\rho_a} \cdot \frac{A}{D_{50}{}^2} = \frac{54}{\pi} \cdot \frac{\rho_b}{\rho_a} \cdot \frac{0,82^2}{1} \cdot \frac{A}{D_{n50}{}^2} = \frac{54 \cdot 0,82^2}{\pi} \cdot \frac{\rho_b}{\rho_a} \cdot S$$

D_{50} [m]	ρ_b [kg/m³]	ρ_a [kg/m³]	ρ_b/ρ_a [-]	
0,020	1510	2700	0,559259259	$S=N_\Delta/6{,}463753336$
0,030	1480	2700	0,548148148	$S=N_\Delta/6{,}335334395$
0,040	1480	2700	0,548148148	$S=N_\Delta/6{,}335334395$

Table 3.1: Conversion from N_Δ to S

In order to make a comparison between the data of THOMPSON & SHUTTLER [1975], the data of VAN DER MEER [1988] and VAN GENT ET AL. [2003] the dataset of THOMPSON & SHUTTLER [1975] also has to be entered in the spreadsheet and transformed.

3.3   Correctness spreadsheet

After the conversion in Figure 3.1 and Figure 3.2 the dataset of THOMPSON & SHUTTLER [1975] is drawn together with the original dataset of VAN DER MEER [1988]. On the background the original graphs from the doctoral thesis of VAN DER MEER [1988] are given in which the dataset of THOMPSON & SHUTTLER [1975] was also included.
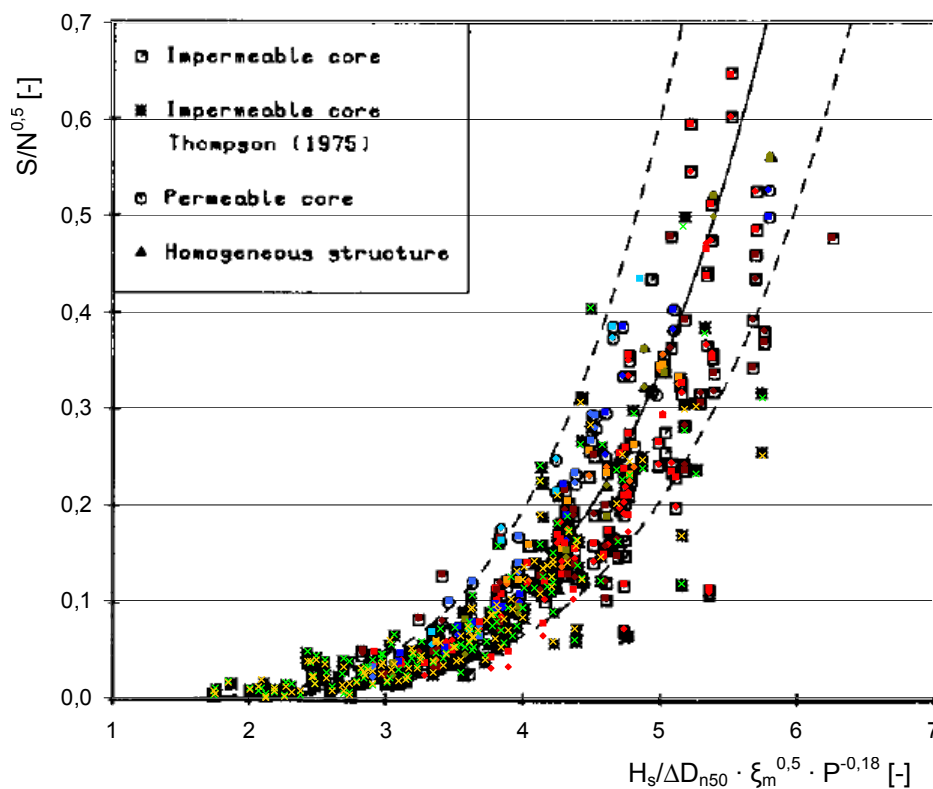
Figure 3.1: THOMPSON & SHUTTLER [1975] and VAN DER MEER [1988] for plunging waves

Besides the differences in the dataset of VAN DER MEER [1988] that were described before, no noteworthy differences between the original graph of VAN DER MEER [1988] and the new graph can be seen in Figure 3.1. Small differences can occur because of scaling effects due to the document scanning of small round off errors.

In Figure 3.2 a few deviating points, indicated with red circles, in the dataset of THOMPSON & SHUTTLER [1975] can be seen. Probably in VAN DER MEER [1988] again some mistakes were made with the critical Iribarren parameter, ξ_c. The reason why these deviations cannot be found the graph for plunging waves is that this graph is has very dense areas in which individual points are hard to distinguish.
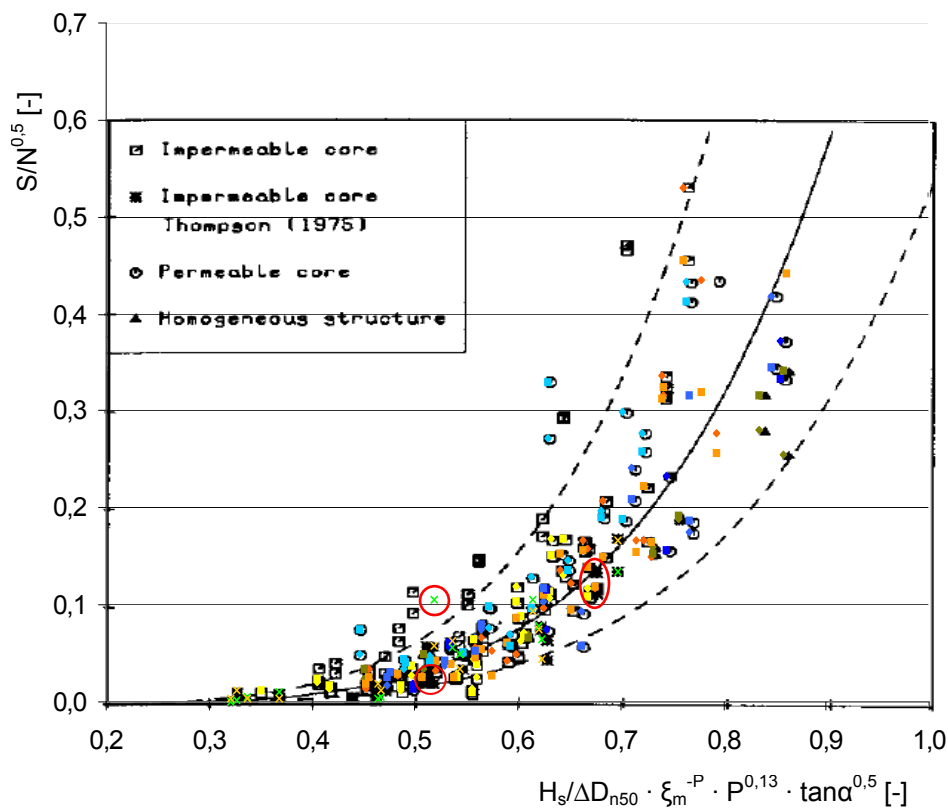
Figure 3.2: THOMPSON & SHUTTLER [1975] and VAN DER MEER [1988] for surging waves

3.4   Conversion dataset to $T_{m-1,0}$ and $H_{2\%}$ values

After this all parameters need to be written in the same format as the dataset of VAN GENT ET AL. [2003]. In this way a clear comparison of the datasets can be made. This means that the dataset of THOMPSON & SHUTTLER [1975] also has to be rewritten in terms of $H_{2\%}$ and $T_{m-1,0}$.

3.4.1 Wave height

In the dataset of THOMPSON & SHUTTLER [1975] the wave height is given in H_3. This is another notation for the significant wave height, H_s. In order to rewrite this wave height to the wave height exceeded by 2% of the waves, $H_{2\%}$, the point model of BATTJES & GROENENDIJK [2000] can be used.

For Rayleigh distributed waves the significant wave height estimated from the wave spectrum, H_{m0}, can be calculated with the following approximation.

$$H_{m0} = 4,005... \cdot \sqrt{m_0}$$

Real time wave observations by LONGUET & HIGGINS [1980] and numerical simulations by GODA [1988] show that the significant wave height measured from a zero crossing analysis, $H_{1/3}$, may be 5% to 10% lower than the significant wave height as estimated from the spectrum. GODA [1988] suggests $H_{1/3} = 0,95 H_{m0}$, which results in:

$$H_{1/3} = 3,804 \cdot \sqrt{m_0}$$

When the zero-th order spectral moment is known the root-mean-square wave height, H_{rms}, of each test can be calculated. With this H_{rms} the transitional wave height, H_{tr}, is normalised to the normalised transitional wave height as described in paragraph A1.

In table 2 of BATTJES & GROENENDIJK [2000] the characteristic normalised wave heights are given as a function of the normalised transitional wave height, $\tilde{H}_{tr}$. Out of this table the ratio $H_{2\%}/H_{1/3}$ can be calculated.

Using this approach for all tests of the dataset of THOMPSON & SHUTTLER [1975] the ratio $H_{2\%}/H_s$ has been calculated. The spreadsheet shows that for all tests the ratio $H_{2\%}/H_{1/3}$ is equal to 1,4.

3.4.2 Wave period

According to INFRAM, I489 [2001] the ratio $T_{m-1,0}/T_p$ is equal to 1,1, in which the peak period, T_p, is calculated from the mean period, T_m, using $T_p = 1,15 T_m$.

3.5 New graphs of dataset THOMPSON & SHUTTLER [1975]

Because no specific details are known about the stones used by THOMPSON & SHUTTLER [1975] it is assumed that the stones used in this research are of the standard type which was also used by VAN DER MEER [1988]. Therefore no correction factors are needed for this dataset. With these adaptations the datasets of THOMPSON & SHUTTLER [1975] are drawn again in Figure 3.3 and Figure 3.4.
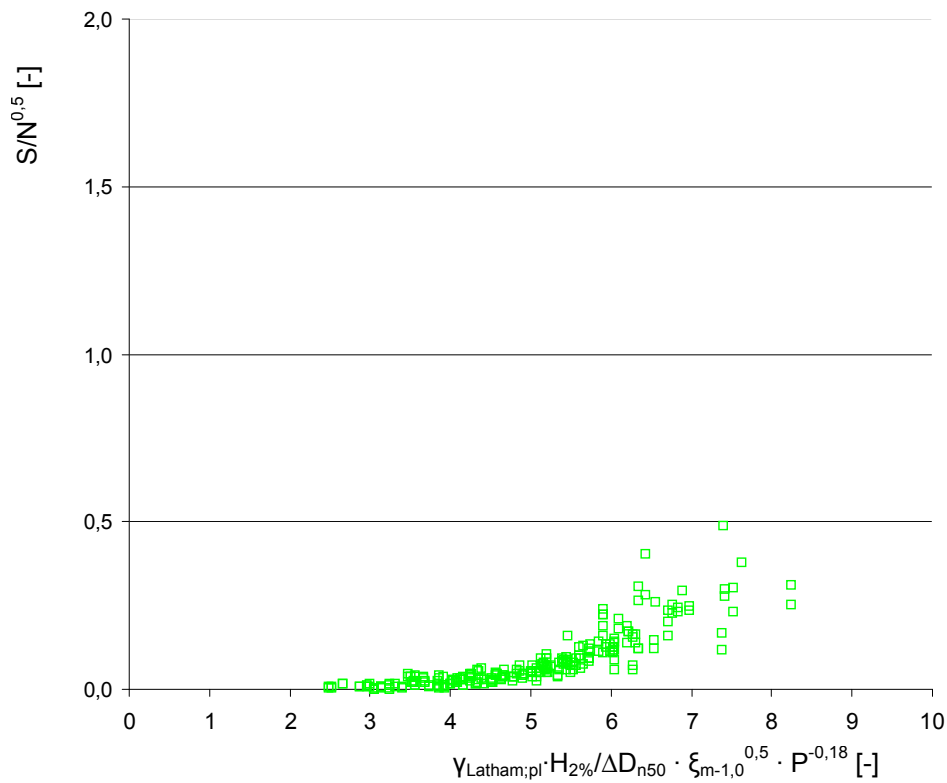
Figure 3.3: Plunging waves THOMPSON & SHUTTLER [1975]
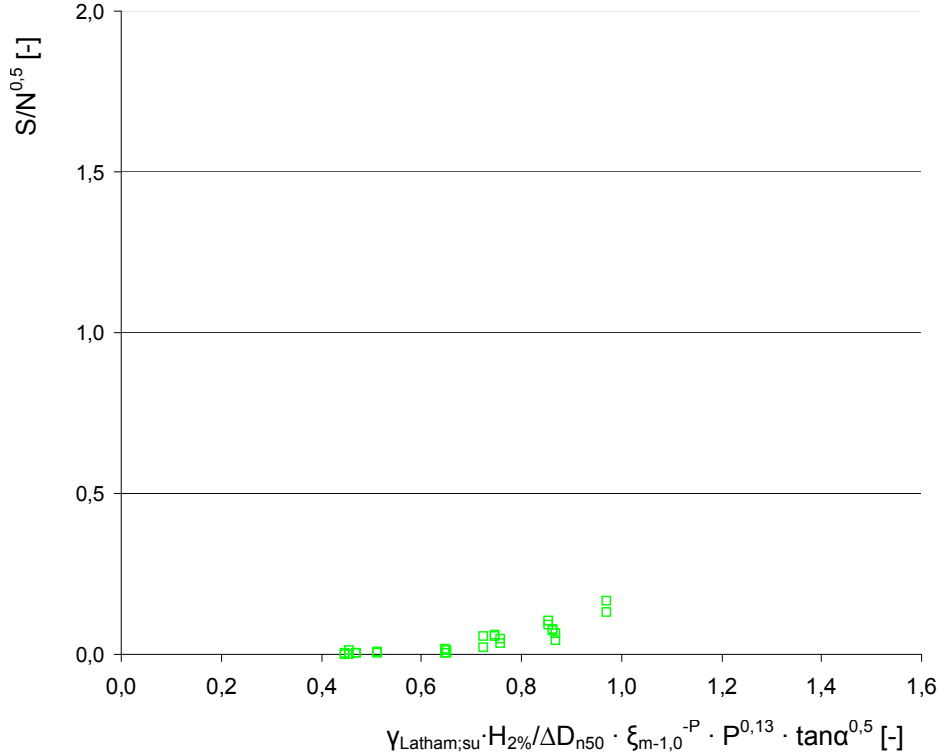
Figure 3.4: Surging waves THOMPSON & SHUTTLER [1975]

With these graphs the dataset of THOMPSON & SHUTTLER [1975] will be compared with the datasets of VAN DER MEER [1988] and VAN GENT ET AL. [2003] in Chapter 5.

Chapter 4

VAN GENT

4.1   Introduction

Before the dataset of VAN GENT ET AL. [2003] can be compared with the datasets of THOMPSON & SHUTTLER [1975] and VAN DER MEER [1988] the dataset of VAN GENT ET AL. [2003] had to be entered in an Excel spreadsheet. Because only graphs from the dataset of VAN GENT ET AL. [2003] were available during this M.Sc. Thesis the data was read from the graphs and entered in the spreadsheet to be able to compare the data likewise.

4.2   Correctness spreadsheet

Using the original graphs of VAN GENT ET AL. [2003] the correctness of the spreadsheet checked. In Figure 4.1 the graph for plunging waves is plotted (in grey) with on the background original graph from VAN GENT ET AL. [2003]. In the same way the graph for surging waves is treated. In Figure 4.2 the graph for surging waves is plotted together with the original graph from VAN GENT [2003]. With these graphs the dataset of VAN GENT ET AL. [2003] is compared with the datasets of VAN DER MEER [1988] and THOMPSON & SHUTTLER [1975]. No corrections or changes were made to the dataset of VAN GENT ET AL. [2003], which also means that the assumption is made that the stones used are of the standard stone type (γ_{Latham} = 1,0).
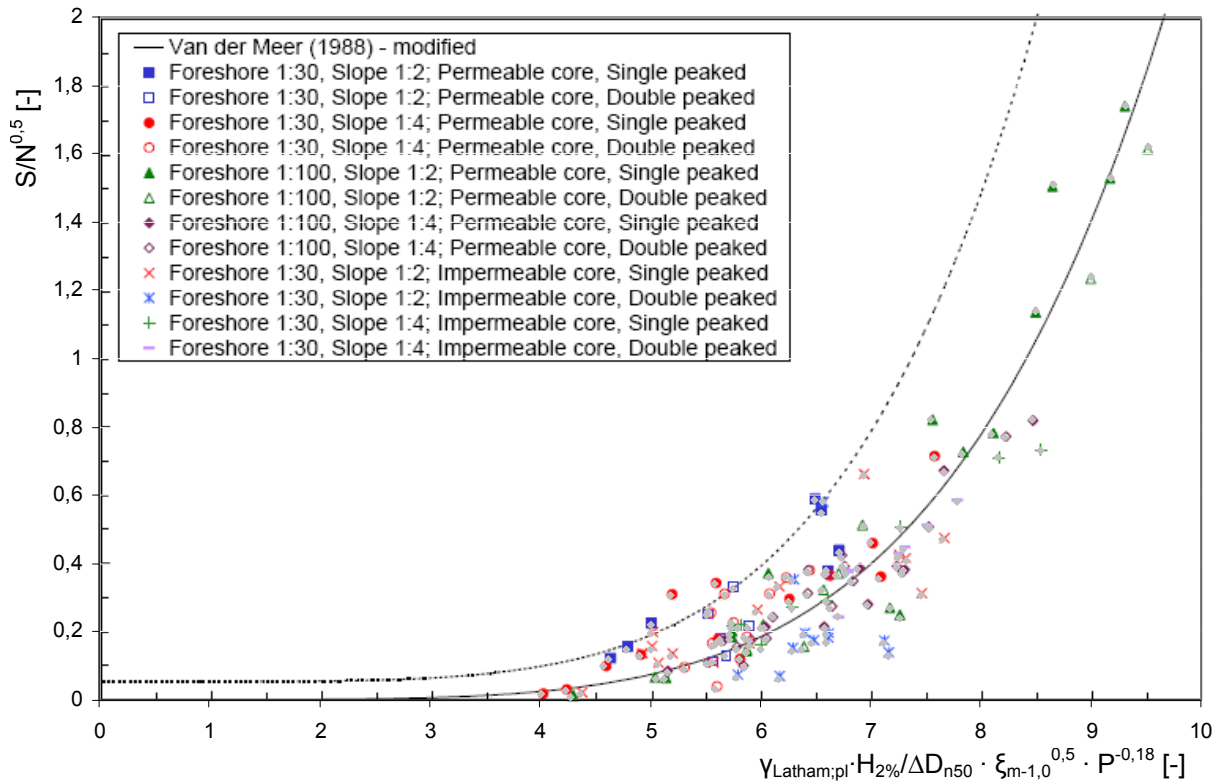
Figure 4.1: Plunging waves, reconstructed graph (grey), original graph (VAN GENT ET AL. [2003])
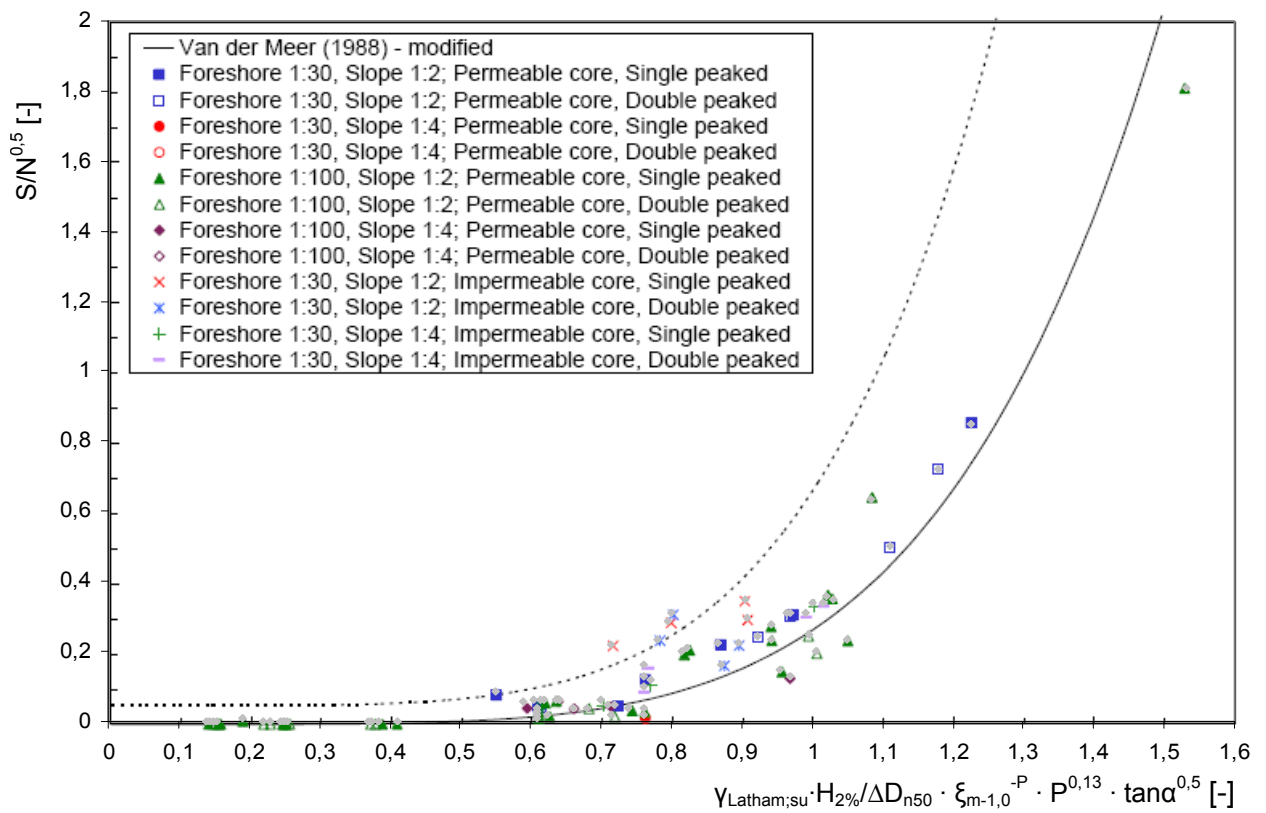
Figure 4.2: Surging waves, reconstructed graph (grey), original graph VAN GENT ET AL. [2003]

Chapter 5

COMPARISON OF DATASETS

5.1 Plunging waves

In Figure 5.1 to Figure 5.4 the graphs of VAN DER MEER [1988] (red), THOMPSON & SHUTTLER [1975] (green) and VAN GENT ET AL. [2003] (blue) have been plotted together.
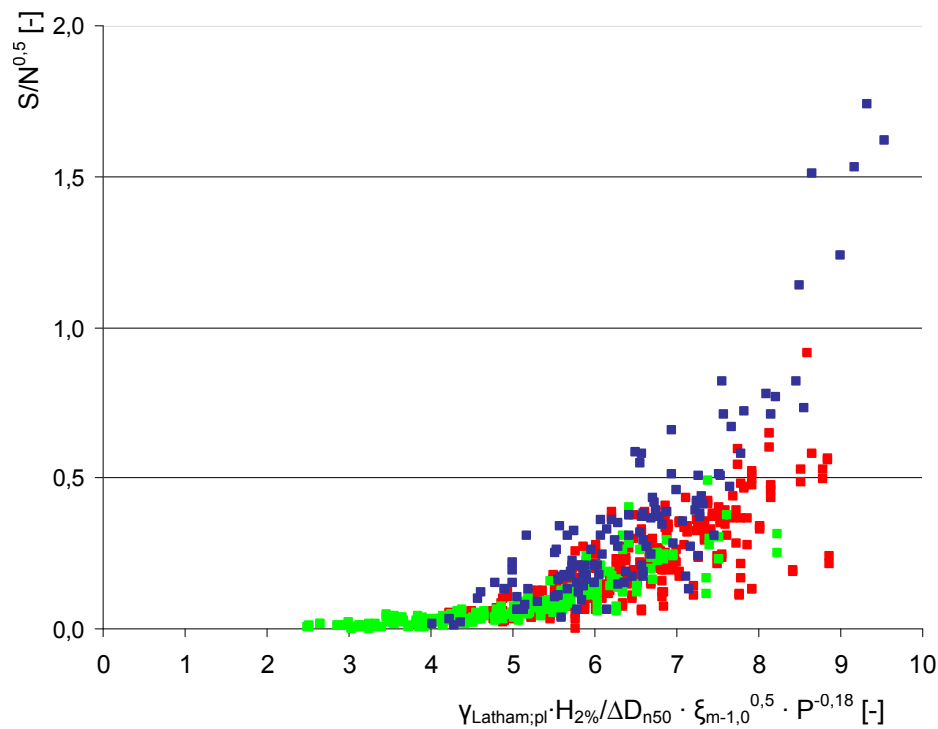
Figure 5.1: Plunging waves: THOMPSON & SHUTTLER [1975] (green), VAN DER MEER [1988] (red), VAN GENT ET AL. [2003] (blue
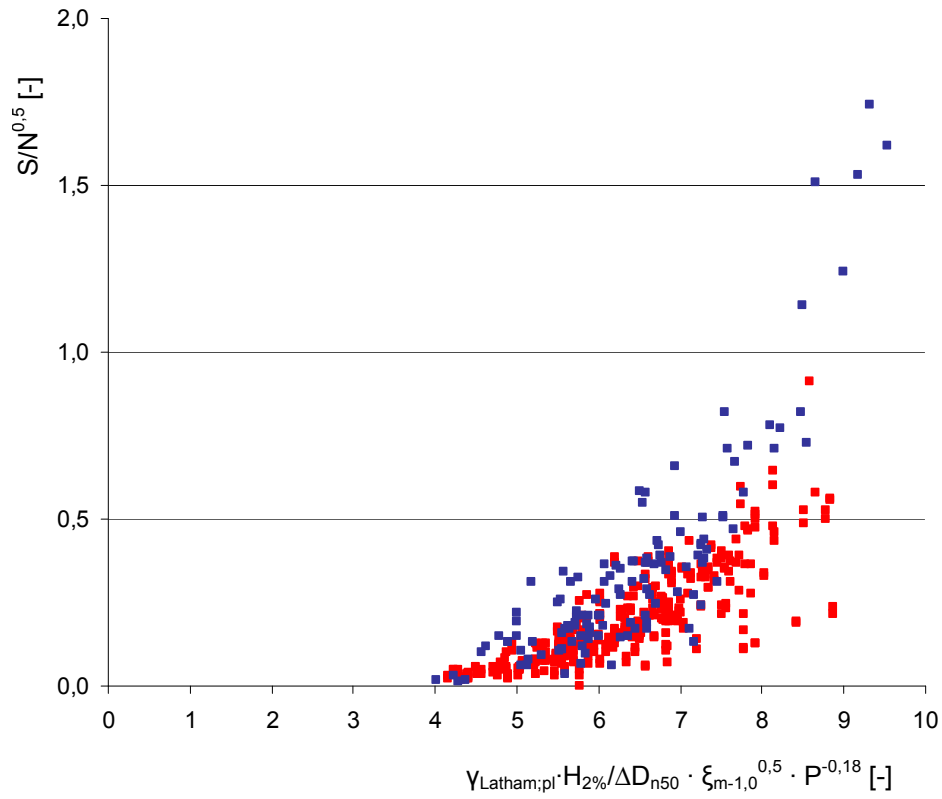
Figure 5.2: Plunging waves: VAN DER MEER [1988] (red), VAN GENT ET AL. [2003] (blue)
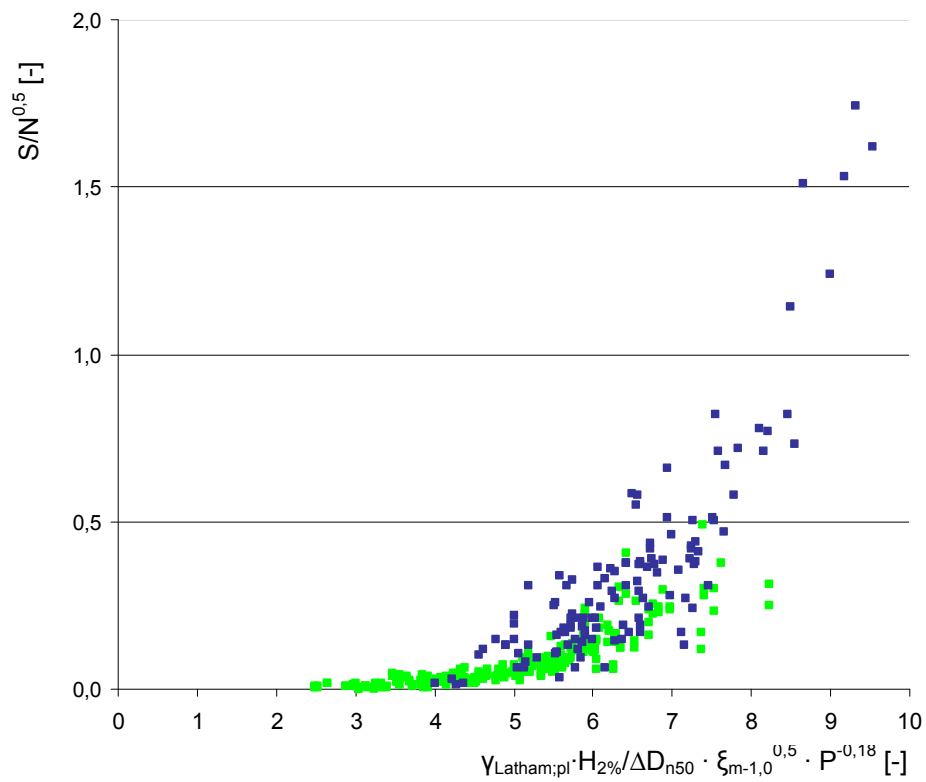
Figure 5.3: Plunging waves: THOMPSON & SHUTTLER [1975] (green), VAN GENT ET AL. [2003] (blue)
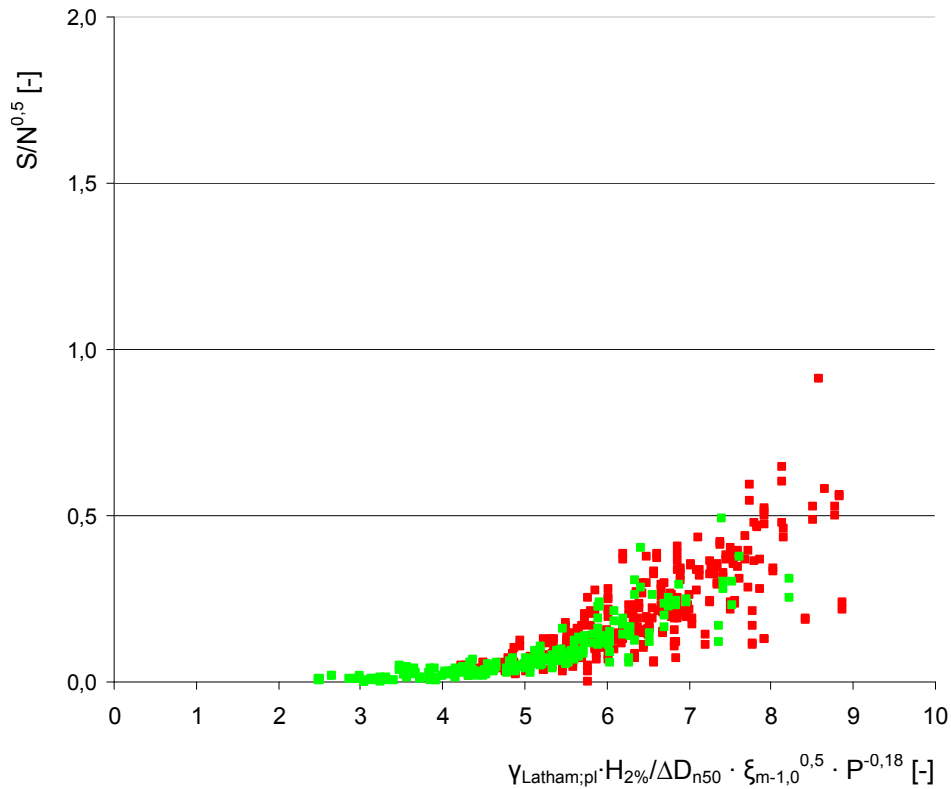
Figure 5.4: Plunging waves: THOMPSON & SHUTTLER [1975] (green), VAN DER MEER [1988] (red)

In the graphs for plunging waves the datasets still don't really correspond to each other. The dataset of VAN GENT ET AL. [2003] still tends to show more damage than the datasets of VAN DER MEER [1988] and THOMPSON & SHUTTLER [1975]. The datasets of VAN DER MEER [1988] and THOMPSON & SHUTTLER [1975] however show a similar trend.

5.2 Surging waves

Subsequently in Figure 5.5 to Figure 5.8 the graphs of VAN DER MEER [1988] (red), THOMPSON & SHUTTLER [1975] (green) and VAN GENT ET AL. [2003] (blue) have been plotted together. Also in these graphs a certain distinction between the data of VAN GENT ET AL. [2003] and the data of VAN DER MEER [1988] and THOMPSON & SHUTTLER [1975] can be seen.
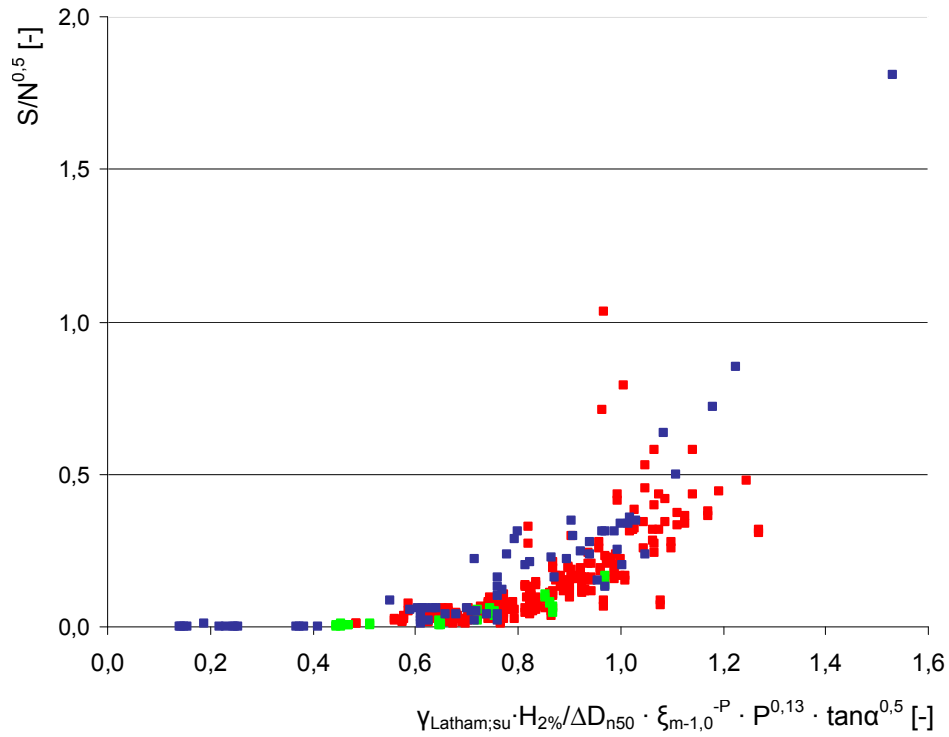
Figure 5.5: Surging waves: THOMPSON & SHUTTLER [1975] (green), VAN DER MEER [1988] (red), VAN GENT ET AL. [2003] (blue)
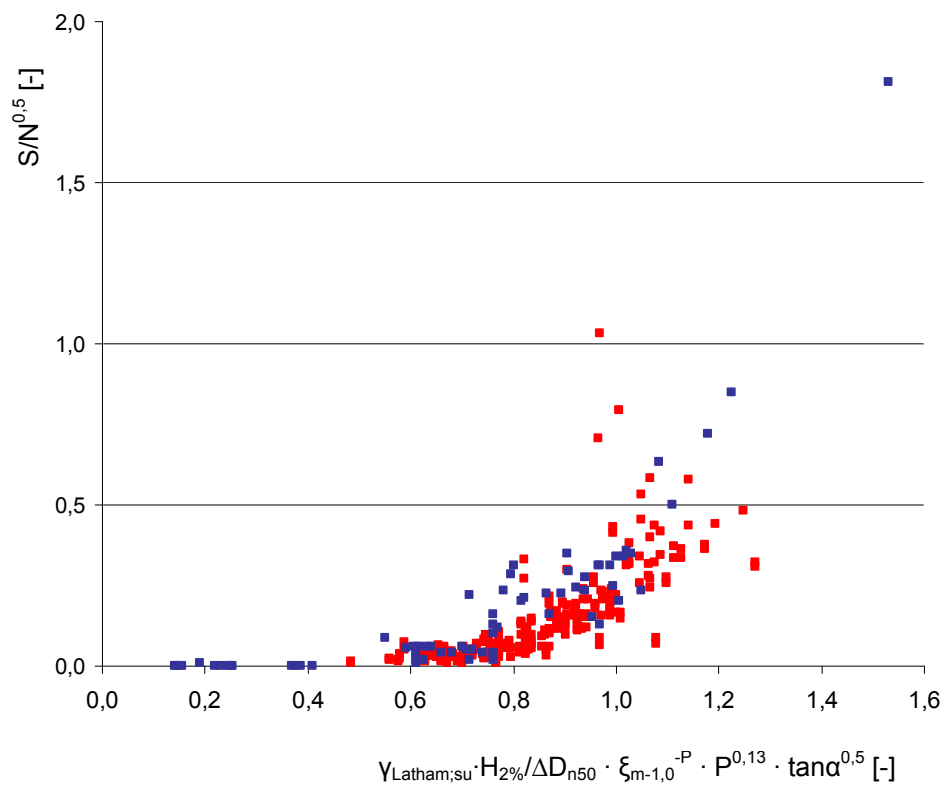
Figure 5.6: Surging waves: VAN DER MEER [1988] (red), VAN GENT ET AL. [2003] (blue)
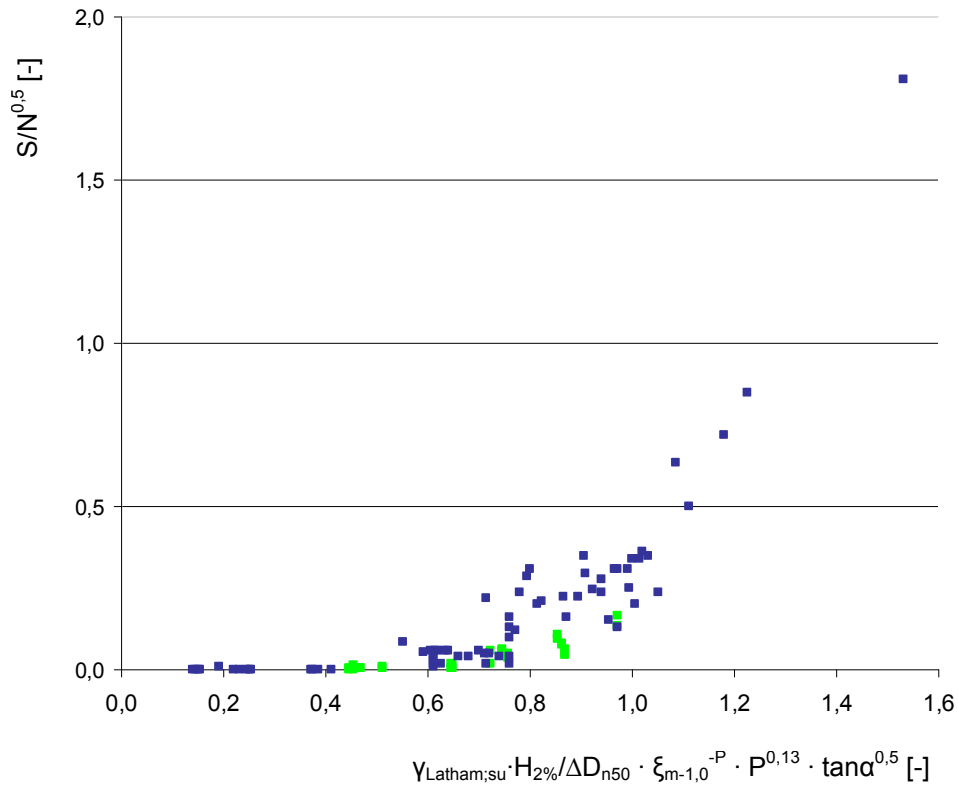
Figure 5.7: Surging waves: THOMPSON & SHUTTLER [1975] (green), VAN GENT ET AL. [2003] (blue)
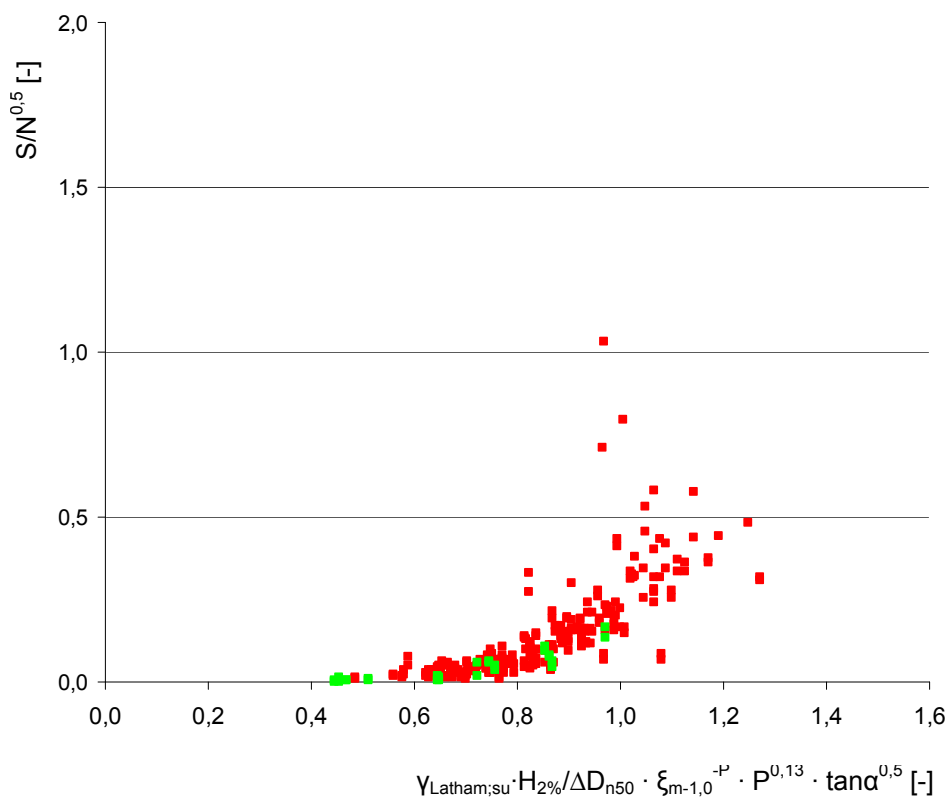
Figure 5.8: Surging waves: THOMPSON & SHUTTLER [1975] (green), VAN DER MEER [1988] (red)

5.3 Maximum accepted damage levels

In the dataset of VAN DER MEER [1988] damage levels vary between S=0 and S=33, in the dataset of THOMPSON & SHUTTLER [1975] damage levels vary between S=0 and S=17 and in the dataset of VAN GENT ET AL. [2003] damage levels vary between S=0 and S=62, although 95% of the tests resulted in damage levels smaller than S=30.

In Table 5.1 the values of S are presented for different slope angles. This table is applicable on the datasets of VAN DER MEER [1988] and THOMPSON & SHUTTLER [1975].

Slope	Initial damage	Intermediate damage	Failure
1:1,5	2	3 – 5	8
1:2	2	4 – 6	8
1:3	2	6 – 9	12
1:4	3	8 – 12	17
1:6	3	8 – 12	17

Table 5.1: Damage levels THOMPSON & SHUTTLER [1975] and VAN DER MEER [1988]

In Table 5.1 it can be seen that damage levels above the values represented in the right column always mean that the structure has failed and needs to be repaired. This means that damage levels above these values are not realistic to be used by a designer and therefore for design practice useless to be plotted in the graphs. In general designers would even use lower maximal acceptable damage levels to increase safety of the structure.

For the datasets of VAN DER MEER [1988] and THOMPSON & SHUTTLER [1975] maximum acceptable damage levels according to Table 5.1 can easy be applied in the graphs, by deleting all points that increase the maximum value.

For the dataset of VAN GENT ET AL. [2003] damage levels can be applied according to Table 5.2. For this dataset the slope angles have been read from the original graphs. In he dataset of VAN GENT ET AL. [2003] in most tests the profile is measured after N=1000 waves. However for some tests the profile has been measured after N=3000 waves. Because it is not known which data point belongs to the tests with N=3000 waves it is assumed that for all tests

N=1000. This is a safe assumption for the upper boundary, because the value of $S/N^{0,5}$ will only decrease when N=3000 would be applied.

Slope	Initial damage	Failure
1:2	2	8
1:4	2	17

Table 5.2: Damage levels VAN GENT ET AL. [2003]

Finally in Figure 5.9 and Figure 5.10 the graphs are plotted with the use of maximum damage levels. To be able to make a good comparison in these graphs on both axes the same scales are used as in the graphs in Figure 5.1 to Figure 5.8. In paragraph 5.4 and 5.5 the graphs are plotted on a more detailed scale.
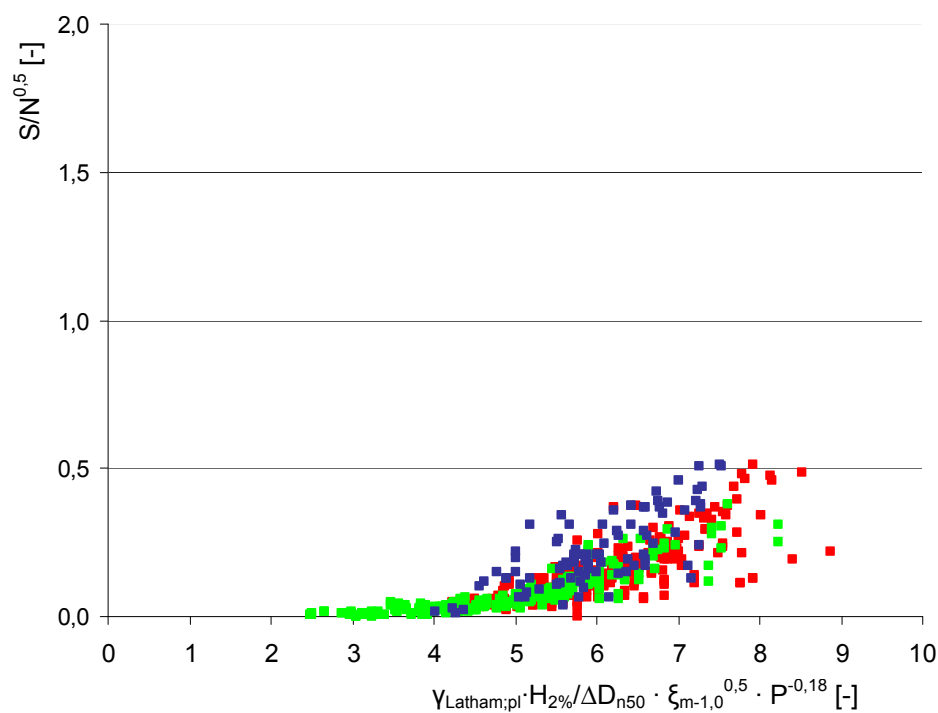
Figure 5.9: Plunging waves: THOMPSON & SHUTTLER [1975] (green), VAN DER MEER [1988] (red), VAN GENT ET AL. [2003] (blue) with maximal acceptable damage levels
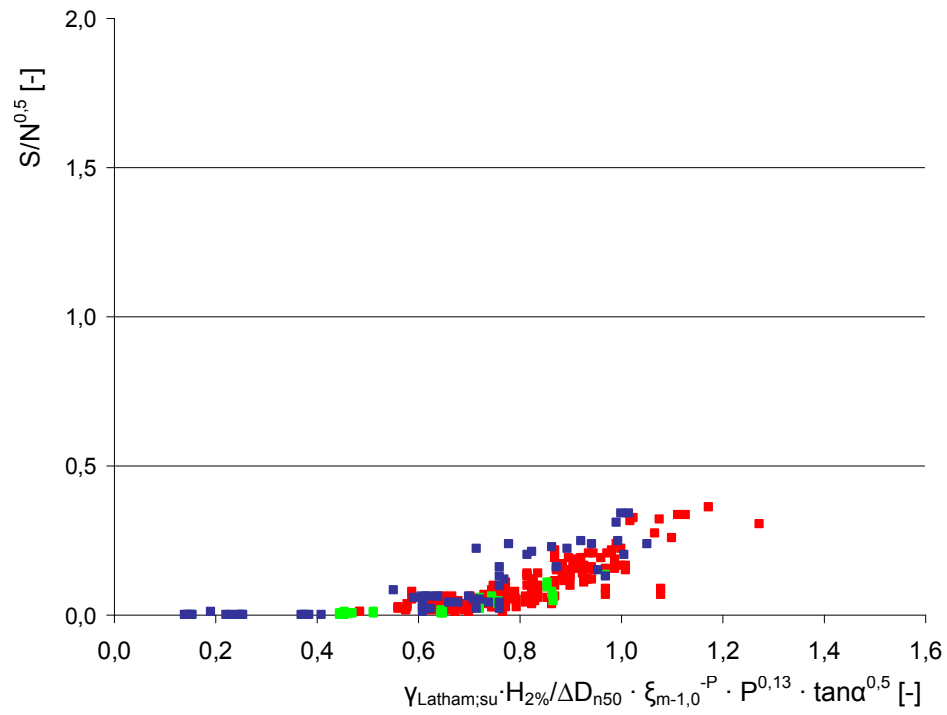
Figure 5.10: Surging waves: THOMPSON **& S**HUTTLER **[1975] (green), V**AN DER **M**EER **[1988] (red), V**AN **G**ENT **E**T **A**L**. [2003] (blue) with maximal acceptable damage levels**

5.4   Detailed graphs for plunging waves

In Figure 5.11 and FigureA.6 (Appendix E) again the graphs of VAN DER MEER [1988], THOMPSON & SHUTTLER [1975] and VAN GENT ET AL. [2003] are plotted together.
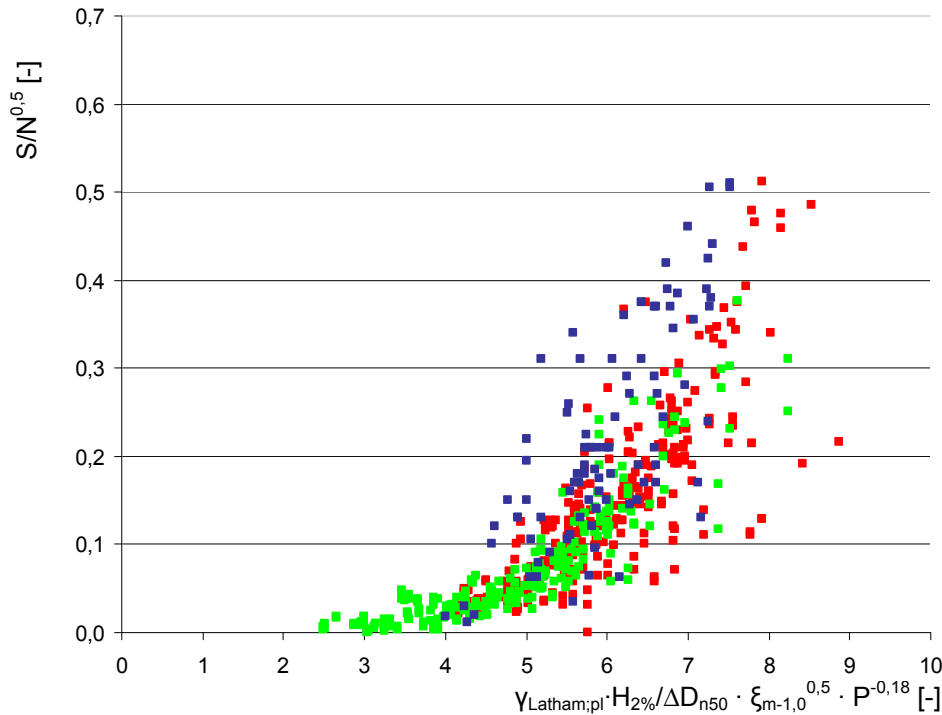
Figure 5.11: Plunging waves: THOMPSON & SHUTTLER [1975] (green), VAN DER MEER [1988] (red), VAN GENT ET AL. [2003] (blue) with maximal acceptable damage levels
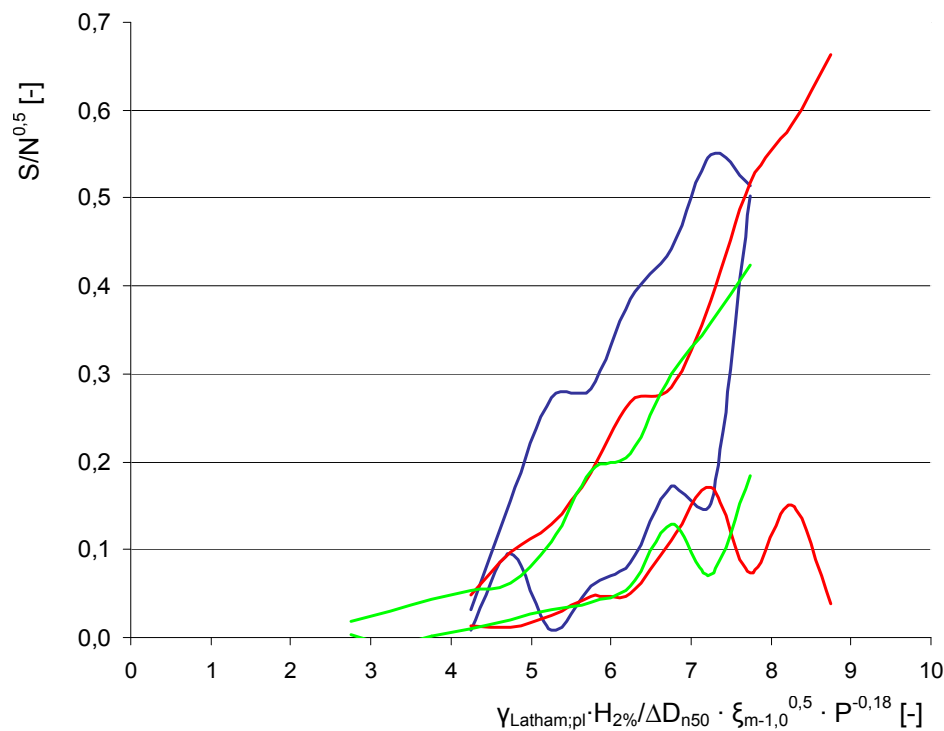
Figure 5.12: Plunging waves: 5% and 95% Exceedance lines, THOMPSON & SHUTTLER [1975] (green), VAN DER MEER [1988] (red), VAN GENT ET AL. [2003] (blue)

In Figure 5.12 the 5%- and 95%-exceedance lines of the datasets of VAN DER MEER [1988], THOMPSON & SHUTTLER [1975] and VAN GENT ET AL. [2003] have been plot for plunging waves. Figure 5.11 and Figure 5.12 again show the differences between the dataset of VAN GENT ET AL. [2003] and the datasets of VAN DER MEER [1988] and THOMPSON & SHUTTLER [1975]. The 5%-exceedance line of the dataset of VAN GENT ET AL. [2003] is on the whole range of the graph higher than those of VAN DER MEER [1988] and THOMPSON & SHUTTLER [1975].

5.5 Detailed graphs for surging waves

Also for surging waves in Figure 5.13 and FigureA.7 (Appendix E) the graphs have been plotted on a detailed scale and in Figure 5.14 the 5%- and 95%-exceedance lines have been plotted.
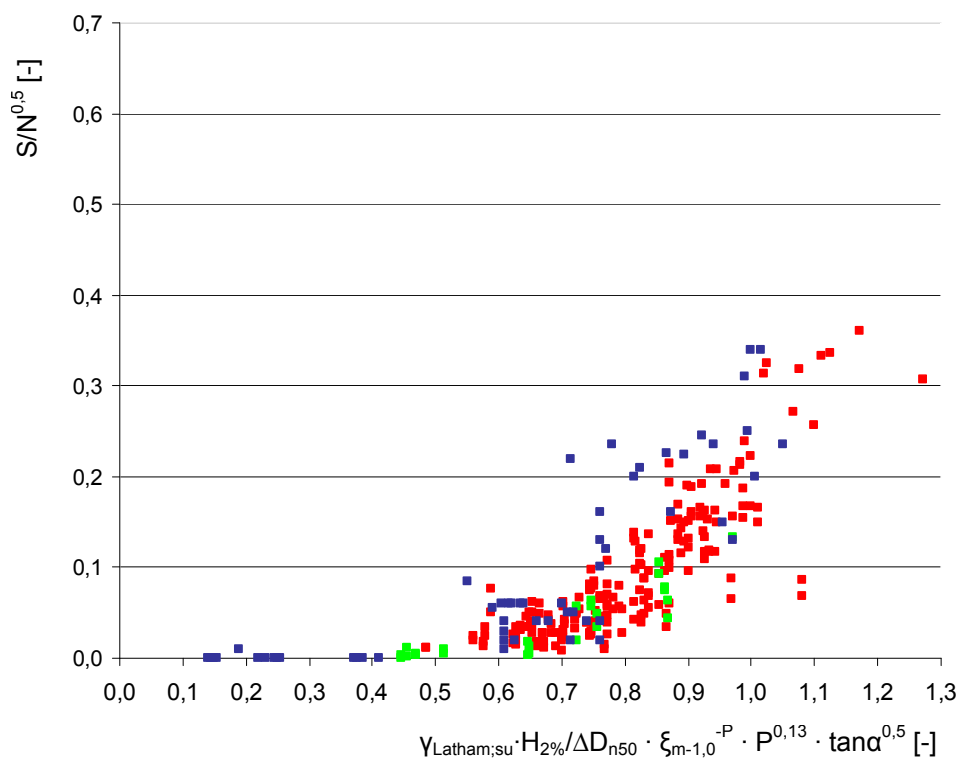
Figure 5.13: Surging waves: THOMPSON & SHUTTLER [1975] (green), VAN DER MEER [1988] (red), VAN GENT ET AL. [2003] (blue) with maximal acceptable damage levels
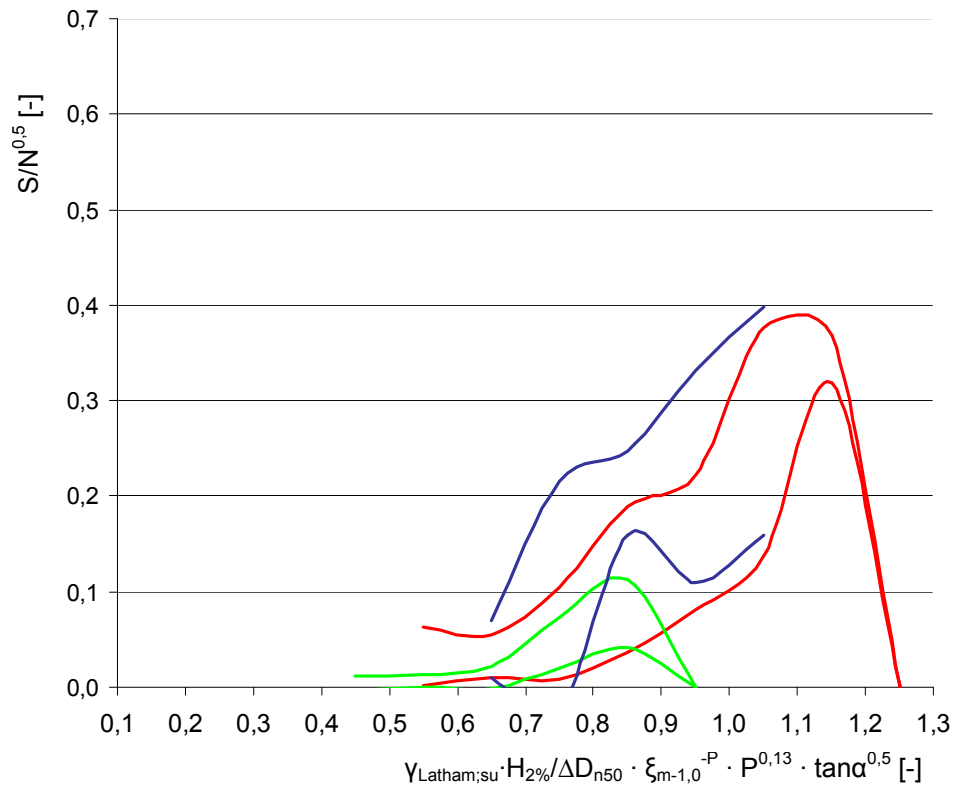
Figure 5.14: Surging waves: 5% and 95% Exceedance lines, THOMPSON & SHUTTLER [1975] (green), VAN DER MEER [1988] (red), VAN GENT ET AL. [2003] (blue)

In Figure 5.14 it can be seen that also for surging waves the 5% exceedance line of the dataset of VAN GENT ET AL. [2003] is higher than the 5% exceedance lines of VAN DER MEER [1988] and THOMPSON & SHUTTLER [1975].

Although differences can be seen on both graphs for plunging and surging waves it must be remarked that the correct use of the maximum damage levels in the dataset of VAN GENT ET AL. [2003] could imply a downward shift of the 5% exceedance line (upper blue line). In this a correct use of the maximum damage levels means the use of N=3000 in determining the maximum damage level $S/N^{0,5}$ for those tests in which the profile was measured after N=3000 waves.

Chapter 6

STATISTICS

6.1 Introduction

In the previous chapter it could be concluded that differences appear between the datasets of VAN GENT ET AL. [2003], VAN DER MEER [1988] and THOMPSON & SHUTTLER [1975]. In this chapter the datasets will be compared on a statistical way.

6.2 Basic statistics for plunging waves

Before a detailed statistic investigation can be done first basic statistical values have to be determined of the datasets. With a step size of 0,5 on the horizontal axis the mean, standard deviation, minimum, maximum, band width, 5%- and 95%-exceedance values and the number of tests per step were determined from the datasets of VAN GENT ET AL. [2003], VAN DER MEER [1988] and THOMPSON & SHUTTLER [1975]. These values are presented in Table 6.1. In Figure 6.1 and Figure 6.2 the mean and the standard deviation have been plotted.

$\gamma_{Latham;pl} \cdot H_{2\%}/\Delta D_{n50} \cdot \xi_{m-1,0}^{0,5} \cdot P^{-0,18}$	$S/N^{0,5}$							
Dataset *VAN DER MEER* [1988]								
	Mean	**Sd.**	**Min.**	**Max.**	**Band width**	**95%**	**5%**	**Nr.**
4,25	0,031	0,011	0,016	0,050	0,035	0,01	0,05	16
4,75	0,055	0,026	0,023	0,126	0,103	0,01	0,10	24
5,25	0,077	0,032	0,031	0,163	0,132	0,02	0,13	39
5,75	0,118	0,043	0,000	0,254	0,254	0,05	0,19	53
6,25	0,159	0,066	0,058	0,374	0,316	0,05	0,27	50
6,75	0,197	0,053	0,072	0,306	0,234	0,11	0,28	41
7,25	0,277	0,065	0,172	0,369	0,197	0,17	0,38	18
7,75	0,296	0,135	0,110	0,511	0,401	0,07	0,52	17
8,25	0,367	0,131	0,192	0,476	0,284	0,15	0,58	4
8,75	0,351	0,190	0,216	0,485	0,269	0,04	0,66	2

$\gamma_{Latham;pl} \cdot H_{2\%}/\Delta D_{n50} \cdot \xi_{m-1,0}^{0,5} \cdot P^{-0,18}$	$S/N^{0,5}$							
Dataset *VAN GENT ET AL.* [2003]								
	Mean	**Sd.**	**Min.**	**Max.**	**Band width**	**95%**	**5%**	**Nr.**
4,25	0,020	0,007	0,012	0,029	0,017	0,01	0,03	4
4,75	0,126	0,018	0,100	0,150	0,050	0,10	0,16	5
5,25	0,141	0,080	0,062	0,310	0,248	0,01	0,27	10
5,75	0,171	0,068	0,035	0,340	0,305	0,06	0,28	28
6,25	0,235	0,091	0,062	0,375	0,313	0,09	0,39	17
6,75	0,308	0,082	0,170	0,420	0,250	0,17	0,44	14
7,25	0,351	0,121	0,130	0,505	0,375	0,15	0,55	11
7,75	0,508	0,004	0,505	0,510	0,005	0,50	0,51	2

$\gamma_{Latham;pl} \cdot H_{2\%}/\Delta D_{n50} \cdot \xi_{m-1,0}^{0,5} \cdot P^{-0,18}$	$S/N^{0,5}$							
Dataset *THOMPSON & SHUTTLER* [1975]								
	Mean	**Sd.**	**Min.**	**Max.**	**Band width**	**95%**	**5%**	**Nr.**
2,75	0,011	0,004	0,005	0,018	0,013	0,00	0,02	8
3,25	0,011	0,012	0,001	0,047	0,047	-0,01	0,03	20
3,75	0,023	0,012	0,003	0,043	0,040	0,00	0,04	28
4,25	0,032	0,013	0,013	0,065	0,052	0,01	0,05	28
4,75	0,041	0,012	0,019	0,071	0,052	0,02	0,06	30
5,25	0,070	0,023	0,026	0,158	0,132	0,03	0,11	40
5,75	0,115	0,045	0,052	0,241	0,189	0,04	0,19	29
6,25	0,134	0,046	0,058	0,263	0,205	0,06	0,21	22
6,75	0,215	0,052	0,121	0,294	0,173	0,13	0,30	11
7,25	0,216	0,087	0,117	0,299	0,182	0,07	0,36	4
7,75	0,304	0,073	0,232	0,377	0,145	0,18	0,42	3

Table 6.1: Basic statistical values for plunging waves
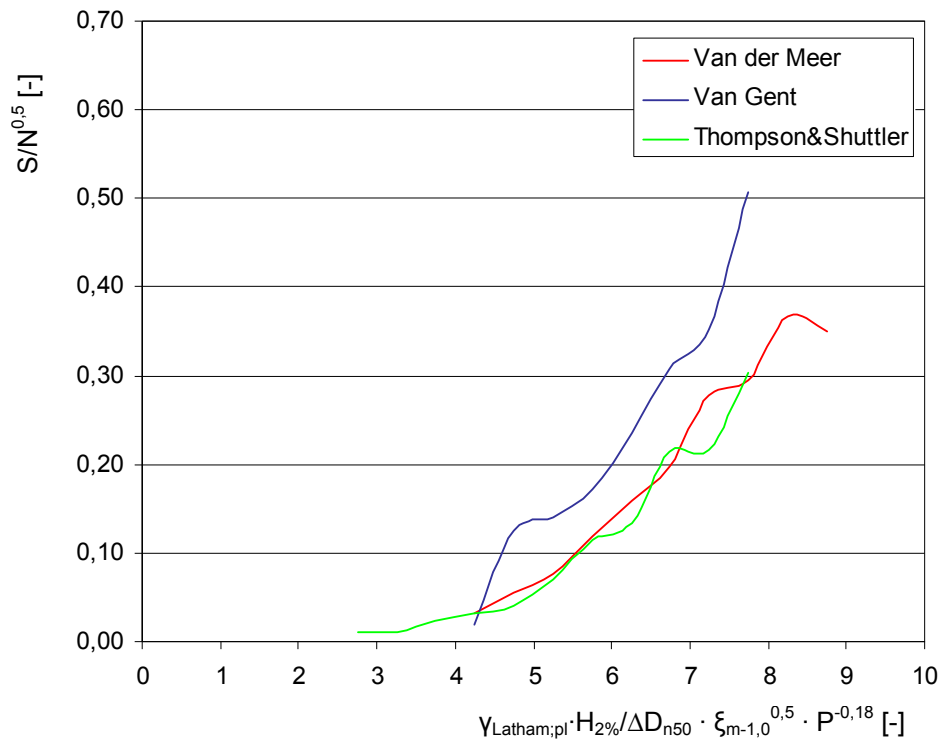
Figure 6.1: Mean values (step size 0,5) for plunging waves
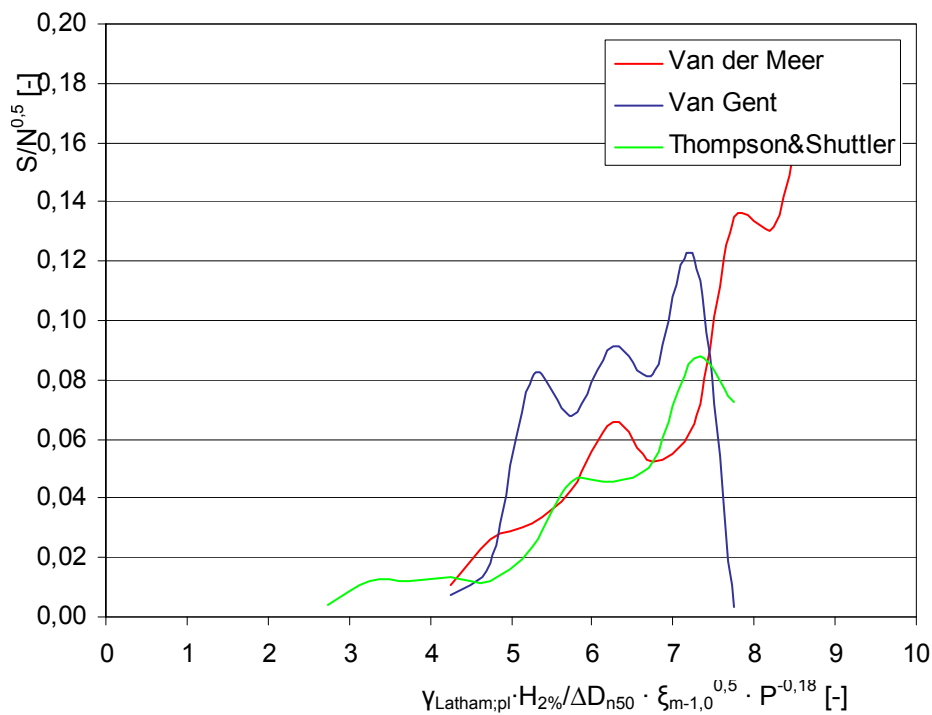
Figure 6.2: Standard deviation (step size 0,5) for plunging waves

In Figure 6.1 it can be seen that the mean values of $S/N^{0,5}$ of the dataset of VAN GENT ET AL. [2003] are higher than those of the datasets of VAN DER MEER [1988] and THOMPSON & SHUTTLER [1975]. In   Figure 6.2 it can be seen that on average the values of the standard deviation of the dataset of VAN GENT ET AL. [2003] are higher than those of the datasets of VAN DER MEER [1988] and THOMPSON & SHUTTLER [1975].

6.3   Basic statistics for surging waves

In the same way in Table 6.2. basic statistic values have been determined for the tests with surging waves. For surging waves on the horizontal axis the step size is 0,1.

Dataset VAN DER MEER [1988]								
	$S/N^{0,5}$							
$\gamma_{Lath} \cdot H_{2\%}/\Delta D_{n50} \cdot \xi_{m-1,0}^{-P} \cdot P^{0,13} \cdot \tan\alpha^{0,5}$	Mean	Sd.	Min.	Max.	Band width	95%	5%	Nr.
0,55	0,032	0,019	0,013	0,076	0,063	0,00	0,06	10
0,65	0,032	0,013	0,008	0,062	0,054	0,01	0,05	40
0,75	0,056	0,029	0,010	0,163	0,152	0,01	0,10	52
0,85	0,112	0,046	0,038	0,239	0,201	0,04	0,19	42
0,95	0,152	0,042	0,065	0,222	0,157	0,08	0,22	36
1,05	0,257	0,073	0,149	0,324	0,175	0,14	0,38	7
1,15	0,344	0,015	0,333	0,361	0,028	0,32	0,37	3
1,25	0,306		0,306	0,306	0,000			1

Dataset VAN GENT ET AL. [2003]								
	$S/N^{0,5}$							
$\gamma_{Lath} \cdot H_{2\%}/\Delta D_{n50} \cdot \xi_{m-1,0}^{-P} \cdot P^{0,13} \cdot \tan\alpha^{0,5}$	Mean	Sd.	Min.	Max.	Band width	95%	5%	Nr.
0,15	0,002	0,004	0,000	0,010	0,010	-0,01	0,01	5
0,25	0,000	0,000	0,000	0,000	0,000			5
0,35	0,000	0,000	0,000	0,000	0,000			3
0,45	0,000		0,000	0,000	0,000			1
0,55	0,055		0,055	0,055	0,000			1
0,65	0,040	0,018	0,010	0,060	0,050	0,01	0,07	11
0,75	0,096	0,073	0,020	0,235	0,215	-0,02	0,22	13
0,85	0,204	0,027	0,160	0,225	0,065	0,16	0,25	5
0,95	0,220	0,068	0,130	0,310	0,180	0,11	0,33	6
1,05	0,279	0,072	0,200	0,340	0,140	0,16	0,40	4
1,15	0,002	0,004	0,000	0,010	0,010	-0,01	0,01	5

Dataset THOMPSON & SHUTTLER [1975]								
	$S/N^{0,5}$							
$\gamma_{Lath} \cdot H_{2\%}/\Delta D_{n50} \cdot \xi_{m-1,0}^{-P} \cdot P^{0,13} \cdot \tan\alpha^{0,5}$	Mean	Sd.	Min.	Max.	Band width	95%	5%	Nr.
0,45	0,004	0,004	0,000	0,012	0,012	0,00	0,01	6
0,55	0,007	0,004	0,004	0,010	0,006	0,00	0,01	2
0,65	0,010	0,007	0,003	0,018	0,015	0,00	0,02	4
0,75	0,047	0,016	0,020	0,063	0,043	0,02	0,07	6
0,85	0,077	0,022	0,044	0,106	0,062	0,04	0,11	6
0,95	0,134		0,134	0,134	0,000			1

Table 6.2: Basic statistical values for surging waves

For surging waves the mean and the standard deviation have been plotted in Figure 6.3 and Figure 6.4.
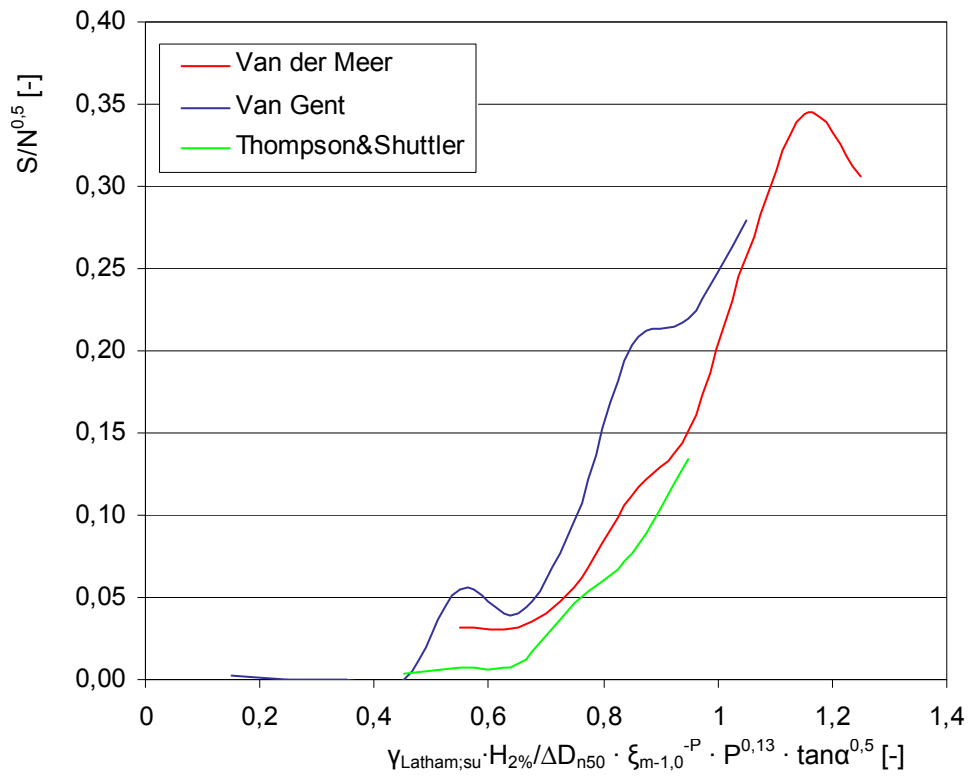
Figure 6.3: Mean values (step size 0,1) for surging waves
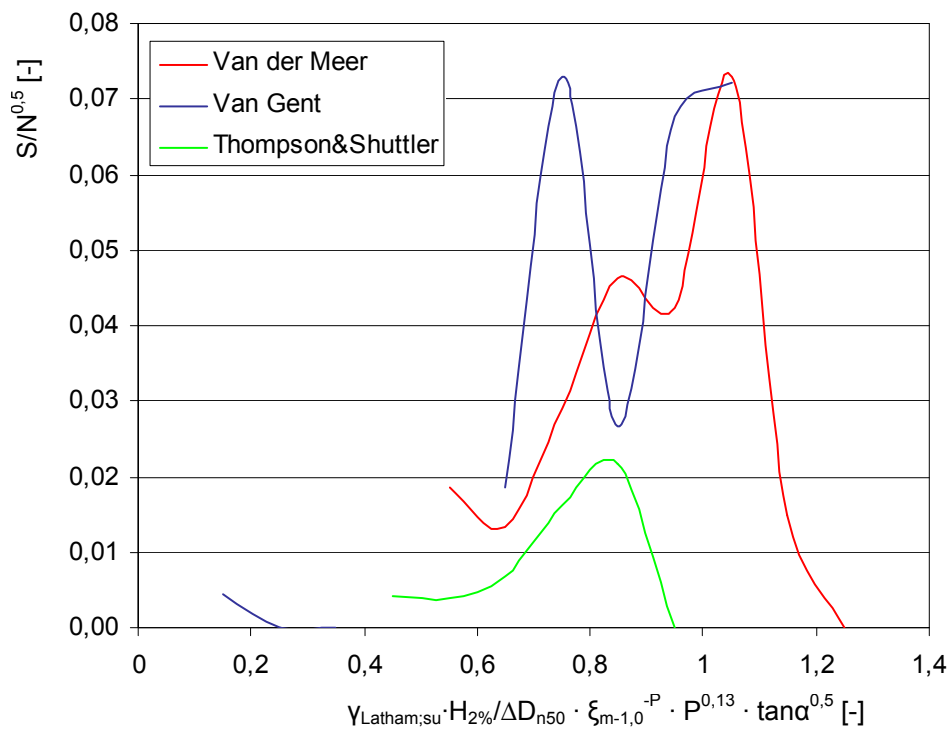
Figure 6.4: Standard deviation (step size 0,1) for surging waves

Figure 6.3 shows that also for surging waves the mean of the dataset of VAN GENT ET AL. [2003] is higher than the mean of VAN DER MEER [1988] and THOMPSON & SHUTTLER [1975]. In Figure 6.4 it can be seen that the standard deviation of the dataset of VAN GENT ET AL. [2003] increases to quite high values in the first part of the graph, where after it decreases to values comparable to those of the dataset of VAN DER MEER [1988].

6.4   The T-test

To test whether the datasets of VAN GENT ET AL. [2003], VAN DER MEER [1988] and THOMPSON & SHUTTLER R [1975] are statistically different the T-test will be used. The T-test is described in Appendix A4 . For the T-test a on the horizontal axis a step size of 0,5 is taken for plunging waves and a step size of 0,1 is taken for surging waves. For each step the datasets were compared. For all results a confidence level of 95% is applied.

6.4.1 *VAN GENT ET AL. [2003] – VAN DER MEER [1988]*

The first datasets to be statistically compared with the T-test are the datasets of VAN GENT ET AL. [2003] and VAN DER MEER [1988]. The results of the T-test for these datasets are given in Table 6.3 and Table 6.4.

$\gamma_{Latham;pl} \cdot H_{2\%}/\Delta D_{n50} \cdot \xi_{m-1,0}^{0,5} \cdot P^{-0,18}$	t_{obs}	dof	$t^*_{95\%}$	T-test
4,25	-2,64	18	1,33	Significant different
4,75	7,33	27	1,31	Significant different
5,25	2,45	47	1,30	Significant different
5,75	3,76	79	1,29	Significant different
6,25	3,19	65	1,30	Significant different
6,75	4,71	53	1,30	Significant different
7,25	1,88	27	1,31	Significant different
7,75	6,43	17	1,33	Significant different

Table 6.3: The T-test for VAN GENT ET AL. [2003] and VAN DER MEER [1988] for plunging waves

$\gamma_{Lath} \cdot H_{2\%}/\Delta D_{n50} \cdot \xi_{m-1,0}^{-P} \cdot P^{0,13} \cdot \tan\alpha^{0,5}$	t_{obs}	dof	$t^*_{95\%}$	T-test
0,65	1,36	49	1,30	Significant different
0,75	1,91	63	1,30	Significant different
0,85	6,59	45	1,30	Significant different
0,95	2,40	40	1,30	Significant different
1,05	0,48	9	1,38	

Table 6.4: The T-test for VAN GENT ET AL. [2003] and VAN DER MEER [1988] for surging waves

From Table 6.3 and Table 6.4 it can be concluded that the datasets of VAN DER MEER [1988] and VAN GENT ET AL. [2003] are statistically significant different both for plunging and surging waves.

6.4.2 *THOMPSON & SHUTTLER [1975] - VAN DER MEER [1988]*

Subsequently the results of the T-tests for the comparison of the datasets of VAN DER MEER [1988] and THOMPSON & SHUTTLER [1975] are shown in Table 6.5 and Table 6.6.

$\gamma_{Latham;pl} \cdot H_{2\%}/\Delta D_{n50} \cdot \xi_{m-1,0}^{0,5} \cdot P^{-0,18}$	t_{obs}	dof	$t^*_{95\%}$	T-test
4,25	-0,13	42	1,30	
4,75	2,37	52	1,30	Significant different
5,25	1,07	77	1,29	
5,75	0,25	80	1,29	
6,25	1,81	70	1,29	Significant different
6,75	-0,96	50	1,30	
7,25	1,33	20	1,33	Significant different
7,75	-0,15	18	1,33	

Table 6.5: The T-test for THOMPSON & SHUTTLER [1975] and VAN DER MEER [1988]

$\gamma_{Lath} \cdot H_{2\%}/\Delta D_{n50} \cdot \xi_{m-1,0}^{-P} \cdot P^{0,13} \cdot \tan\alpha^{0,5}$	t_{obs}	dof	$t^*_{95\%}$	T-test
0,55	3,85	10	1,37	Significant different
0,65	5,56	42	1,30	Significant different
0,75	1,24	56	1,30	
0,85	3,15	46	1,30	Significant different

Table 6.6: The T-test for THOMPSON & SHUTTLER [1975] and VAN DER MEER [1988] for surging waves

From Table 6.5 and Table 6.6 it can be concluded that for plunging waves the datasets of VAN DER MEER [1988] and THOMPSON & SHUTTLER [1975] not significantly different on most points. For surging waves however the datasets are significantly different on 3 out of 4 points.

6.4.3 *THOMPSON & SHUTTLER [1975] - VAN GENT ET AL. [2003]*

The results of the T-tests for the comparison of the datasets of THOMPSON & SHUTTLER [1975] and VAN GENT ET AL. [2003] are shown in Table 6.7 and Table 6.8.

$\gamma_{Latham;pl} \cdot H_{2\%}/\Delta D_{n50} \cdot \xi_{m-1,0}^{0,5} \cdot P^{-0,18}$	t_{obs}	dof	$t^*_{95\%}$	T-test
4,25	-2,79	30	1,31	Significant different
4,75	10,08	33	1,31	Significant different
5,25	2,74	48	1,30	Significant different
5,75	3,62	55	1,30	Significant different
6,25	4,18	37	1,31	Significant different
6,75	3,45	23	1,32	Significant different
7,25	2,39	13	1,35	Significant different
7,75	4,85	3	1,64	Significant different

Table 6.7: The T-test for THOMPSON & SHUTTLER [1975] and VAN GENT ET AL. [2003]

$\gamma_{Lath} \cdot H_{2\%}/\Delta D_{n50} \cdot \xi_{m-1,0}^{-P} \cdot P^{0,13} \cdot \tan\alpha^{0,5}$	t_{obs}	dof	$t^*_{95\%}$	T-test
0,65	-4,66	13	1,4	Significant different
0,75	-2,31	17	1,3	Significant different
0,85	-8,59	9	1,4	Significant different

Table 6.8: The T-test for THOMPSON & SHUTTLER [1975] and VAN GENT ET AL. [2003] for surging waves

In Table 6.7 and Table 6.8 it can be seen that for plunging and surging waves the datasets of THOMPSON & SHUTTLER [1975] and VAN GENT ET AL. [2003] are on all points significantly different.

Chapter 7

DESIGN PRACTICE

7.1   Introduction

In design practise usually the maximum damage level is used as an input parameter. The maximum accepted damage level depends on how much damage the designer of the breakwater allows on the breakwater. The choice of a damage level strongly depends on the chosen safety level and available finances. Other input parameters are the wave height, permeability, slope angle, wave period (in ξ) and the number of waves. This means that the only real output parameter is the stone diameter.

For some reason the graphs which have been described before are always presented with the diameter on the horizontal axis and the damage level in the vertical axis. When designing a breakwater in general the designer has a given maximum damage level and is interested in a corresponding stone diameter. Therefore is would be easier to draw the graphs on the other way around. This is done in Figure 7.1 for plunging waves and in Figure 7.2 for surging waves.
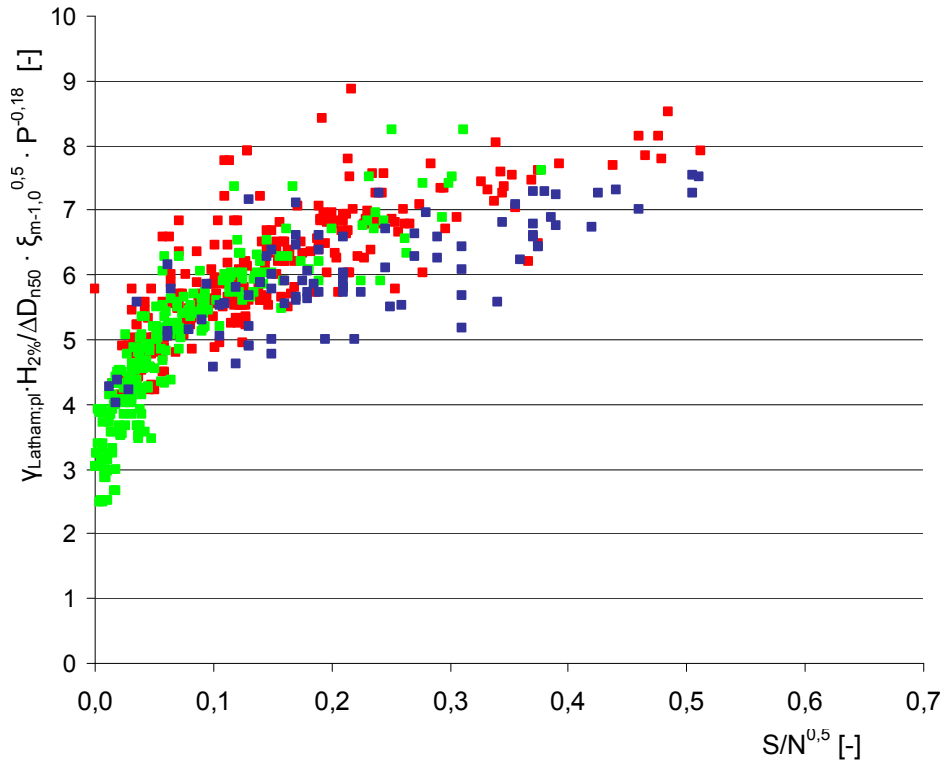
Figure 7.1: Plunging waves with switched axes, VAN DER MEER [1988] (red), THOMPSON & SHUTTLER [1975] (green), VAN GENT ET AL. [2003] (blue)
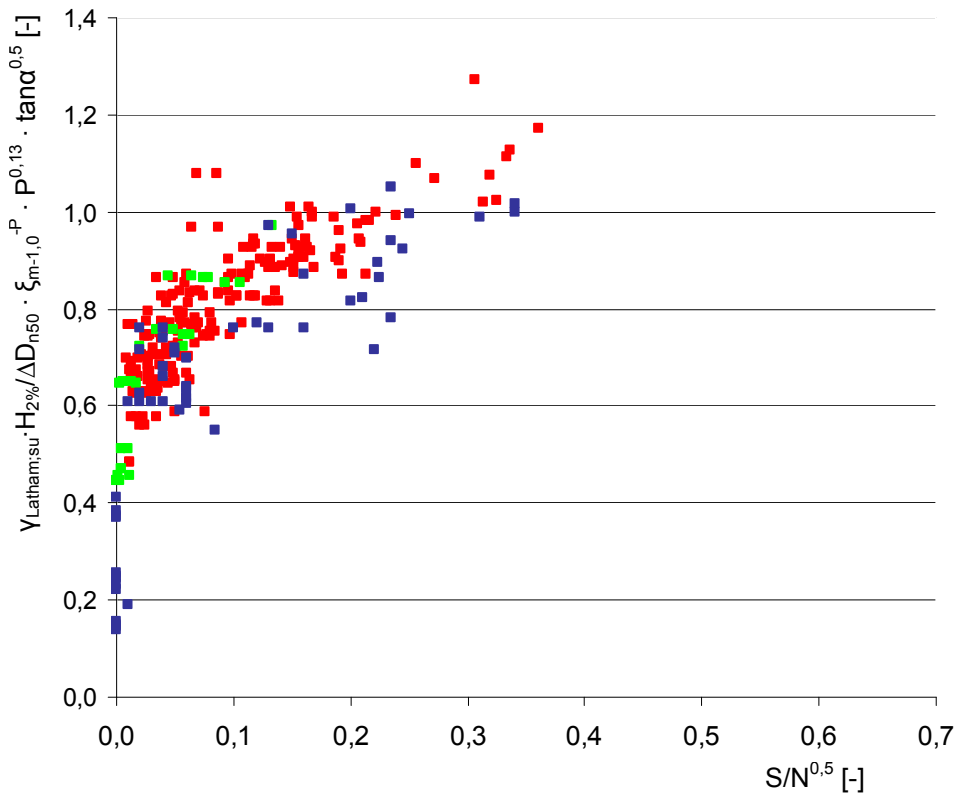
Figure 7.2: Surging waves with switched axes, VAN DER MEER [1988] (red), THOMPSON & SHUTTLER [1975] (green), VAN GENT ET AL. [2003] (blue)

When the graphs are presented this way a designer has to choose a damage level and then find a corresponding stone diameter on the vertical axis. Depending on the requested safety the designer can move in upward direction along the vertical axis. A design in the lower area would be a very conservative design, a design on the upper regions is a rather unsafe design. In Figure 7.3 and Figure 7.4 in the same way the 5%- and 95% exceedance lines have been plot with switched axes.
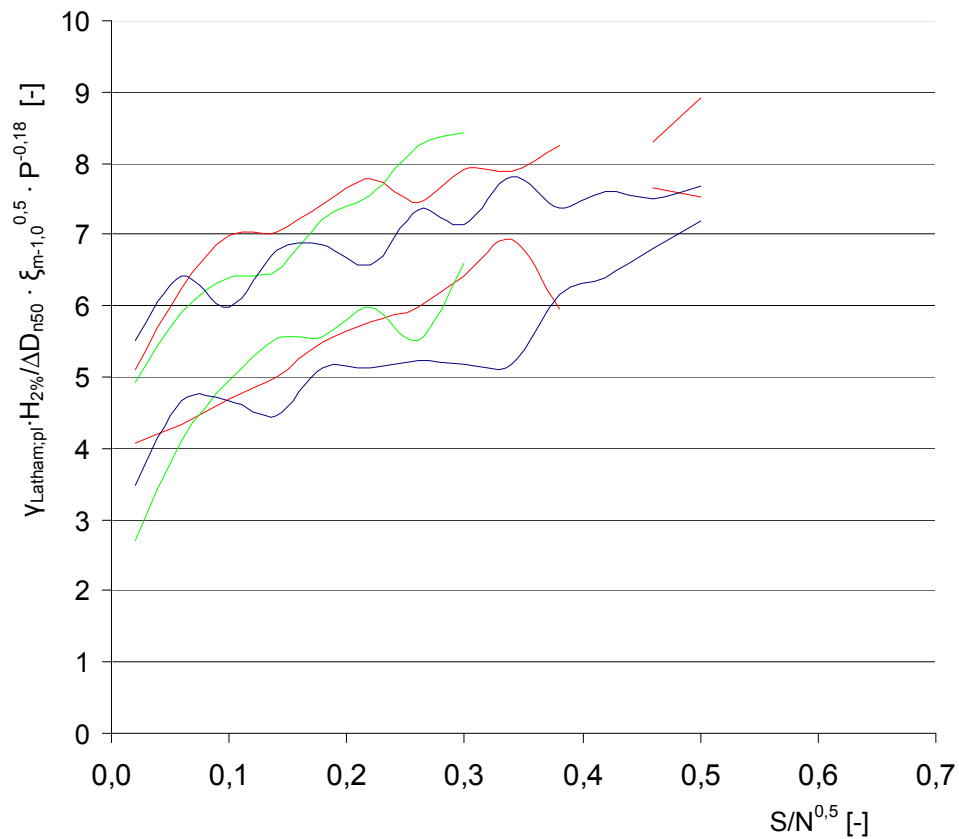
Figure 7.3: 5% and 95% exceedance lines for plunging waves with switched axes, VAN DER MEER [1988] (red), THOMPSON & SHUTTLER [1975] (green), VAN GENT ET AL. [2003] (blue)
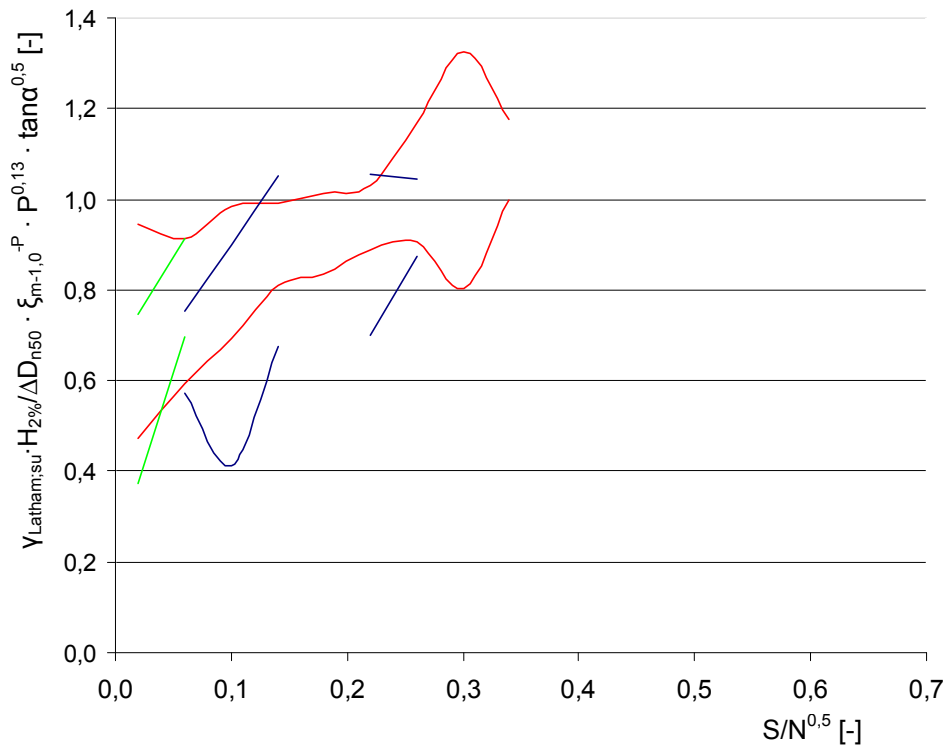
Figure 7.4: 5% and 95% exceedance lines for surging waves with switched axes, VAN DER MEER [1988] (red), THOMPSON & SHUTTLER [1975] (green), VAN GENT ET AL. [2003] (blue)

7.2 Basic statistics for plunging waves

To see whether there are any statistic differences in the graphs with switched axis similar statistic data is acquired as in Chapter 6 will be done with these graphs. For plunging and surging waves on the horizontal axis for the damage parameter a step size = 0,04 is used. The statistical data for plunging and surging waves are presented in Table 7.1. Further in Figure 7.5 and Figure 7.6 the mean values and standard deviations of the values of $\gamma_{Lath} \cdot H_{2\%} / \Delta D_{n50} \cdot \xi_{m-1,0}^{-P} \cdot P^{0,13} \cdot \tan\alpha^{0,5}$ have been plotted as a function of the damage level $S/N^{0,5}$. These figures confirm the findings discussed before that the dataset of VAN GENT ET AL. [2003] shows on average more damage than the datasets of VAN DER MEER [1988] and THOMPSON & SHUTTLER [1975].

Dataset VAN DER MEER [1988]								
$\gamma_{Latham;pl} \cdot H_{2\%} / \Delta D_{n50} \cdot \xi_{m-1,0}^{0,5} \cdot P^{-0,18}$								
$S/N^{0,5}$	Mean	Sd.	Min.	Max.	Band width	95%	5%	Nr.
0,02	4,59	0,32	4,16	5,23	1,07	4,06	5,11	22
0,06	5,28	0,58	4,23	6,84	2,61	4,33	6,23	45
0,1	5,84	0,69	4,86	7,77	2,91	4,70	6,98	36
0,14	6,02	0,62	4,94	7,92	2,98	5,00	7,04	48
0,18	6,45	0,59	5,50	8,41	2,92	5,48	7,43	23
0,22	6,78	0,61	5,73	8,87	3,14	5,77	7,79	31
0,26	6,71	0,44	5,77	7,26	1,49	5,99	7,44	11
0,3	7,17	0,46	6,71	7,72	1,02	6,41	7,92	4
0,34	7,41	0,29	7,03	8,03	0,99	6,93	7,89	9
0,38	7,10	0,70	6,21	7,72	1,52	5,95	8,25	5
0,42	7,69		7,69	7,69	0,00			1
0,46	7,98	0,20	7,79	8,15	0,36	7,66	8,30	4
0,5	8,22	0,42	7,92	8,52	0,60	7,53	8,92	2

Dataset VAN GENT ET AL. [2003]								
$\gamma_{Latham;pl} \cdot H_{2\%} / \Delta D_{n50} \cdot \xi_{m-1,0}^{0,5} \cdot P^{-0,18}$								
$S/N^{0,5}$	Mean	Sd.	Min.	Max.	Band width	95%	5%	Nr.
0,02	3,81	0,67	2,49	5,34	2,85	2,71	4,92	95
0,06	4,99	0,55	3,47	6,27	2,80	4,09	5,90	58
0,1	5,67	0,44	5,12	7,37	2,25	4,94	6,40	27
0,14	6,02	0,29	5,47	6,53	1,06	5,54	6,49	22
0,18	6,39	0,50	5,90	7,37	1,47	5,57	7,21	7
0,22	6,77	0,48	5,90	7,52	1,63	5,98	7,56	7
0,26	6,88	0,83	5,91	8,23	2,33	5,51	8,25	6
0,3	7,51	0,56	6,88	8,23	1,35	6,60	8,43	4

Dataset THOMPSON & SHUTTLER [1975]								
$\gamma_{Latham;pl} \cdot H_{2\%} / \Delta D_{n50} \cdot \xi_{m-1,0}^{0,5} \cdot P^{-0,18}$								
$S/N^{0,5}$	Mean	Sd.	Min.	Max.	Band width	95%	5%	Nr.
0,02	4,50	0,63	4,01	5,59	1,58	3,47	5,53	5
0,06	5,53	0,53	5,05	6,16	1,11	4,65	6,41	4
0,1	5,32	0,39	4,57	5,85	1,28	4,67	5,97	8
0,14	5,61	0,71	4,62	7,16	2,54	4,45	6,78	15
0,18	5,98	0,53	5,00	7,12	2,12	5,12	6,85	16
0,22	5,85	0,44	5,00	6,58	1,58	5,13	6,56	8
0,26	6,29	0,64	5,51	7,26	1,75	5,24	7,34	7
0,3	6,16	0,60	5,18	6,97	1,79	5,19	7,14	7
0,34	6,49	0,80	5,58	7,08	1,50	5,17	7,81	3
0,38	6,77	0,37	6,22	7,29	1,07	6,16	7,38	11
0,42	6,99	0,37	6,73	7,25	0,52	6,39	7,59	2
0,46	7,15	0,21	7,00	7,30	0,30	6,80	7,50	2
0,5	7,44	0,15	7,27	7,53	0,26	7,20	7,68	3

Table 7.1: Basic statistical values for plunging waves with switched axes
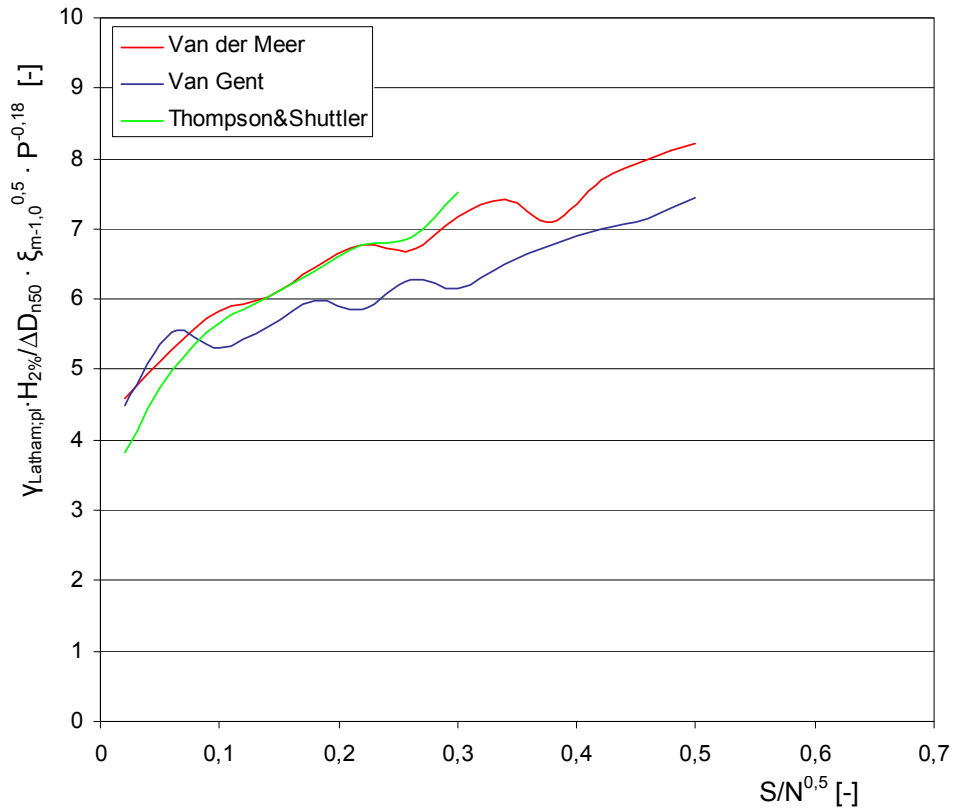
Figure 7.5: Mean values (step size = 0,04) for plunging waves with switched axes
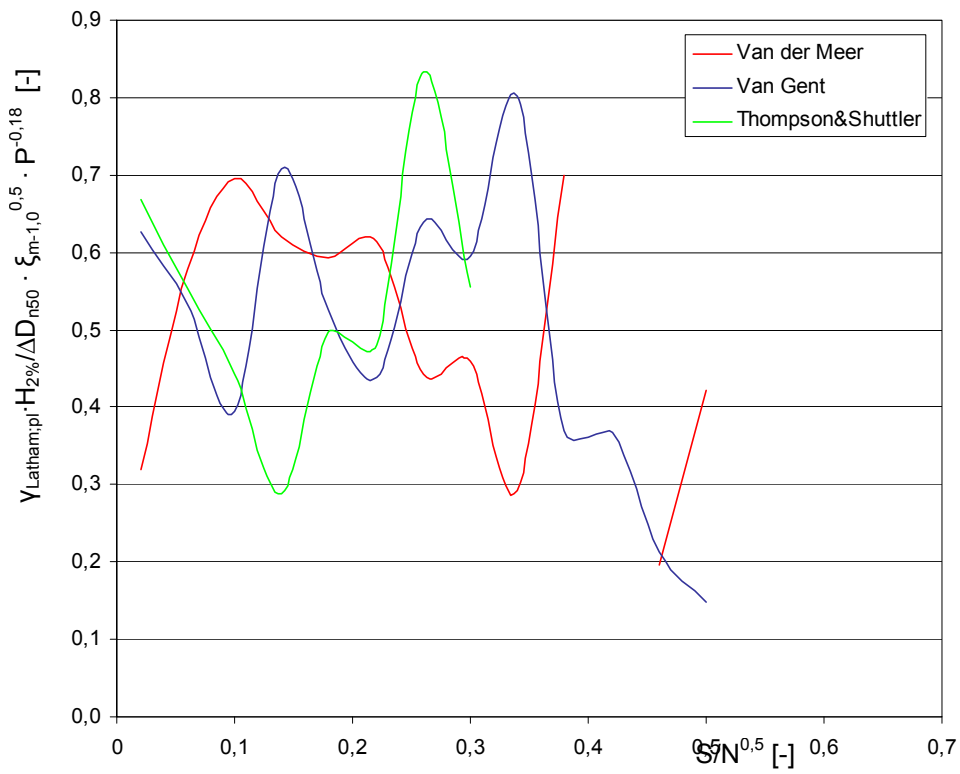
Figure 7.6: Standard deviation (step size = 0,04) for plunging waves with switched axes

7.3 Basic statistics for surging waves

In the same the datasets for surging waves have been treated in Table 7.2, Figure 7.7 and Figure 7.8.

Dataset VAN DER MEER [1988]								
$\gamma_{Lath} \cdot H_{2\%}/\Delta D_{n50} \cdot \xi_{m-1,0}^{-P} \cdot P^{0,13} \cdot \tan\alpha^{0,5}$								
$S/N^{0,5}$	Mean	Sd.	Min.	Max.	Band width	95%	5%	Nr.
0,02	0,71	0,14	0,48	1,25	0,76	0,47	0,95	71
0,06	0,75	0,10	0,44	1,08	0,64	0,59	0,91	54
0,10	0,84	0,09	0,59	1,08	0,48	0,69	0,98	35
0,14	0,90	0,05	0,78	1,01	0,23	0,81	0,99	26
0,18	0,92	0,05	0,81	1,01	0,20	0,84	1,01	18
0,22	0,96	0,04	0,87	1,00	0,13	0,89	1,03	8
0,26	1,04	0,08	0,95	1,10	0,15	0,91	1,17	3
0,30	1,06	0,16	0,89	1,27	0,38	0,80	1,33	4
0,34	1,09	0,06	1,02	1,13	0,10	1,00	1,18	3
0,38	1,17		1,17	1,17	0,00			1
Dataset VAN GENT ET AL. [2003]								
$\gamma_{Lath} \cdot H_{2\%}/\Delta D_{n50} \cdot \xi_{m-1,0}^{-P} \cdot P^{0,13} \cdot \tan\alpha^{0,5}$								
$S/N^{0,5}$	Mean	Sd.	Min.	Max.	Band width	95%	5%	Nr.
0,06	0,66	0,06	0,59	0,76	0,17	0,57	0,75	14
0,10	0,66	0,15	0,55	0,76	0,21	0,41	0,90	2
0,14	0,86	0,11	0,76	0,97	0,21	0,68	1,05	4
0,18	0,87		0,87	0,87	0,00			1
0,22	0,88	0,11	0,72	1,05	0,34	0,70	1,05	9
0,26	0,96	0,05	0,92	1,00	0,07	0,87	1,04	2
0,30	0,99		0,99	0,99	0,00			1
0,34	1,01	0,01	1,00	1,02	0,01	0,99	1,02	2
Dataset THOMPSON & SHUTTLER [1975]								
$\gamma_{Lath} \cdot H_{2\%}/\Delta D_{n50} \cdot \xi_{m-1,0}^{-P} \cdot P^{0,13} \cdot \tan\alpha^{0,5}$								
$S/N^{0,5}$	Mean	Sd.	Min.	Max.	Band width	95%	5%	Nr.
0,02	0,56	0,11	0,45	0,76	0,31	0,37	0,74	14
0,06	0,80	0,07	0,72	0,87	0,15	0,70	0,91	8

Table 7.2: Basic statistical values for surging waves
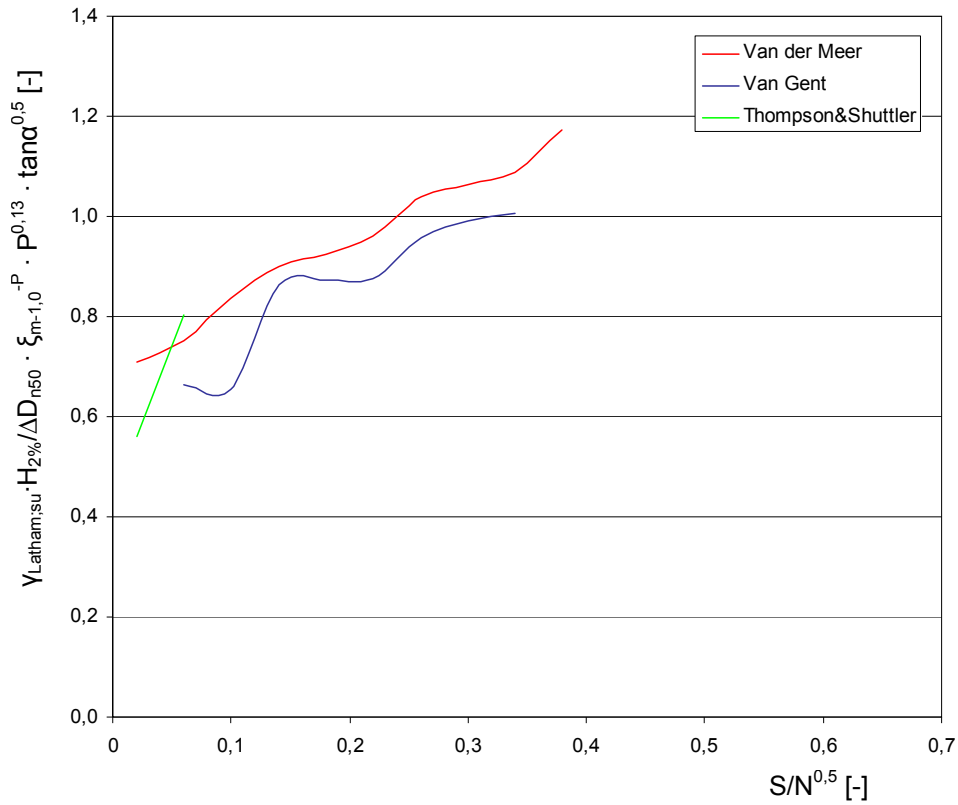
Figure 7.7: Mean values (step size = 0,04) for surging waves with switched axes
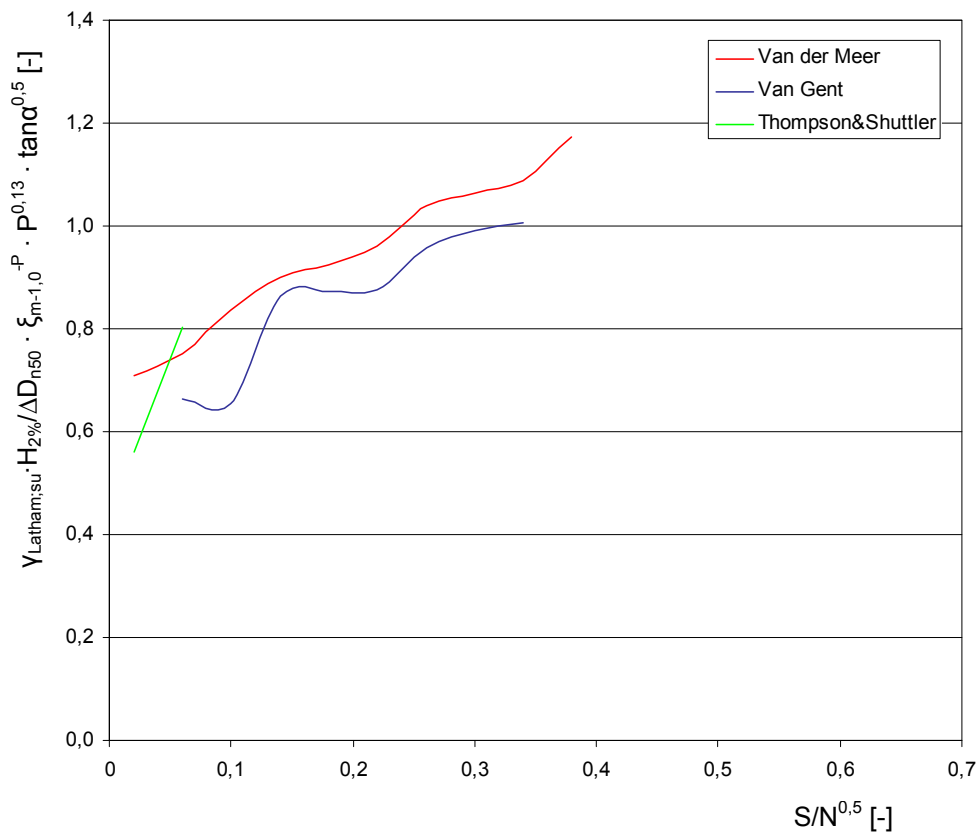
Figure 7.8: Standard deviation (step size = 0,04) for surging waves with switched axes

7.4 The T-test

The datasets of VAN GENT ET AL. [2003], VAN DER MEER [1988] and THOMPSON & SHUTTLER [1975] with switched axes will again be compared using the T-test. The T-test is described in Appendix A4 . For the T-test the step size = 0,04 is taken for plunging and surging waves. For each step the datasets were compared. For all results a confidence level of 95% is applied.

7.4.1 *VAN GENT ET AL. [2003] – VAN DER MEER [1988]*

The results of the T-test for the datasets of VAN GENT ET AL. [2003] and VAN DER MEER [1988] are presented in Table 7.3 and Table 7.4.

$S/N^{0,5}$	t_{obs}	dof	$t^*_{95\%}$	T-test
0,02	-0,32	25	1,32	
0,06	0,88	47	1,30	
0,1	-2,87	42	1,30	Significant different
0,14	-2,01	61	1,30	Significant different
0,18	-2,60	37	1,31	Significant different
0,22	-4,91	37	1,31	Significant different
0,26	-1,54	16	1,34	Significant different
0,3	-3,12	9	1,38	Significant different
0,34	-1,94	10	1,37	Significant different
0,38	-0,99	14	1,35	
0,42	-2,69	1	3,08	
0,46	-4,62	4	1,53	Significant different
0,5	-2,51	3	1,64	Significant different

Table 7.3: The T-test for VAN GENT ET AL. [2003] and VAN DER MEER [1988] for plunging waves

$S/N^{0,5}$	t_{obs}	dof	$t^*_{95\%}$	T-test
0,06	-4,51	66	1,30	Significant different
0,1	-1,72	35	1,31	Significant different
0,14	-0,61	28	1,31	
0,18	-4,11	17	1,33	Significant different
0,22	-2,14	15	1,34	Significant different
0,26	-1,36	3	1,64	
0,3	-0,93	3	1,64	
0,34	-2,44	3	1,64	Significant different

Table 7.4: The T-test for VAN GENT ET AL. [2003] and VAN DER MEER [1988] for surging waves

From Table 7.3 and Table 7.4. it can be concluded that the datasets of VAN DER MEER [1988] and VAN GENT ET AL. [2003] are in the majority of steps statistically significant different for plunging and surging waves.

7.4.2 *THOMPSON & SHUTTLER [1975] - VAN DER MEER [1988]*

Subsequently the results of the T-tests for the comparison of the datasets of VAN DER MEER [1988] and THOMPSON & SHUTTLER [1975] are shown in Table 7.5 and Table 7.6.

$S/N^{0,5}$	t_{obs}	dof	$t^*_{95\%}$	T-test
0,02	8,00	115,00	1,29	Significant different
0,06	2,56	101,00	1,29	Significant different
0,10	1,19	61,00	1,30	
0,14	0,05	68,00	1,29	
0,18	0,27	28,00	1,31	
0,22	0,03	36,00	1,31	
0,26	-0,46	15,00	1,34	
0,30	-0,96	6,00	1,44	

Table 7.5: The T-test for THOMPSON & SHUTTLER [1975] and VAN DER MEER [1988]

$S/N^{0,5}$	t_{obs}	dof	$t^*_{95\%}$	T-test
0,02	4,33	77	1,293	Significant different
0,06	-1,93	52	1,298	Significant different

Table 7.6: The T-test for THOMPSON & SHUTTLER [1975] and VAN DER MEER [1988] for surging waves

From Table 7.5 and Table 7.6 it can be concluded that for plunging waves the datasets of VAN DER MEER [1988] and THOMPSON & SHUTTLER [1975] are not significantly different except for the left part of the graph (step 0,02 and 0,06). For surging waves the datasets are significantly different on all points, but here only a few points seemed comparable.

7.4.3 *THOMPSON & SHUTTLER [1975] - VAN GENT ET AL. [2003]*

The results of the T-tests for the comparison of the datasets of THOMPSON & SHUTTLER [1975] and VAN GENT ET AL. [2003] are shown in Table 7.7 and Table 7.8.

$S/N^{0,5}$	t_{obs}	dof	$t^*_{95\%}$	T-test
0,02	-2,36	98	1,29	Significant different
0,06	-1,94	60	1,30	Significant different
0,1	2,13	33	1,31	Significant different
0,14	2,10	35	1,31	Significant different
0,18	1,78	21	1,32	Significant different
0,22	3,88	13	1,35	Significant different
0,26	1,42	11	1,36	Significant different
0,3	3,77	9	1,38	Significant different

Table 7.7: The T-test for THOMPSON & SHUTTLER [1975] and VAN GENT ET AL. [2003]

$S/N^{0,5}$	t_{obs}	dof	$t^*_{95\%}$	T-test
0,06	-5,11	20	1,325	Significant different

Table 7.8: The T-test for THOMPSON & SHUTTLER [1975] and VAN GENT ET AL. [2003] for surging waves

In Table 7.7 and Table 7.8 it can be seen that for plunging and surging waves the datasets of THOMPSON & SHUTTLER [1975] and VAN GENT ET AL. [2003] are on all points significantly different.

Chapter 8

ELABORATION DIFFERENCES

8.1 Introduction

In this chapter possible explanations for the differences between the datasets as shown in the previous chapter will be discussed.

8.2 Influence of shallow foreshores

Experiments by a number of M.Sc. Students at Delft University of Technology have shown that acceleration and phase shift affect the stability of stones under wave attack. DESSENS [2004] investigated stone stability in an accelerating flow and found that combinations of a fixed velocity with different accelerations show differences in movement. The amount of movement increases for an increase in acceleration combined with a constant or slightly decreasing velocity, which proves that there is a relation between the stability of the stones and a combination of the velocity and acceleration generated forces.

TROMP [2004] and TERILLE [2004] did a series of experiments with a 1:2 construction on a 1:30 and 1:8 foreshore. From these experiments it was concluded that near-bed velocities are not the only forces on the bed. Accelerations cause pressure gradients that tend to move stones,

which makes accelerations play a role in the threshold of motion. Furthermore it could be seen that the role of acceleration in the threshold of motion increases when the waves get more peaked. TROMP [2004] also showed that phase shift between the moments of maximum velocity and the maximum acceleration might play a role in this subject. When waves enter shallow water their shape changes, which causes changes in the phase shift between maximum velocity and maximum acceleration. This phase shift might be of great importance for the stability of stones. An example of this is shown in Figure 8.1 where at t=0.00s the maximal velocity is reached, while acceleration is zero, which is the behaviour of a normal wave in deep water conditions with a phase difference between velocity and acceleration of π/2. At t=0.15s it can be seen that acceleration is maximum, while velocity is certainly not zero. In this situation acceleration can play a role in stability.
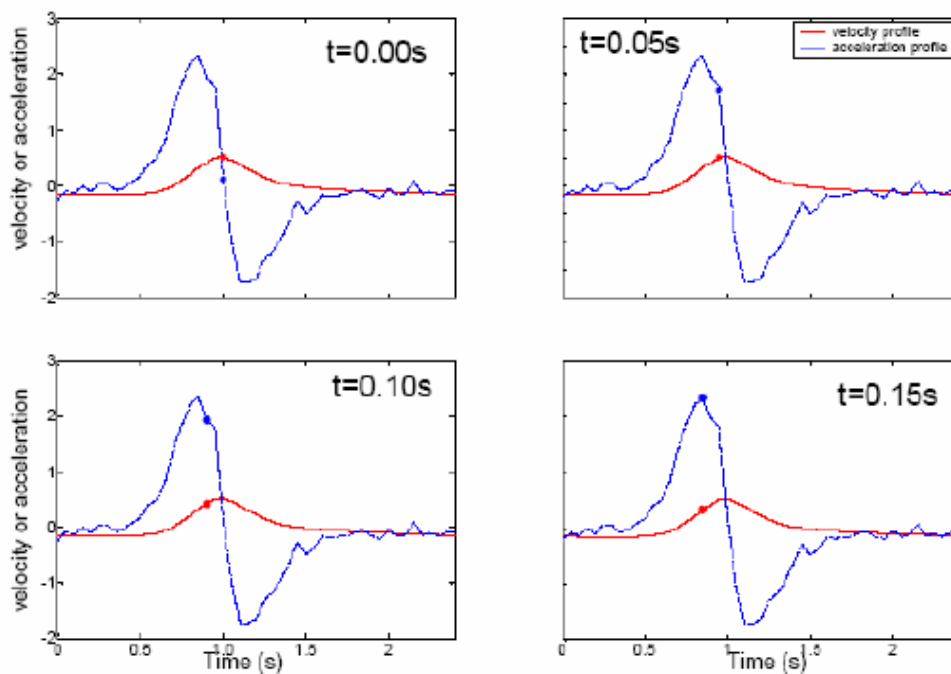
Figure 8.1: Decrease of phase shift between velocity (red) and acceleration (blue)

HOVESTAD [2005] and OORTMAN [2006] did experiments with different foreshore slopes in which the wave heights and the wave spectra were kept equal at the toe. Differences in damage occurred and it appeared that the wave shape (the steepness of the wave front) is different for the different slopes. On the steep foreshores, the wave fronts were steeper than on less steep foreshores. According to HOVESTAD [2005] this might explain the higher damage levels for constructions with a steep foreshore.

Structures with a steep foreshore on average show more damage than structures with a less steep foreshore even if the spectrum at the toe of the structure is identical. In VAN GENT ET AL. [2003] most of the tests were done with shallow foreshores with two different slope angles (1:100 and 1:30). In VAN DER MEER [1988] only a limited number of tests (tests 274 to 289) were done with shallow foreshores with a slope angle of 1:30.

To check whether the influence of the foreshore can be seen in the dataset of VAN DER MEER [1988] in Figure 8.2 and Figure 8.3 the tests with shallow foreshores of VAN DER MEER [1988] (in red) are plotted together with all data of VAN GENT ET AL. [2003] (in blue). The complete datasets of VAN DER MEER [1988] and THOMPSON & SHUTTLER [1975] are plotted in grey on the background. For plunging waves this is done in Figure 8.2. In all graphs maximum accepted damage levels are applied.
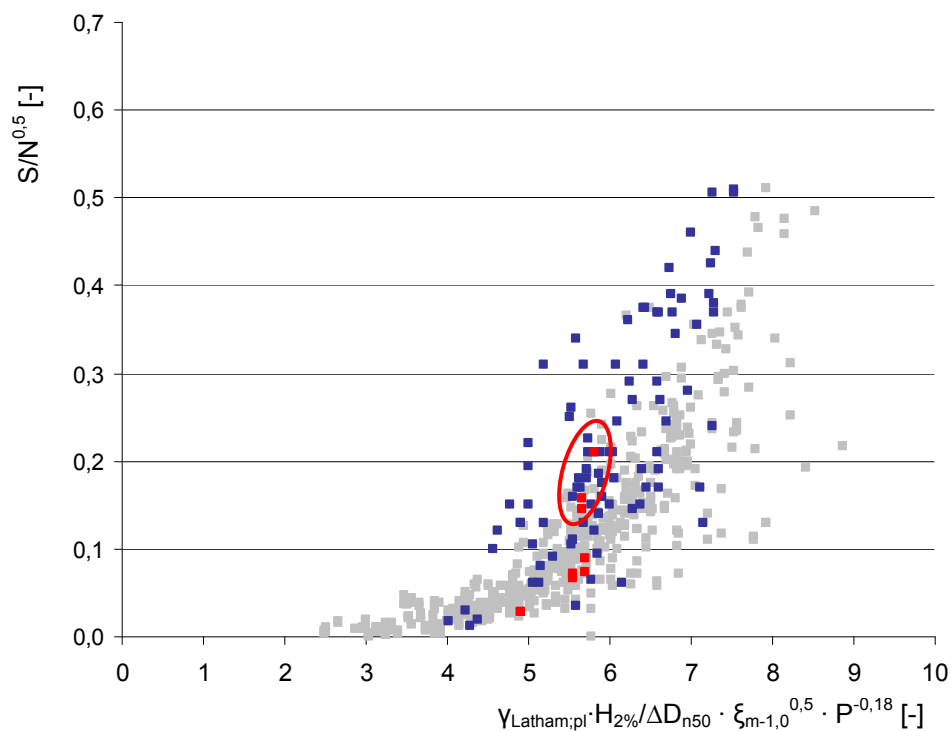
Figure 8.2: Plunging waves: VAN DER MEER [1988] and THOMPSON & SHUTTLER [1975] (grey), VAN DER MEER [1988] with shallow foreshores (red), VAN GENT ET AL. [2003] (blue)

In Figure 8.2 it can be seen the tests with shallow foreshores from the dataset of VAN DER MEER [1988] do not deviate in an extreme way from of the datasets of VAN DER MEER [1988] and THOMPSON & SHUTTLER [1975]. However a close look shows that some red data points, indicated with a red circle, show a bit more damage than the average of the dataset of VAN DER MEER [1988]. In Figure 8.3 it can be seen that for surging waves the tests with shallow foreshores of VAN DER MEER [1988] don't show differences from the rest of the dataset.

From this it can be concluded that in the tests of VAN DER MEER [1988] no convincing influence of shallow foreshores can be seen, because the points that indicate the tests with shallow foreshores do not show convincing deviations as compared with the rest of the test results of VAN DER MEER [1988].
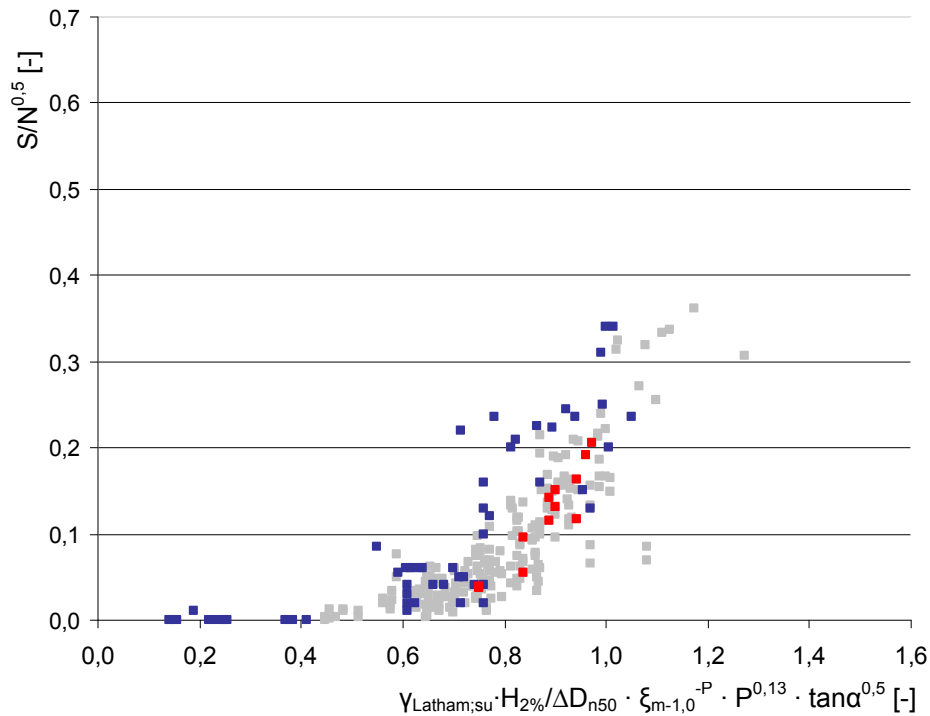
Figure 8.3: Surging waves: VAN DER MEER [1988] and THOMPSON & SHUTTLER [1975] (grey), VAN DER MEER [1988] with shallow foreshores (red), VAN GENT ET AL. [2003] (blue)

Because in VAN GENT ET AL. [2003] two different slope angles were used for the foreshore it is also very interesting to check if any differences can be seen in damage for these two slope angles. Therefore in Figure 8.4 the dataset for plunging waves of VAN GENT ET AL. [2003] is plotted with the data with $\cot\beta=30$ in dark blue and in light blue the data with $\cot\beta=100$. The tests from VAN DER MEER [1988] with shallow foreshores are presented in red. The same is done for surging waves in Figure 8.5.

In Figure 8.4 it can be seen that for plunging waves in the left part of the graph a certain distinction appears between the data with $\cot\beta=30$ and $\cot\beta=100$. The data with $\cot\beta=30$ tends to show more damage than the data with $\cot\beta=100$. But on the other hand the data cloud of the data with $\cot\beta=30$ is very large for yet unknown reasons. In further research possible reasons for the large spread in data with $\cot\beta=30$ have to be investigated.
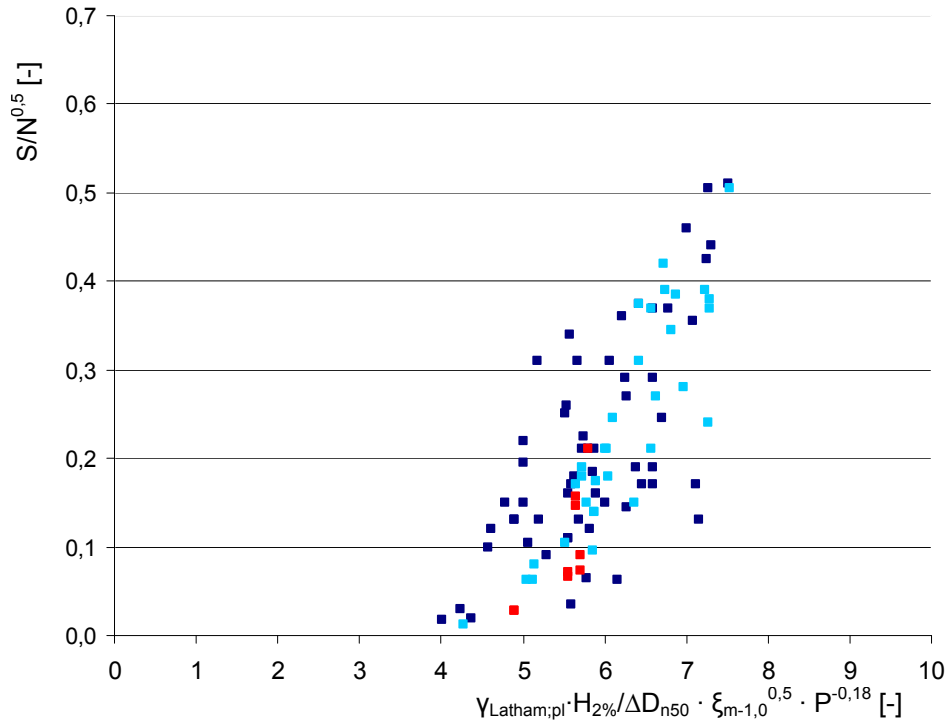
Figure 8.4: Plunging waves: VAN GENT ET AL. [2003] cotβ=30 (dark blue), cotβ=100 (light blue), VAN DER MEER [1988] with cotβ=30 (red)
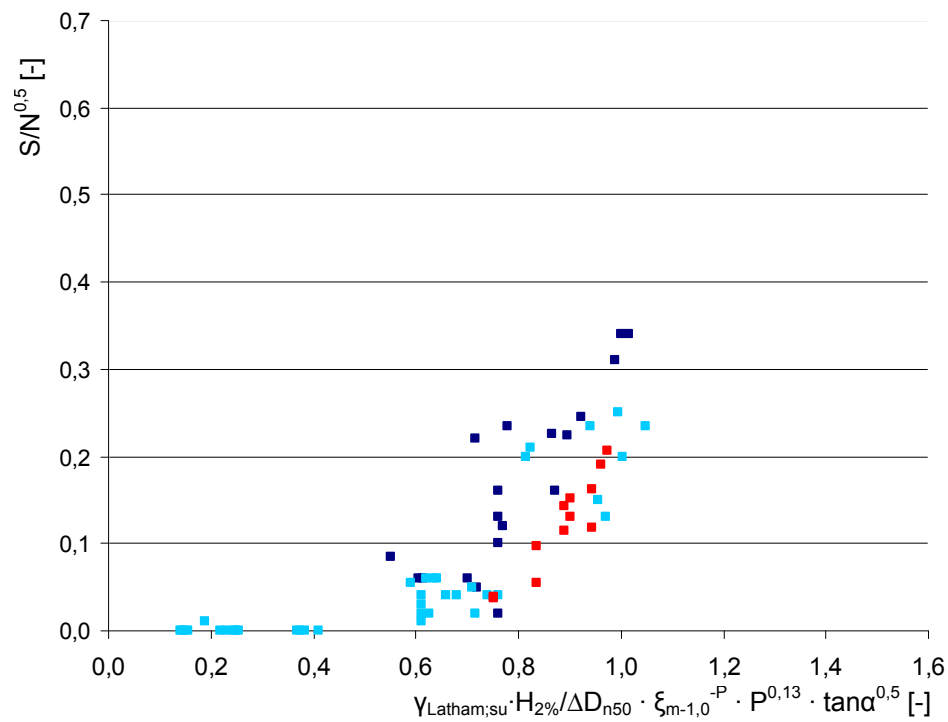
Figure 8.5: Surging waves: VAN GENT ET AL. [2003] cotβ=30 (dark blue), cotβ=100 (light blue), VAN DER MEER [1988] with cotβ=30 (red)

For surging waves in Figure 8.5 the data with cotβ=30 shows more damage than the data with cotβ=100 on the whole range. Therefore from Figure 8.5 it can be concluded that for surging waves the slope of the foreshore has influence on the stability.

In both graphs it can be seen that the tests with shallow foreshores (cotβ=30) from the dataset of VAN DER MEER [1988] mostly correspond to the data from VAN GENT ET AL. [2003] with cotβ=100, especially in the graph for surging waves. This would mean, if the model setup is equal for both datasets, that besides the influence on stability of the foreshore slope angle also other mechanisms that have not been investigated before might have influence on stability. A possible mechanism that might have influence on stability is the amount of wave breaking, which will be discussed in paragraph 8.4. To prove such influences a detailed analysis of the dataset of VAN GENT ET AL. [2003] is required, which cannot be done in this M.Sc. Thesis because of the unavailability of this dataset.

Because from the previous section it can be concluded that there is an influence of the foreshore slope angle on stability a first question that has to be answered is what the difference is between a foreshore slope and a slope that is a part of the construction. When for example a slope of 1:8 is schematised as a part of the structure the structure would exist of 2 different slope angles. VAN DER MEER [1988] did a few tests with an 1:30 foreshore slope and VAN GENT ET AL. [2003] used an 1:100 and a 1:30 foreshore slope. To recognise a shallow foreshore we can distinguish 2 conditions (depth and width). According to VAN DER MOST [1979] a foreshore is shallow when the water depth is sufficiently small ($d_{foreshore}/L_0 < {}^1/_{20}$). The purpose of a foreshore is to let waves break before they reach the structure, what will decrease the wave height. When we speak of a shallow foreshore the width of the sloping foreshore must be at least $2L_0$ to let wave breaking occur.

To describe the possible influence of a shallow foreshore a connection has to be found between the shape of the foreshore and stability. The shape of a wave depends on the water depth and the shape of the foreshore. Entering shallow water the wave steepness increases and finally the waves will break when the wave steepness reaches critical values. Accelerations, velocities and phase shift, which obviously affect stability according to previous sections, depend on the shape of the wave. The wave steepness might be a good descriptor for this. The shape of a foreshore can be expressed in the water depth and the slope angle. In this way a possible descriptor for the influence of the foreshore might be a

foreshore Iribarren parameter, ξ_β, in which the wave steepness and the slope angle of the foreshore can be combined. A definition for the foreshore Iribarren parameter is given below.

$$\xi_\beta = \frac{\tan \beta}{\sqrt{H_{2\%}/L}}$$

Where:

β   =   the foreshore slope angle

$H_{2\%}$ =   the wave height exceeded by 2% of the waves

L   =   the wave length (based on $T_{m-1,0}$)

To explain the influence of the foreshore Iribarren parameter, ξ_β, 4 different model setups will be distinguished which are presented in Figure 8.6 to Figure 8.9. At first in Figure 8.6 the standard model setup of VAN DER MEER [1988] with deep water at the toe of the construction and no sloping foreshore can be seen. In this situation cotβ=∞, which makes ξ_β=0.
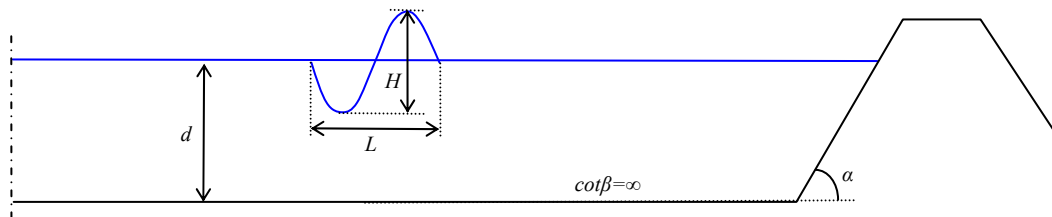
Figure 8.6: Model setup with deep water at toe and foreshore slope cotβ=∞
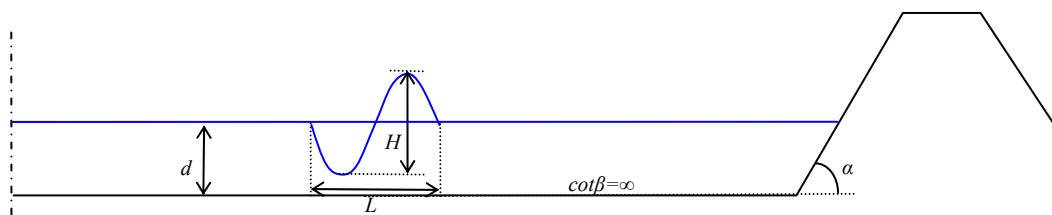
Figure 8.7: Model setup with shallow water at toe and foreshore slope cotβ=∞

Figure 8.7 shows a setup with shallow water at the toe of the construction and also no sloping foreshore. Also in this situation cotβ=∞, which makes ξ_β=0. In the latter two model setups no difference in the foreshore Iribarren parameter can be found. The differences in damage between these two setups are fully overcome by the use the spectral period, $T_{m-1,0}$, and the wave height exceeded by 2% of the waves, $H_{2\%}$.
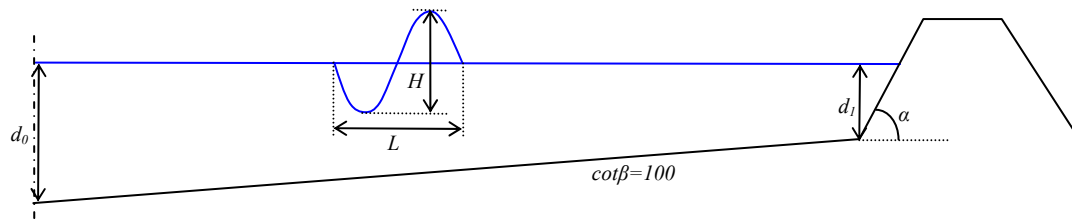
Figure 8.8: Model setup with shallow water at toe and foreshore slope cotβ=100

Figure 8.8 shows a situation with shallow water at the toe of the structure and a foreshore slope of cot β=100 and Figure 8.9 shows a situation with shallow water at the toe of the construction and a foreshore slope of cot β=30. With equal wave characteristics the value of ξ_β is higher for the situation in Figure 8.9 than for the situation in Figure 8.8. Also according to the hypothesis that damage increases as the foreshore slope gets steeper, with equal wave characteristics, the expected damage in the situation in Figure 8.9 will be higher than in the situation in Figure 8.8. Including a parameter based on ξ_β would include the effects on stability of the foreshore slope angle.
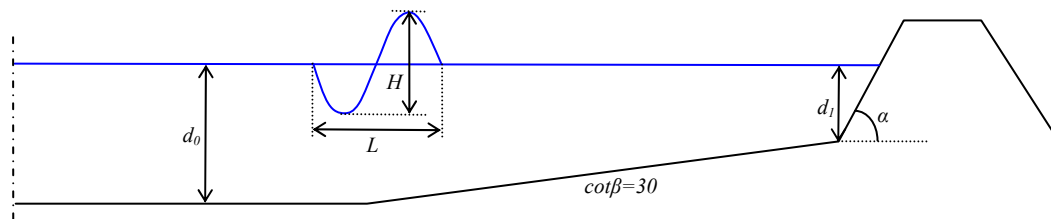
Figure 8.9: Model setup with shallow water at toe and foreshore slope cotβ=30

Because in VAN DER MEER [1988] only 16 tests were done with shallow foreshores no good reliable regression analysis can be done, but nevertheless the behaviour of a foreshore Iribarren parameter can be analysed for these 16 tests. Therefore in Table 8.1 values of the foreshore Iribarren parameter are calculated for all 16 tests with shallow foreshores of VAN DER MEER [1988].

Because tests with a 1:100 foreshore do not exist in the dataset of VAN DER MEER [1988] in Table 8.1 four tests have been created with a 1:100 foreshore slope and similar wave characteristics as the tests with a 1:30 foreshore slope to analyse the influence of the foreshore slope angle on the foreshore Iribarren parameter and the correction factors. These imaginary tests are indicated with a star. On the bottom row values of the foreshore Iribarren parameter are given for the tests of VAN DER MEER [1988] without shallow foreshores. Because the difference in damage between the datasets of VAN DER MEER [1988] and VAN GENT ET AL.

[2003] is about 10 to 15% in Table 8.1 it is tried to get a correction factor in a format $(1+\xi_\beta^n)$, with values of 1,1 to 1,15 for 1:30 foreshore slopes. It can be seen that for 1:30 foreshore slopes this correction factor is higher than for 1:100 foreshore slopes which is in correspondence with the occurring damage. For situations with $\cot\beta=\infty$ the correction factor is 1,0. Of course in a future real regression analysis of these factors more accurate techniques need to be applied.

Test nr.	d	$\cot\beta$	ξ_β	ξ_β^2	$(1+\xi_\beta^2)$	$\xi_\beta^{1,5}$	$(1+\xi_\beta^{1,5})$	$\xi_\beta^{1,3}$	$(1+\xi_\beta^{1,3})$	$\xi_\beta^{1,2}$	$(1+\xi_\beta^{1,2})$
	[m]	[-]	[-]	[-]	[-]	[-]	[-]	[-]	[-]	[-]	[-]
274	0,40	30	0,19	0,04	1,04	0,09	1,09	0,11	1,11	0,13	1,13
275	0,40	30	0,23	0,05	1,05	0,11	1,11	0,12	1,12	0,14	1,14
276	0,40	30	0,21	0,04	1,04	0,10	1,10	0,13	1,13	0,15	1,15
277	0,40	30	0,18	0,03	1,03	0,08	1,08	0,15	1,15	0,17	1,17
278	0,40	30	0,24	0,06	1,06	0,12	1,12	0,14	1,14	0,17	1,17
279	0,40	30	0,27	0,07	1,07	0,14	1,14	0,16	1,16	0,18	1,18
280	0,40	30	0,23	0,05	1,05	0,11	1,11	0,16	1,16	0,19	1,19
281	0,40	30	0,25	0,06	1,06	0,12	1,12	0,18	1,18	0,20	1,20
282	0,20	30	0,25	0,06	1,06	0,13	1,13	0,12	1,12	0,15	1,15
283	0,20	30	0,25	0,06	1,06	0,13	1,13	0,12	1,12	0,14	1,14
284	0,20	30	0,25	0,06	1,06	0,12	1,12	0,13	1,13	0,15	1,15
285	0,20	30	0,24	0,06	1,06	0,12	1,12	0,13	1,13	0,15	1,15
286	0,20	30	0,21	0,04	1,04	0,09	1,09	0,16	1,16	0,18	1,18
287	0,20	30	0,20	0,04	1,04	0,09	1,09	0,16	1,16	0,19	1,19
288	0,20	30	0,20	0,04	1,04	0,09	1,09	0,17	1,17	0,19	1,19
289	0,20	30	0,21	0,04	1,04	0,09	1,09	0,17	1,17	0,19	1,19
*	0,40	100	0,07	0,00	1,00	0,01	1,01	0,03	1,03	0,03	1,03
*	0,40	100	0,07	0,00	1,00	0,01	1,01	0,03	1,03	0,03	1,03
*	0,20	100	0,07	0,00	1,00	0,02	1,02	0,03	1,03	0,04	1,04
*	0,20	100	0,07	0,00	1,00	0,02	1,02	0,03	1,03	0,04	1,04
Other	0,80	∞	0,00	0,00	1,00	0,00	1,00	0,00	1,00	0,00	1,00

Table 8.1: Behaviour of foreshore Iribarren parameter for tests of VAN DER MEER [1988]

From this the stability formulae of VAN DER MEER [1988] can be changed into the following formulae:

Plunging waves:
$$\frac{S}{\sqrt{N}} = \left(\left(1+\xi_\beta^{\,n}\right) \cdot \gamma_{Lath;pl} \cdot \frac{1}{c_{pl}} \cdot \frac{H_s}{\Delta D_{n50}} \cdot \xi_{\alpha;m-1,0}^{\,0,5} \cdot P^{-0,18} \cdot \frac{H_{2\%}}{H_s} \right)^5$$

Surging waves:
$$\frac{S}{\sqrt{N}} = \left(\left(1+\xi_\beta^{\,n}\right) \cdot \gamma_{Lath;su} \cdot \frac{1}{c_{su}} \cdot \frac{H_s}{\Delta D_{n50}} \cdot \xi_{\alpha;m-1,0}^{\,-P} \cdot P^{0,13} \cdot \tan\alpha^{0,5} \cdot \frac{H_{2\%}}{H_s} \right)^5$$

Where:

n = factor to be found by regression analysis. Probably n≈1.2to 1.5

In further research to this topic relations between the geometry of the foreshore and the damage level have to be investigated in which the geometry of the foreshore can be given by the foreshore Iribarren parameter, ξ_β. To prove such relationships if possible damage curves have to be plotted in which these relations can be shown in a better way. This can be done by making 3d-curves showing relations between $H_{2\%}/\Delta D_{n50}$, $\xi_{construction}$, $cot\alpha$, $S/\sqrt{N}$ and $\xi_{foreshore}$. By making 3d graphs these curves can be compared with the damage curves of VAN DER MEER [1988]. An important factor in this is the wave height. A clear definition for the place where the wave height has to be measured has to be defined. VAN DER MEER [1988] assumed that the incoming wave height is equal to the wave height at the construction, because in his investigation no shallow foreshore was present. When a shallow foreshore is present the wave height at the construction might be affected by processes occurring on the shallow foreshore, which means that the wave height should be measured at the intersection of mean water level and the construction. Another possibility is to set up a model to calculate the wave height at the toe of the construction out of the incoming wave height and the geometry of the foreshore (BATTJES & GROENENDIJK [2000]).

8.3   Influence of double peaked spectra

In earlier chapters it was already concluded that the wideness of single peaked spectra does not influence stability. In VAN GENT ET AL. [2003] however also double peaked spectra were used. To check whether a double peaked spectrum might have a different effect on stability than a single peaked spectrum in Figure 8.10 from the dataset of VAN GENT ET AL. [2003] for plunging waves the data with single peaked spectra is compared with the data with double peaked spectra. In these graphs also a distinction is made between structures with a 1:30 and 1:100 foreshore, because in previous sections it could be concluded that the foreshore slope angle also influences stability.
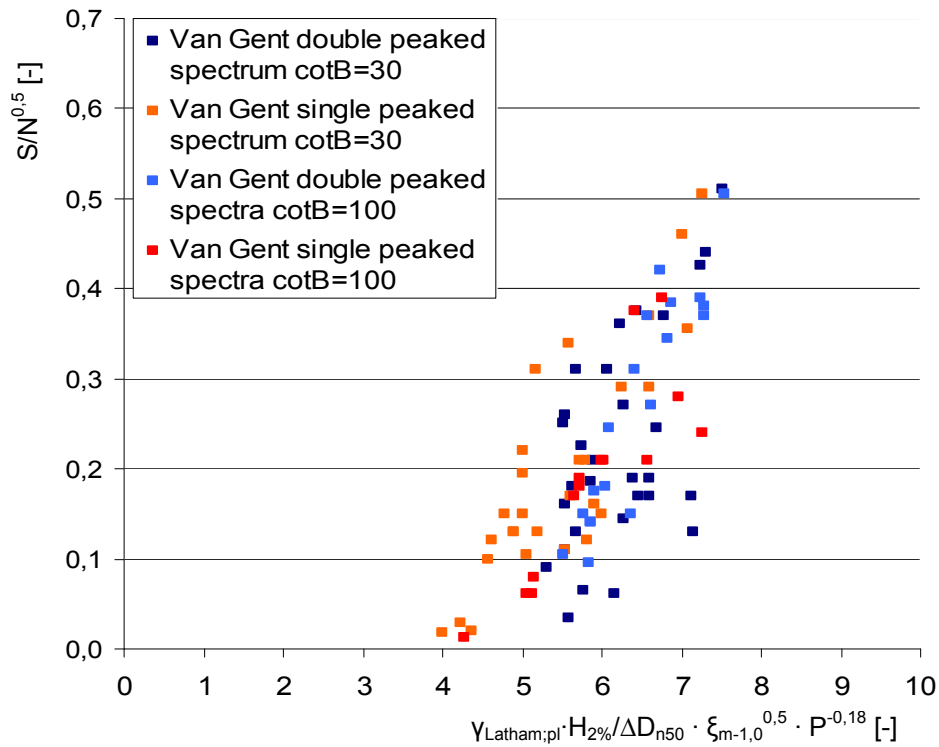
Figure 8.10: Plunging waves: VAN GENT ET AL. [2003] Single peaked spectra, double peaked spectra
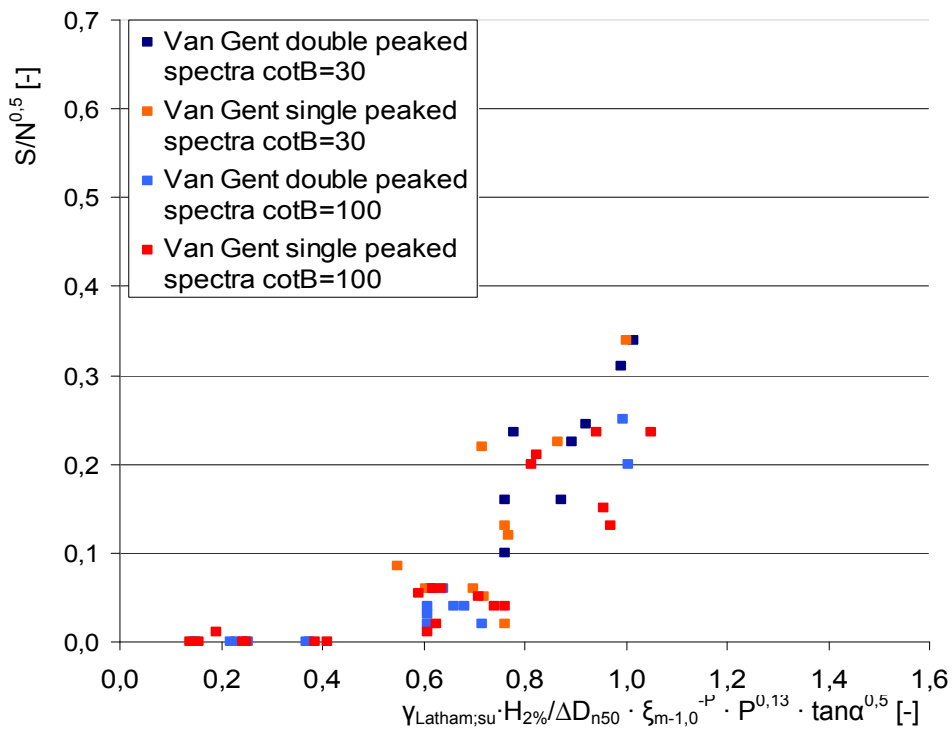
Figure 8.11: Surging waves: VAN GENT ET AL. [2003] Single peaked spectra), double peaked spectra

In Figure 8.10 in general a distinction appears between the data with single peaked and double peaked spectra. It can be seen that the data with single peaked spectra and cotβ=30

on average show more damage than the data with double peaked spectra and cotβ=30, but this may also be caused by the absence of data with double peaked spectra on the left part of the graph. Also there is a lot of scatter in both data clouds. For cotβ=100 there is no clear distinction between single and double peaked spectra. To be able to make a proper conclusion from this more research on this topic is required.

In Figure 8.11 the same graph is given for surging waves. In this graph no clear distinction can be seen between data with double peaked and single peaked spectra.

8.4   Wave breaking

In Figure 8.12 the test results for plunging waves of VAN GENT ET AL. [2003] have been plotted again. A distinction has been made in the amount of wave breaking. Severe wave breaking occurs for $H_{s;toe}$ / $H_{s;deep}$ <0,7, intermediate wave breaking occurs for 0,7 < $H_{s;toe}$ / $H_{s;deep}$ <0,9 and only a small amount of wave breaking occurs for $H_{s;toe}$ / $H_{s;deep}$ > 0,9. In this figure no clear relation can be seen between the amount of wave breaking on the foreshore and the damage level.
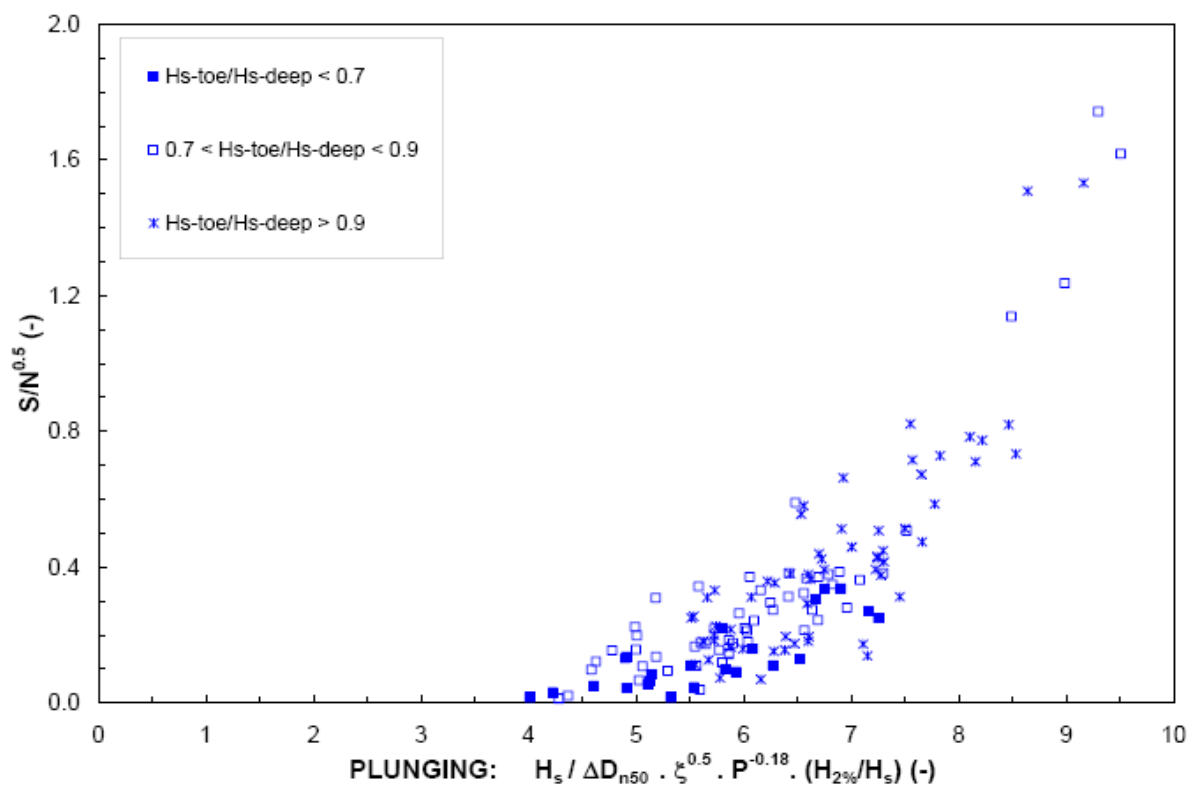
Figure 8.12: Plunging waves VAN GENT ET AL. [2003] with distinction in amount of wave breaking

In future research to this topic more research has to be done to the wave height distribution on the foreshore in the tests of VAN GENT ET AL. [2003] and the effects on stability of the wave breaking processes on the foreshore. This also includes a test whether the wave height relations from BATTJES & GROENENDIJK [2000] are valid for the data of VAN GENT ET AL. [2003].

Because in shallow waters the wave height strongly depends on the water depth for the data of VAN GENT ET AL. [2003] the damage level may also directly be influenced by the water depth instead of the wave height. Also because of difficulties in measuring wave heights of breaking waves it might be better to use the water depth in shallow water conditions, which forms a more fixed value. Therefore in future research to this topic also possible relations between the water depth and the damage level in shallow water conditions have to be investigated.

8.5   Surf beat and wave reflection

Surf beat occurs when deep water waves propagate into shallow water. Entering shallow water they exhibit increasingly strong nonlinearities. One important nonlinear effect is the emergence of low-frequency energy as a consequence of interactions between higher frequency incident wave components. The low-frequency components with periods of several minutes cause water level variations in the surf zone. Compared with wave impact on average surf beat has only a minor contribution to the forces acting on the stones and therefore it is in most situations neglectable. However when wave heights are low (in the order of centimetres), the effects of surf beat on stability may not be neglectable. The same can be said for the effects of wave reflection. In model tests of VAN DER MEER [1988] and THOMPSON & SHUTTLER [1988] the wave height varies between 0,02m and 0,26m for the small scale tests, which indicates that surf beat and wave reflection may have affected the stability of stones during these tests, especially for the lower wave heights.

In Figure 8.13 the datasets of VAN DER MEER [1988] and THOMPSON & SHUTTLER [1975] have been plotted. In these graphs a distinction is made between $H_s<0,10m$ (blue) and $H_s>0,10m$ (red). In these graphs it can be seen that the data with $H_s<0,10m$ does not show different damage patterns than the data with $H_s>0,10m$. Also it can be seen that the amount of scatter is about equal for both groups of data. From this it can be concluded that for the datasets of

VAN DER MEER [1988] and THOMPSON & SHUTTLER [1975] the influence of small scale effects like surf beat and wave reflection can not be visualized by making a distinction between smaller and larger significant wave heights. However this does not mean that these small scale effects do not influence stability.
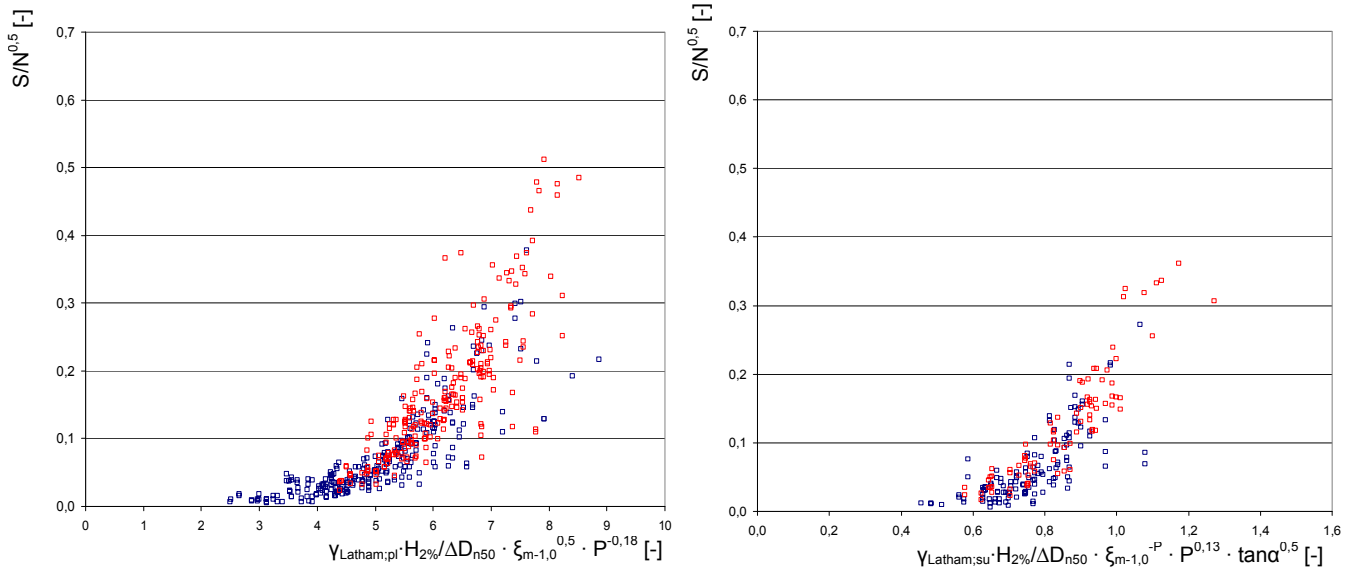
Figure 8.13: Plunging waves (left) and surging waves (right) of VAN DER MEER [1988] and THOMPSON & SHUTTLER with distinction in $H_s<0,10m$ (blue) and $H_s>0,10m$ (red)

Chapter 9

CONCLUSIONS & RECOMMENDATIONS

9.1   General conclusion

The main conclusion from this report is that the foreshore slope angle influences stability in the dataset of VAN GENT ET AL. [2003]. After transforming the datasets of THOMPSON & SHUTTLER [1975] and VAN DER MEER [1988] into comparable datasets with the dataset of VAN GENT ET AL. [2003] still differences can be seen between the datasets of VAN DER MEER [1988] / THOMPSON & SHUTTLER [1975] and the dataset of VAN GENT ET AL. [2003]. These differences are visible in the reconstructed graphs and have been statistically confirmed by using the T-test. In this for all 3 datasets the wave height was expressed in the wave height exceeded by 2% of the waves, $H_{2\%}$, and the wave period was expressed in the spectral wave height, $T_{m-1,0}$. Transformation of the original datasets of VAN DER MEER [1988] and THOMPSON & SHUTTLER [1975], in which for the wave height the significant wave height, H_s, was used and for the wave period the mean wave period, T_m, was used, was done on a individual basis. This means no generally applicable ratios where used which were used for the comparison in VAN GENT [2004]. Besides the correct transformation of wave height and

wave period also the influences of stone roundness, which caused some deviations in the original dataset of VAN DER MEER [1988], and maximum acceptable damage levels were incorporated in this M.Sc. Thesis.

In the final graphs it can be seen that on average the data of VAN GENT ET AL. [2003] still shows more damage than the data of VAN DER MEER [1988] and THOMPSON & SHUTTLER [1975]. The datasets of VAN DER MEER [1988] and THOMPSON & SHUTTLER [1975] do not show significant differences. An explanation for these differences can be found in the fact that most of the tests of VAN GENT ET AL. [2003] were tests with shallow water conditions (shallow foreshores), while the majority of the tests of VAN DER MEER [1988] and THOMPSON & SHUTTLER [1975] were done in deep water conditions. Experiments of a number of M.Sc. students at Delft University of Technology indicated that wave deformation on shallow foreshores causes different damage patterns as compared with standard waves. On average constructions with steep foreshores show more damage than constructions with less steep foreshores. This was also visible in the data of VAN GENT ET AL. [2003]. The influence of acceleration and the phase shift between velocity and acceleration may also play an important role in this (VERHAGEN [2005]).

9.2   Recommendations

To get a better understanding of the differences between the datasets more research to this topic is required. However a possible explanation can be the influence of acceleration and phase shift because of wave deformation, other possible differences between the experiments must also be taken into account. In this M.Sc. Thesis it already became clear that stone roundness had a quite spectacular influence on stability, but it might just as well be possible that many other at present unknown factors play a role on stability too.

Further research to this topic requires the availability and accessibility of the dataset of VAN GENT ET AL. [2003]. A first thing to be done would be to check if in the dataset of VAN GENT ET AL. [2003] itself also a distinction occurs between tests results with deep water conditions and shallow water conditions. The inclusion of a new factor, based on the foreshore Iribarren parameter as described in paragraph 8.2, in the modified formulae of VAN DER MEER [1988] should lead to a decrease of the differences between the datasets of VAN DER MEER [1988] / THOMPSON & SHUTTLER [1975] and VAN GENT ET AL. [2003].

REFERENCES

BATTJES, J.A., & GROENENDIJK, H.W. [2000]
Wave height distribution on shallow foreshores
Coastal engineering 40, Elsevier

DESSENS, M. [2004]
The influence of flow acceleration on stone stability
M.Sc. Thesis, Delft University of Technology

GENT, M.R.A. VAN, SMALE, A., KUIPER, C. [2003]
Stability of rock slopes with shallow foreshores
Proc. Coastal structures 2003, Portland, ASCE

GENT, M.R.A. VAN [2004]
On the stability of rock slopes
Keynote NATO Workshop May 2004 Bulgaria

Goda, Y. [1988]
On the Methodology of Selecting Design Wave Height
Coastal engineering 1988

A review on statistical interpretation of wave data.
Report of the Port and Harbour Research Institute, Japan

HOVESTAD, M. [2005]
Breakwaters on steep foreshores
M.Sc. Thesis, Delft University of Technology

INFRAM report i 489 [2001]
Verhouding piekperiode en spectrale periodemaat

LATHAM, J.-P., MANNION, M.B., POOLE, A.B. BRADBURY A.P. AND ALLSOP, N.W.H. [1988]
The influence of armour stone shape and rounding on the stability of breakwater armour layers.
Queen Mary College, University of London, UK

LONGUET-HIGGINS, M.S. [1980]

On the distribution of the heights of sea waves: some effects of nonlinearity and finite band width

J. Geophys.

MEER, J.W. VAN DER [1988]

Rock slopes and gravel beaches under wave attack

Ph.D. Thesis, WL | Delft Hydraulics (report 396) and Delft University of Technology

OORTMAN, N.J. [2006]

Influence of foreshore steepness on wave velocity and acceleration at the breakwater interface.

M.Sc. Thesis, Delft University of Technology

TERILLE, E. [2004]

The threshold of motion of coarse sediment particles by regular non-breaking waves

M.Sc. Thesis, Delft University of Technology, University of Genoa

TERILLE, E. [2004]

Incipient motion of coarse particles under regular shoaling waves

Coastal Engineering December 2004

THOMPSON, D.M., SHUTTLER, R.M. [1975]

Riprap design for wind wave attack. A laboratory study in random waves

Wallingford, EX 707

TROMP, M. [2004]

Influences of fluid accelerations on the threshold of motion

M.Sc. Thesis, Delft University of Technology

VERHAGEN, H.J. [2005]

The effect of foreshore slope on breakwater stability

ASCE, Proc. ICCE 2005

WL | DELFT HYDRAULICS, M1983 DEEL I [1988]

Statistische stabiliteit van stortsteentaluds onder golfaanval. Ontwerp formules.

Verslag modelonderzoek, M1983 deel I

APPENDIX A   THEORY

A1   Wave height distribution on shallow foreshores

The conversion from H_s to $H_{2\%}$ can be done using the point model of BATTJES & GROENENDIJK [2000]. The point model of BATTJES & GROENENDIJK [2000] describes the wave height distribution on a shallow foreshore. This model consists of a Rayleigh distribution, or a Weibull distribution with the exponent equal to 2, for the lower wave heights and a Weibull distribution with a higher exponent for the higher wave heights. This composite Weibull distributed is shown in Figure A.1.
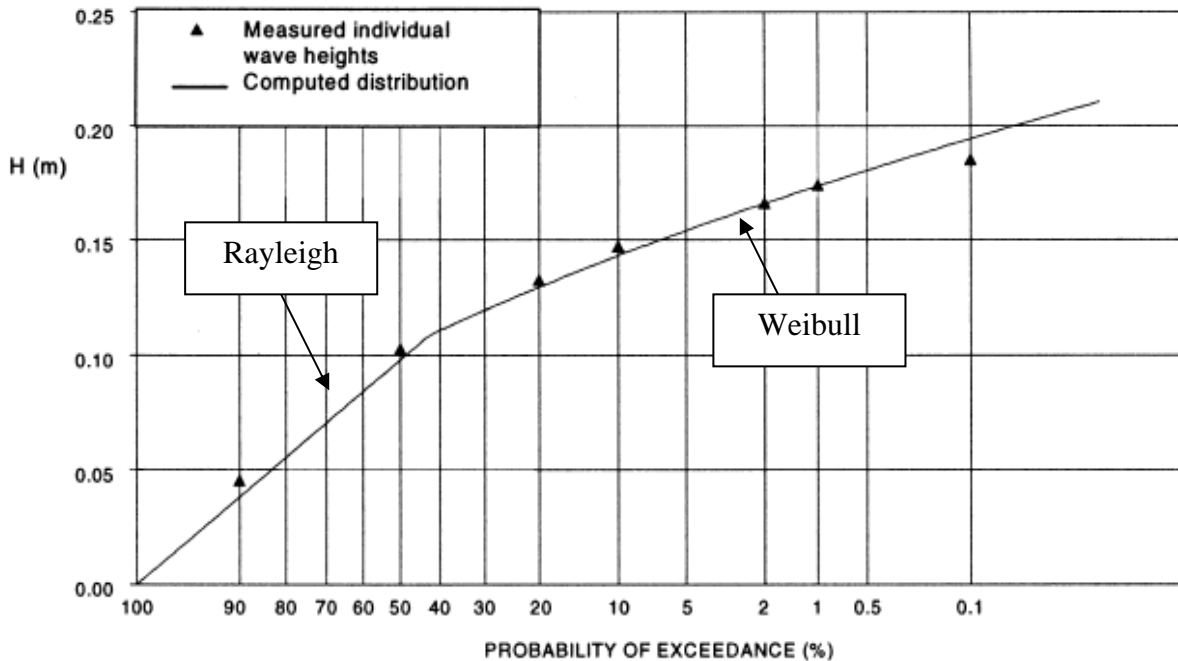
Figure A.1: Probability density function (BATTJES & GROENENDIJK [2000])

The theoretical expression of the composite Weibull distribution is shown below.

$$F(H) \equiv \Pr\{\underline{H} \leq H\} = \begin{cases} F_1(H) = 1 - \exp\left[-\left(\dfrac{H}{H_1}\right)^{k_1}\right] & H \leq H_{tr} \\[4mm] F_2(H) = 1 - \exp\left[-\left(\dfrac{H}{H_2}\right)^{k_2}\right] & H \geq H_{tr} \end{cases}$$

In which:

k_1, k_2 = shape parameters of the distribution determining the curvature

H_1, H_2 = scale parameters

H_{tr} = transition wave height: $H_{tr} = H_{tr} = \beta_{tr} \cdot 0{,}14 \cdot L_c \cdot \tanh\left(\dfrac{2\pi d}{L_c}\right)$

Where:

β_{tr} = slope-dependent coefficient: $\beta_{tr} = c_3 + c_4 \tan\alpha$; ($c_3 = 0{,}46$, $c_4 = 9{,}25$)

L_c = characteristic local wave height defined by: $L_c = \dfrac{gT_c{}^2}{2\pi} \cdot \tanh\left(\dfrac{2\pi d}{L_c}\right)$

The introduction of the wave period in the expression for H_{tr} gave insignificant improvements comparing with the point model using a transitional wave height depending on the bottom slope and depth only. Therefore a simpler parameterisation for the transitional wave height is given by:

$$H_{tr} = (0{,}35 + 5{,}8 \cdot \tan\alpha) \cdot d$$

For the shape parameters k_1 and k_2 BATTJES & GROENENDIJK [2000] uses $k_1 = 2$ and $k_2 = 3{,}6$.

For the root mean square wave height the root mean square of the sampled zero-crossing wave height per record is used. Using the deep-water ratio of $H_{rms}/\sqrt{m_0}$ for broad banded sea as a constraint for the root mean square wave height is found:

$$H_{rms} = (2{,}69 + \beta_{rms} \cdot \psi)\sqrt{m_0} = \left(2{,}69 + 3{,}24 \cdot \dfrac{\sqrt{m_0}}{d}\right)\sqrt{m_0}$$

The only unknown parameters in the model described above are the scale parameters H_1 and H_2. These can be calculated by solving the following expression in terms of the incomplete gamma functions $\gamma(a,x)$ and $\Gamma(a,x)$ (ABRAMOWITZ & STEGUN [1964]). This gives:

$$\tilde{H}_{rms} = \sqrt{\tilde{H}_1{}^2 \cdot \gamma\left[\frac{2}{k_1} + 1 \ , \ \left(\frac{\tilde{H}_{tr}}{\tilde{H}_1}\right)^{k_1}\right] + \tilde{H}_2{}^2 \cdot \Gamma\left[\frac{2}{k_2} + 1 \ , \ \left(\frac{\tilde{H}_{tr}}{\tilde{H}_2}\right)^{k_2}\right]} = 1$$

resulting in:

$$\tilde{H}_{rms} = \sqrt{\tilde{H}_1^2 \cdot \int\limits_0^{\left(\frac{\tilde{H}_{tr}}{\tilde{H}_1}\right)^2} t \cdot \exp(-t)\cdot dt + \tilde{H}_2^2 \cdot \int\limits_{\left(\frac{\tilde{H}_{tr}}{\tilde{H}_2}\right)^{3,6}}^{\infty} t^{\frac{5}{9}} \cdot \exp(-t)\cdot dt} = 1$$

where :
$$\left(\frac{\tilde{H}_{tr}}{\tilde{H}_1}\right)^2 = \left(\frac{\tilde{H}_{tr}}{\tilde{H}_2}\right)^{3,6}$$

In order to make this calculation a lot easier BATTJES & GROENENDIJK [2000] set up a table with the characteristic normalised wave heights as a function of the transitional wave height. To use this table the normalised transitional wave height is needed. This parameter is expressed by:

$$\tilde{H}_{tr} = \frac{H_{tr}}{H_{rms}}$$

Corresponding to each value of the normalised transitional wave height in Table A.1 values of several normalised characteristic wave heights are given in the table. The table from BATTJES & GROENENDIJK [2000] is given on the next page for $H_{2\%}$ and $H_{1/3}$. With these values the ratio $H_{2\%}/H_{1/3}$ is calculated.

H_{tr}	$H_{2\%}$	$H_{1/3}$	$H_{2\%}/H_{1/3}$	H_{tr}	$H_{2\%}$	$H_{1/3}$	$H_{2\%}/H_{1/3}$
0,00	1,548	1,279	1,210	1,50	1,778	1,406	1,265
0,05	1,548	1,279	1,210	1,55	1,799	1,408	1,278
0,10	1,548	1,279	1,210	1,60	1,820	1,410	1,291
0,15	1,548	1,279	1,210	1,65	1,841	1,411	1,305
0,20	1,548	1,279	1,210	1,70	1,863	1,412	1,319
0,25	1,548	1,279	1,210	1,75	1,884	1,413	1,333
0,30	1,548	1,279	1,210	1,80	1,906	1,413	1,349
0,35	1,548	1,279	1,210	1,85	1,927	1,414	1,363
0,40	1,548	1,279	1,210	1,90	1,949	1,414	1,378
0,45	1,549	1,279	1,211	1,95	1,970	1,415	1,392
0,50	1,549	1,280	1,210	2,00	1,985	1,415	1,403
0,55	1,550	1,281	1,210	2,05	1,983	1,415	1,401
0,60	1,552	1,282	1,211	2,10	1,982	1,415	1,401
0,65	1,554	1,284	1,210	2,15	1,981	1,415	1,400
0,70	1,557	1,286	1,211	2,20	1,981	1,415	1,400
0,75	1,561	1,290	1,210	2,25	1,980	1,415	1,399
0,80	1,567	1,294	1,211	2,30	1,979	1,415	1,399
0,85	1,573	1,300	1,210	2,35	1,979	1,415	1,399
0,90	1,582	1,307	1,210	2,40	1,979	1,416	1,398
0,95	1,591	1,315	1,210	2,45	1,979	1,416	1,398
1,00	1,603	1,324	1,211	2,50	1,978	1,416	1,397
1,05	1,616	1,335	1,210	2,55	1,978	1,416	1,397
1,10	1,630	1,346	1,211	2,60	1,978	1,416	1,397
1,15	1,645	1,359	1,210	2,65	1,978	1,416	1,397
1,20	1,662	1,371	1,212	2,70	1,978	1,416	1,397
1,25	1,679	1,381	1,216	2,75	1,978	1,416	1,397
1,30	1,698	1,389	1,222	2,80	1,978	1,416	1,397
1,35	1,717	1,395	1,231	2,85	1,978	1,416	1,397
1,40	1,737	1,399	1,242	2,90	1,978	1,416	1,397
1,45	1,757	1,403	1,252	2,95	1,978	1,416	1,397
				3,00	1,978	1,416	1,397

Table A.1: table from Battjes & Groenendijk [2000] for $H_{2\%}$ and $H_{1/3}$

A2 Wave spectra

Ocean waves can be described by a wave spectrum. The aim of describing waves with a wave spectrum is not to describe one observation of the sea surface in detail. In a wave spectrum the sea surface is described as a stochastic process, which means that all possible observations that could have been made are characterised.

The surface elevation in a time record, η(t), with a duration D is a very chaotic process which can exactly be reproduced as the sum of a large number of harmonic wave components (a Fourier series):

$$\eta(t) = \sum_{i=1}^{N} a_i \cos(2\pi f_i t + \alpha_i)$$

Each wave component has it's own amplitude (a), phase difference (α) and frequency (f). The next step in order to create a wave spectrum is to make an amplitude spectrum. To do this for each frequency interval (Δf=1/D) the corresponding amplitude is plotted. In another observation other values of the corresponding amplitudes will be found, but by repeating the experiment many times (M) and take the average over all experiments the average amplitude spectrum can be found. From this the amplitude density ($\bar{a}_i / \Delta f$) can be calculated for each frequency.

A more meaningful way to describe the waves would be to calculate the variance density ($\frac{1}{2}\overline{a_i^2} / \Delta f$) of each frequency step, because of two reasons:

- the variance is a more relevant statistical quantity than the amplitude;
- the variance is proportional to the wave energy.

By letting the frequency interval approach to zero (Δf → 0) a continuous distribution of the variance density can be made. The variance density spectrum can now be described as:

$$E(f) = \lim_{\Delta f \to 0} \frac{1}{\Delta f_i} E\left\{ \frac{1}{2} \underline{a}_i^2 \right\}$$

By multiplying the variance density spectrum with ρg the energy density spectrum is obtained.

A lot of research has been done to the shape of the wave spectrum. Observations by PIERSON AND MOSKOWITZ [1964] in an assumed fully sea state in deep water resulted in a f^{-5} –shape for higher frequencies. The Pierson-Moskowitz spectrum is given by the following equation:

$$E_{PM}(f) = \alpha_{PM} \cdot g^2 \cdot (2\pi)^{-4} \cdot f^{-5} \cdot \exp\left\{-\frac{5}{4}\left(\frac{f}{f_{PM}}\right)^{-4}\right\}$$

The shape of the wave spectrum depends on the overall appearance of the waves. The narrower the spectrum is, the more regular the waves are. The narrowest spectrum describes a wave record of a harmonic wave. This spectrum is a delta function (spike) at one frequency. The wider the spectrum gets, the more chaotic the wave record is.

Because fully developed sea states do not often occur in reality and observations have shown that in fetch-limited conditions the spectra show a sharper and higher peak than in fully developed conditions. Because of this scientists of JONSWAP (Joint North Sea Wave Project) chose to use the shape of the Pierson-Moskowitz spectrum and enhance its peak with a peak enhancement function. This resulted in:

$$E_{JONSWAP}(f) = \alpha_{PM} \cdot g^2 \cdot (2\pi)^{-4} \cdot f^{-5} \cdot \exp\left\{-\frac{5}{4}\left(\frac{f}{f_{PM}}\right)^{-4}\right\} \cdot \gamma^{\exp\left[-\frac{1}{2}\left(\frac{f/f_{peak}-1}{\sigma}\right)^2\right]}$$

For example in Figure A.2 the Pierson-Moskowitz–spectrum, PM-spectrum, is plotted together with the JONSWAP-spectrum with equal wave conditions.
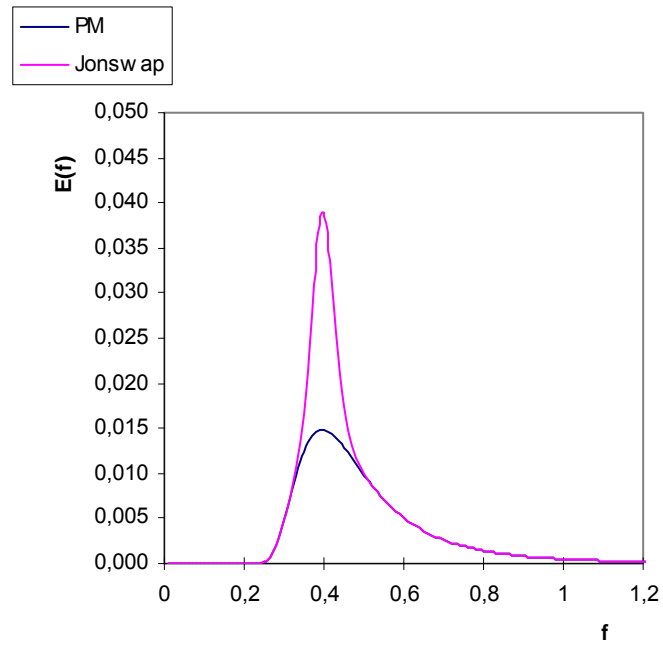
Figure A.2: PM- spectrum and JONSWAP-spectrum

A3   Ratio peak period to spectral period

In INFRAM I489 [2001] the ratio peak period to spectral period has been calculated for various tests. Also for a number of tests from DELFT HYDRAULICS, M1983 PART I [1988] this ratio was investigated. In this paper different definitions for the peak period and the spectral period are given:

T_p The frequency at which the energy in the energy density spectrum is at it's maximum. The peak period is the inverse of the peak frequency ($T_p = 1/f_p$). A disadvantage is that this value depends on the 'smoothness' of the spectrum.

$T_{p;a}$ The peak period using a cut off frequency for the higher frequencies.

$T_{p;b}$ The peak period from the part of the spectrum for which the energy is more than 40% of the maximum value. This value gives a more fixed value than the T_p as described before. This value was calculated over the whole frequency range.

$T_{p;d}$ The peak period from the part of the spectrum for which the energy is more than 80% of the maximum value. This value was calculated over the whole frequency range.

$T_{m-1,0}$ The spectral period $T_{m-1,0} = m_{-1}/m_0$, in which m_{-1} and m_0 are respectively the first negative and the zero-th order moment of the spectrum calculated over the whole frequency range.

$T_{m-1,0;a}$ The spectral period $T_{m-1,0} = m_{-1}/m_0$, in which m_{-1} and m_0 are respectively the first negative and the zero-th order moment of the spectrum using a cut-off frequency for the lower frequencies.

To make this clear in Figure A.3 an example of a spectrum is given. In this figure the cut off frequency is shown and also the meaning of the 40%- and 80% energy value used in T_{pb} and T_{pd} is shown.
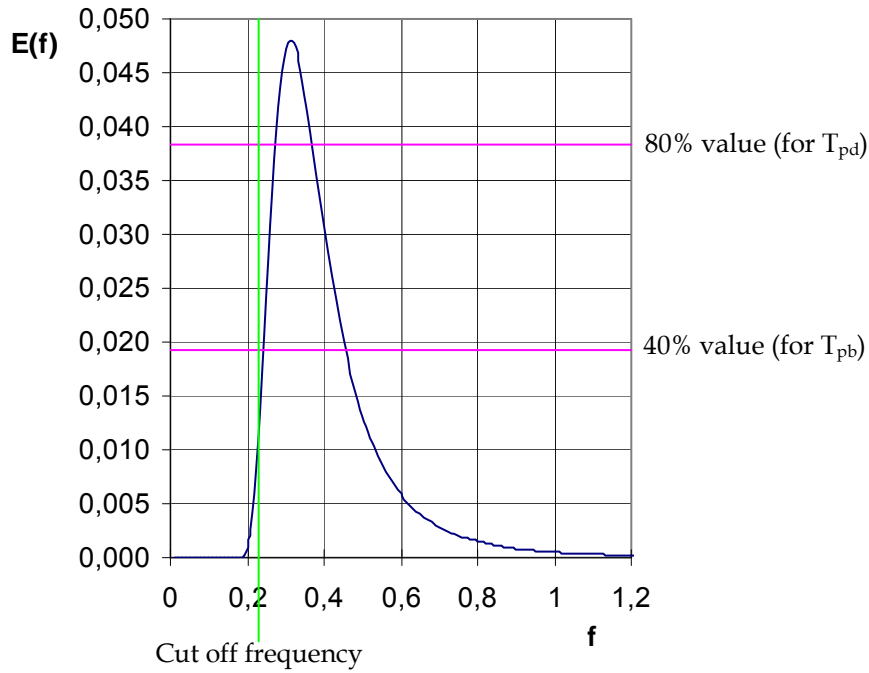
Figure A.3: Wave spectrum with cut-of frequency and 40%- and 80% energy value

In INFRAM I489 [2001] the analysed spectra are digitalised. From these digitalised spectra the peak period, T_p, and the spectral period, $T_{m-1,0}$, are obtained. The results of this are given in Table A.2.

For test 25 the spectral period, $T_{m-1,0}$, has been recalculated in this M.Sc. Thesis. The spectral period, $T_{m-1,0}$ can be calculated using the following expression:

$$T_{m-1,0} = \frac{m_{-1}}{m_0} = \frac{\int_0^\infty f^{-1}E(f)df}{\int_0^\infty f^0 E(f)df} = \frac{\int_0^\infty f^{-1}E(f)df}{\int_0^\infty E(f)df}$$

In order to calculate the spectral period the wave spectrum from test 25 first has to be digitalised. This has been done with a step size of 0,02. After this the surface of each step has been calculated where after the spectral moments, m_{-1} and m_0, can be calculated by calculating the surface under the spectral curve. For test 25 this resulted in a calculated spectral moment, $T_{m-1,0}$, of:

$$T_{m-1,0} = \frac{0,4210}{0,1683} = 2,502s$$

and: $T_{m-1,0;a} = \frac{0,4047}{0,1669} = 2,425s$

These calculated values are very close to the values calculated in INFRAM I489 [2001], where $T_{m-1,0}$ = 2,491s and $T_{m-1,0;a}$ = 2,413s. The small differences can be explained because of the better accuracy in the calculations of INFRAM I489 [2001].

Data from DELFT HYDRAULICS, M1983 PART I [1988]				Calculated with a digitalised spectrum						
testnr.	T_p [s]	H_s [m])	*Spectrum*	*Cut off freq. [Hz]*	T_p [s]	$T_{m-1,0}$ [s]	$T_{m-1,0a}$ [s]	T_{pb} [s]	$T_p/T_{m-1,0}$ [-]	$T_{pb}/T_{m-1,0a}$ [-]
26	3,17	0,117	I	0,2	3,092	3,079	2,887	3,093	1,00	1,07
60	2,17	0,116	I	0,2	1,999	2,153	2,032	2,110	0,93	1,04
21	2,53	0,118	I	0,2	2,664	2,559	2,384	2,471	1,04	1,04
24	2,53	0,109	I	0,2	2,679	2,52	2,372	2,440	1,06	1,03
22	2,56	0,100	I	0,2	2,697	2,561	2,422	2,518	1,05	1,04
23	2,53	0,086	I	0,2	2,687	2,497	2,393	2,503	1,08	1,05
25	2,53	0,071	I	0,2	2,625	2,491	2,413	2,492	1,05	1,03
186	3,23	0,097	II	0,2	3,200	3,244	3,171	3,187	0,99	1,01
161	2,24	0,111	II	0,2	2,220	2,511	2,271	2,244	0,88	0,99
164	1,79	0,119	II	0,2	1,788	1,953	1,819	1,801	0,92	0,99
195	1,40	0,124	II	0,2	1,384	1,462	1,462	1,399	0,95	0,96
175	4,25	0,106	III	0,05	4,354	3,854	3,788	4,076	1,13	1,08
182	3,17	0,112	III	0,05	3,032	2,813	2,813	2,884	1,08	1,03
171	2,67	0,122	III	0,05	2,715	2,357	2,316	2,513	1,15	1,09
188	1,83	0,125	III	0,05	1,701	1,672	1,672	1,768	1,02	1,06

Table A.2: Ratios $T_p / T_{m-1,0}$ for tests from DELFT HYDRAULICS, M1983 PART I [1988]

From this table the average $T_p/T_{m-1,0}$ ratios can be calculated for the different spectral shapes. This is done in Table A.3 where also the standard deviations are given. In this table also the

ratio $T_{pb}/T_{m-1,0a}$ was calculated which shows a smaller standard deviation than the ratio $T_p/T_{m-1,0}$, and thus forms a better fixed value.

	$T_{pb}/T_{m-1,0a}$	Standard Deviation	$T_p/T_{m-1,0}$	Standard Deviation
Spectrum I	1,042	0,013	1,031	0,047
Spectrum II	0,985	0,018	0,933	0,038
Spectrum III	1,061	0,023	1,094	0,052

Table A.3: Average ratios peak period / spectral period and standard deviations

According to INFRAM I489 [2001] the ratios $T_p/T_{m-1,0}$ of the tests from DELFT HYDRAULICS, M1983 PART I [1988] are smaller than the average value from the other tests. The report recommends a fixed ratio $T_p/T_{m-1,0}$ of 1,1. In earlier research it was found that for JONSWAP-spectra this ratio would be 1,11 and for a wider PM-spectrum the ratio would increase to 1,17. For the tests from DELFT HYDRAULICS, M1983 PART I [1988] the report recommends a fixed value of 1,04, instead of 1,1. This difference can be explained when a close look is given to the spectra used in DELFT HYDRAULICS, M1983 PART I [1988]. Therefore in Appendix B the spectra from DELFT HYDRAULICS, M1983 PART I [1988] have been plotted with a real PM-spectrum on the background in red. In Appendix B it can be seen that the spectra from the tests with PM-spectra are significantly narrower on the right tail than the original PM-spectra. This can explain why the peak period, T_p, and the spectral period, $T_{m-1,0}$, converge.

A4   The T-Test

To check whether the means of two datasets, or parts of datasets are statistically different from each other the T-test can be used. The T-test is especially appropriate for posttest analysis of two different groups of randomized experiments. This makes the T-test very applicable on the subject of this M.Sc. Thesis.
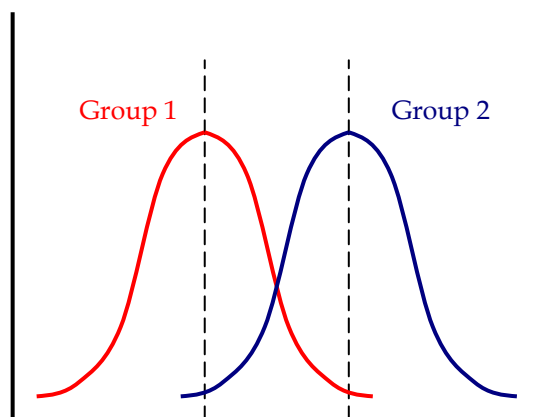
Figure A.4: Idealized distributions for treated and comparison group posttest values

In Figure A.4 the distributions for the group 1 (red) and group 2 (blue) groups in a study are shown. It must be mentioned that the figure shows an idealized distribution, because the actual distribution would usually be a histogram. In Figure A.4 it can be seen where the control and treatment group means are located. The T-test can address whether the means are statistically different or not.

In Figure A.5 examples are given of samples with the same mean, but different variations. In this figure cases with medium, high and low variability are shown. Two groups are most statistically different in the bottom or low-variability case, because there is relatively little overlap between the two bell-shaped curves. In the high variability case, the group difference least, because the two bell-shaped distributions overlap very much.
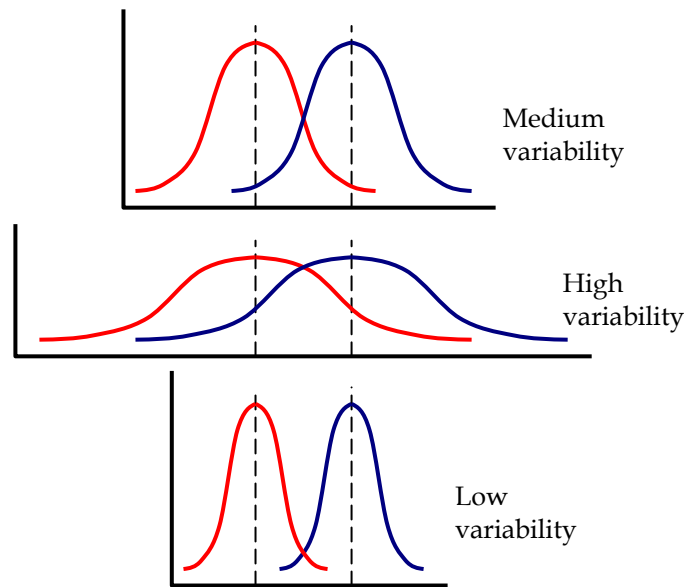
Figure A.5: Three scenarios for differences between means

From this it can be concluded that differences between scores for two groups can be judged by analysing the difference between their means relative to the spread or variability of their scores.

The T-test to determine whether two groups, X and Y, are statistically different is shown below. At first the value of t_{obs} has to be calculated.

$$t_{obs} = \frac{difference\ between\ group\ means}{variability\ of\ groups} = \frac{\bar{X} - \bar{Y}}{\sqrt{\dfrac{s_X^2}{n_X} + \dfrac{s_Y^2}{n_Y}}}$$

Where:

$\bar{X}$	=	group mean of group X (x_1, x_2, ……..x_n)
$\bar{Y}$	=	group mean of group Y (y_1, y_2, ……..y_n)
s_X, s_Y	=	standard deviation of group X or group Y
n_X, n_Y	=	number of tests of group X or group Y

A positive value of t_{obs} indicates that the mean of group X is larger than the mean of group Y and a negative value of t_{obs} indicates that the mean of group X is lower than the mean of group Y. Once the value of t_{obs} is determined the risk level (or alpha level) has to be set. In

most social research, the "rule of thumb" is to set the alpha level at 0.05. This means that five times out of a hundred a statistically significant difference exists between the means even if there was none.

After this the degrees of freedom (dof) for the test need to be determined. In the T-test, the degrees of freedom is the sum of the experiments in both groups minus 2. Given the alpha level, the dof, and the t_{obs}-value, the t-value has to be looked up in a standard table of significance to determine whether the t-value is large enough to be significant. If it is it can be concluded that the two groups are statistically different.

APPENDIX B   SPECTRA VAN DER MEER [1988]

Tests with PM-spectra:

Tests with narrow spectra:

Test 195

Test 164

Test 161

Test 186
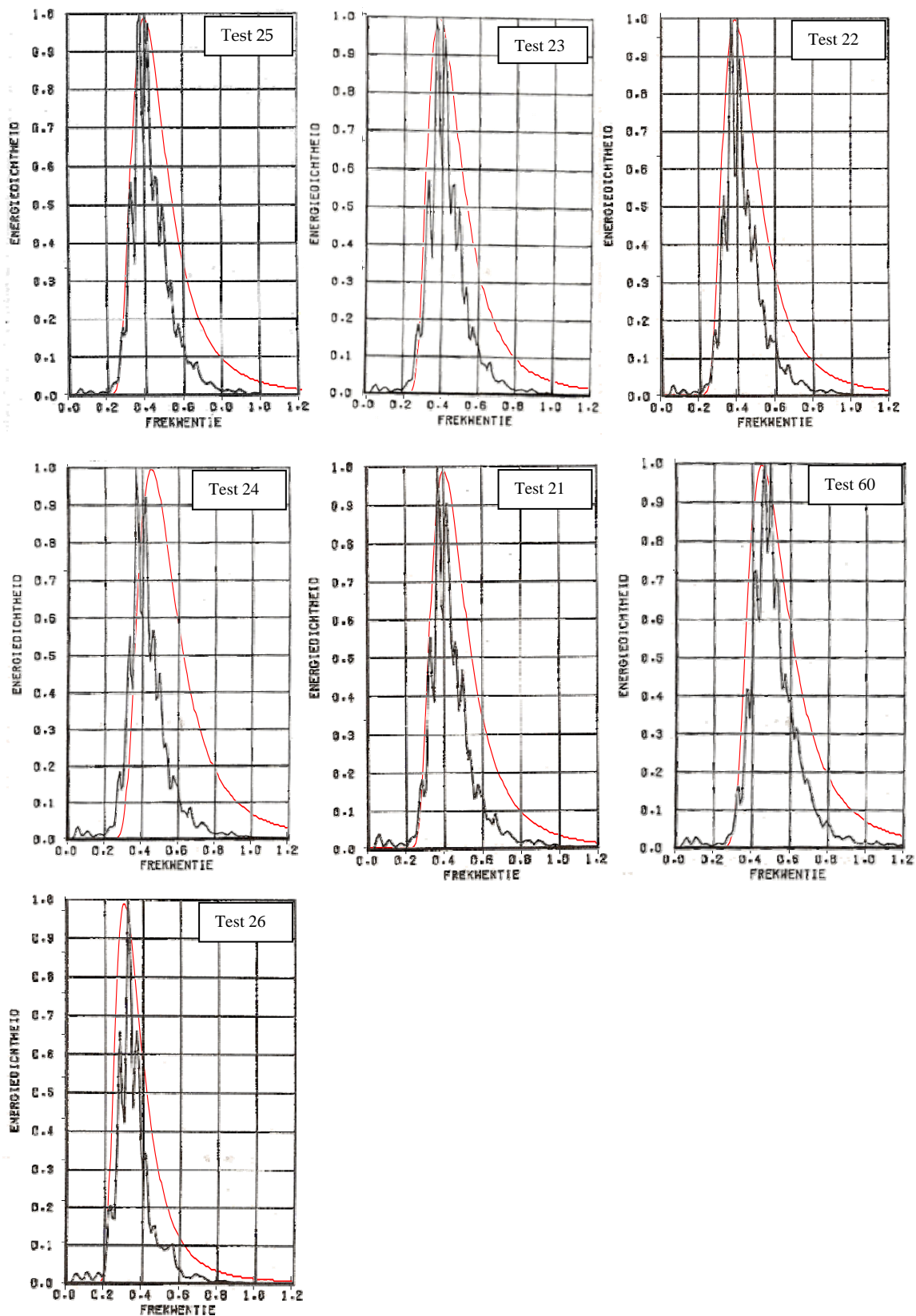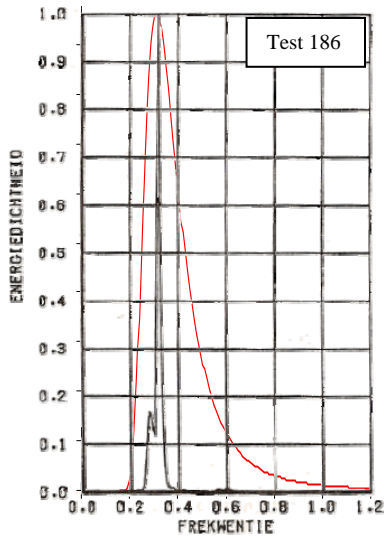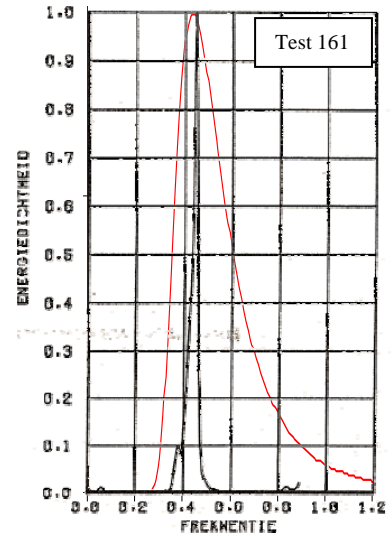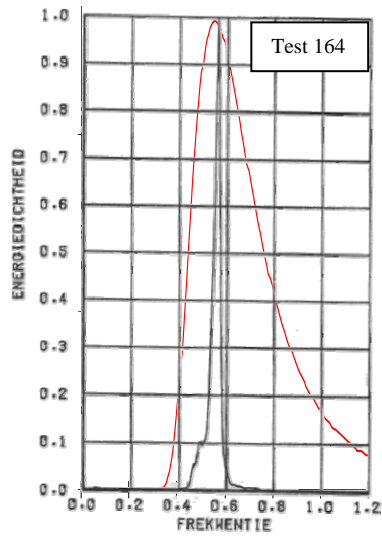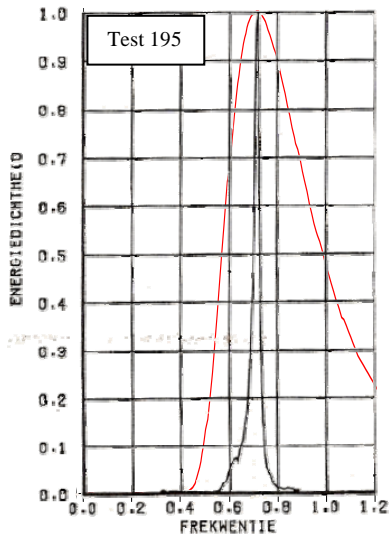
Tests with wide spectra:
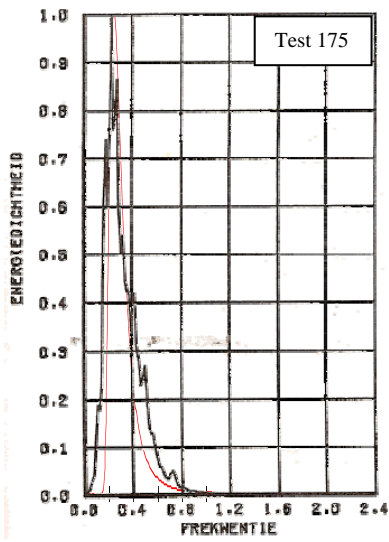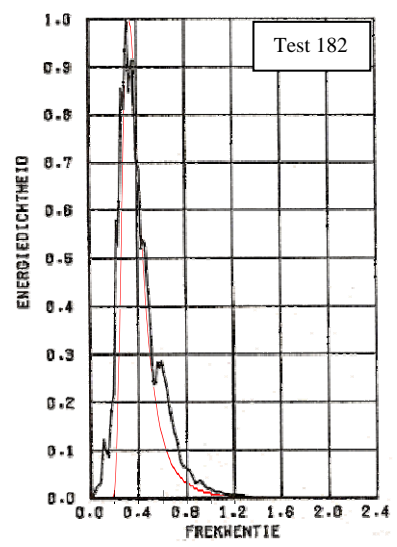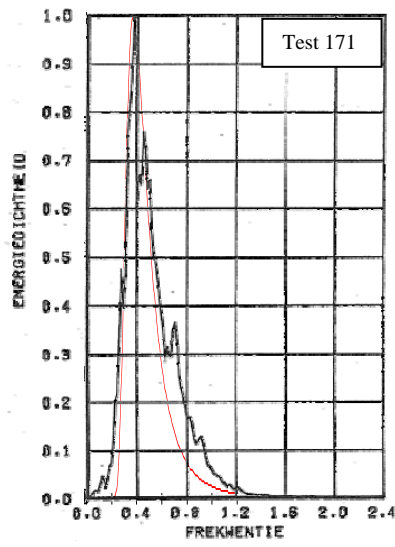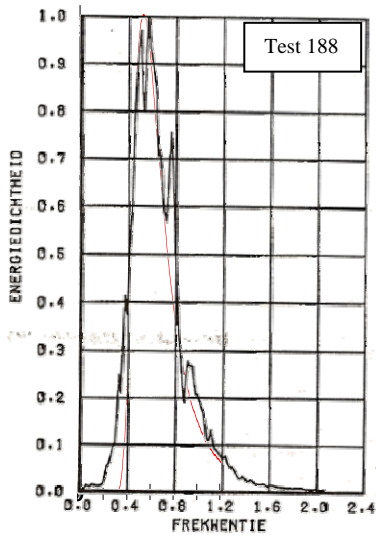
APPENDIX C   STONES VAN DER MEER [1988]
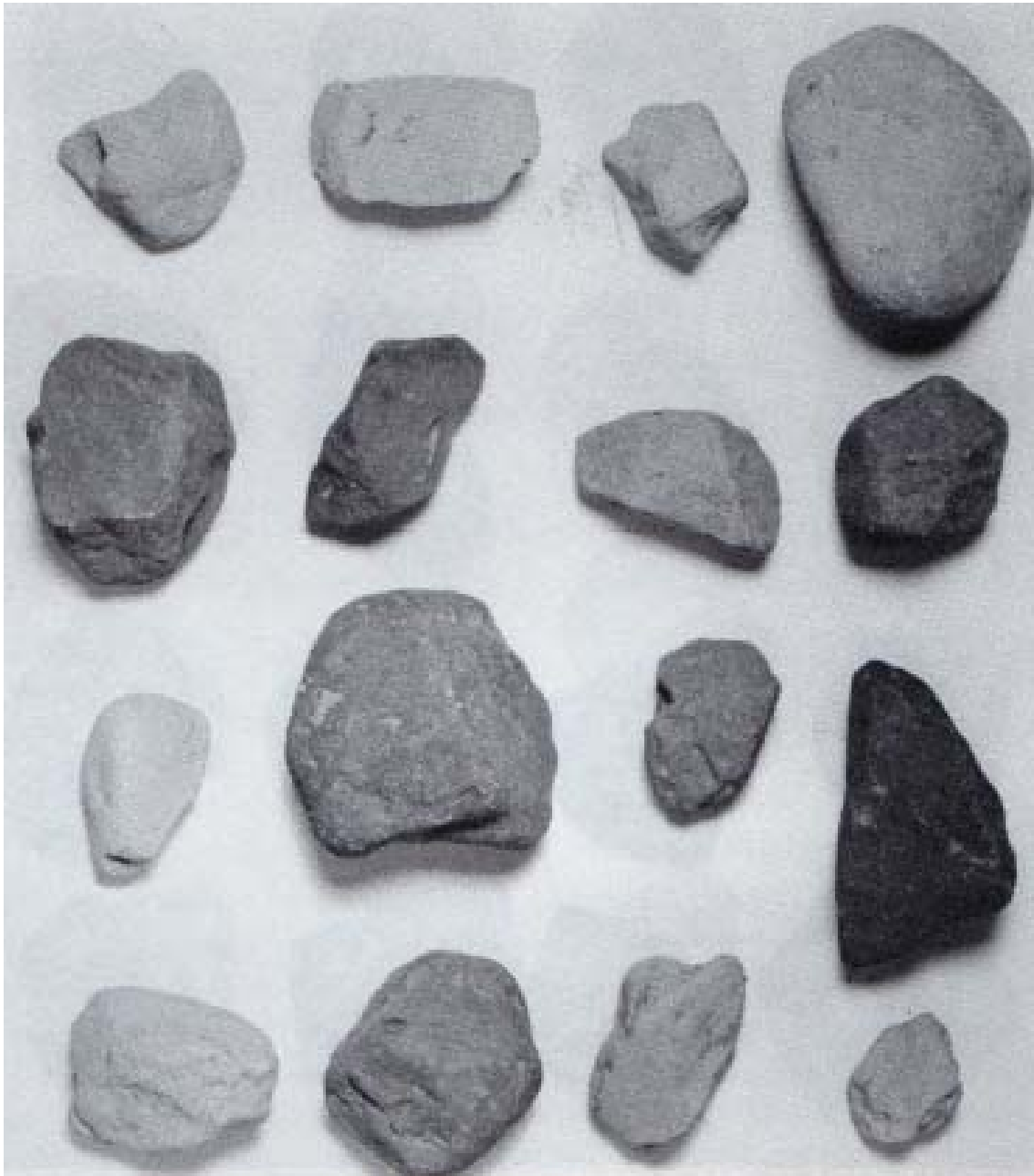
Riprap after 134 tests, 2x painted
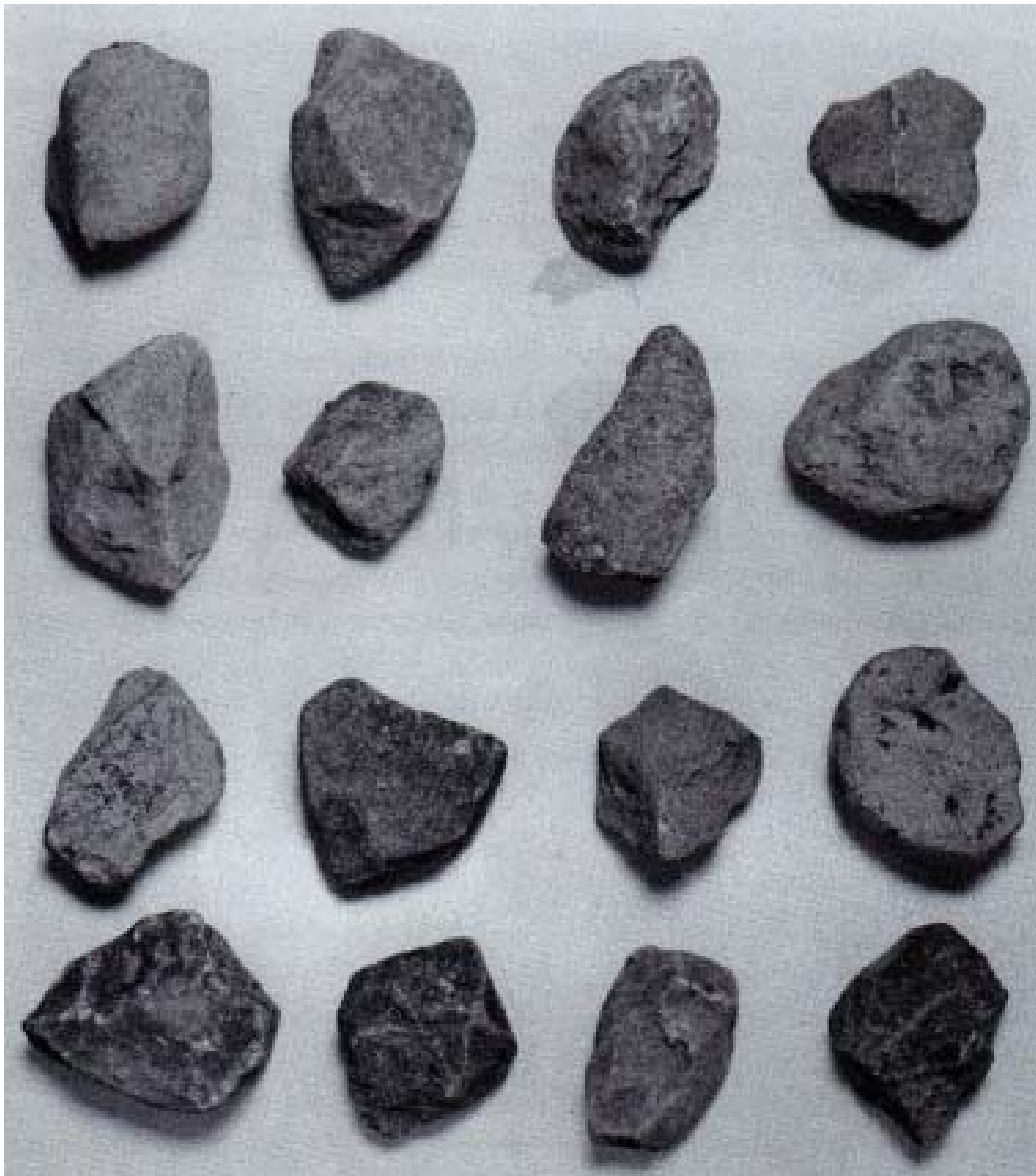
Uniform stone after 106 tests, 1x painted
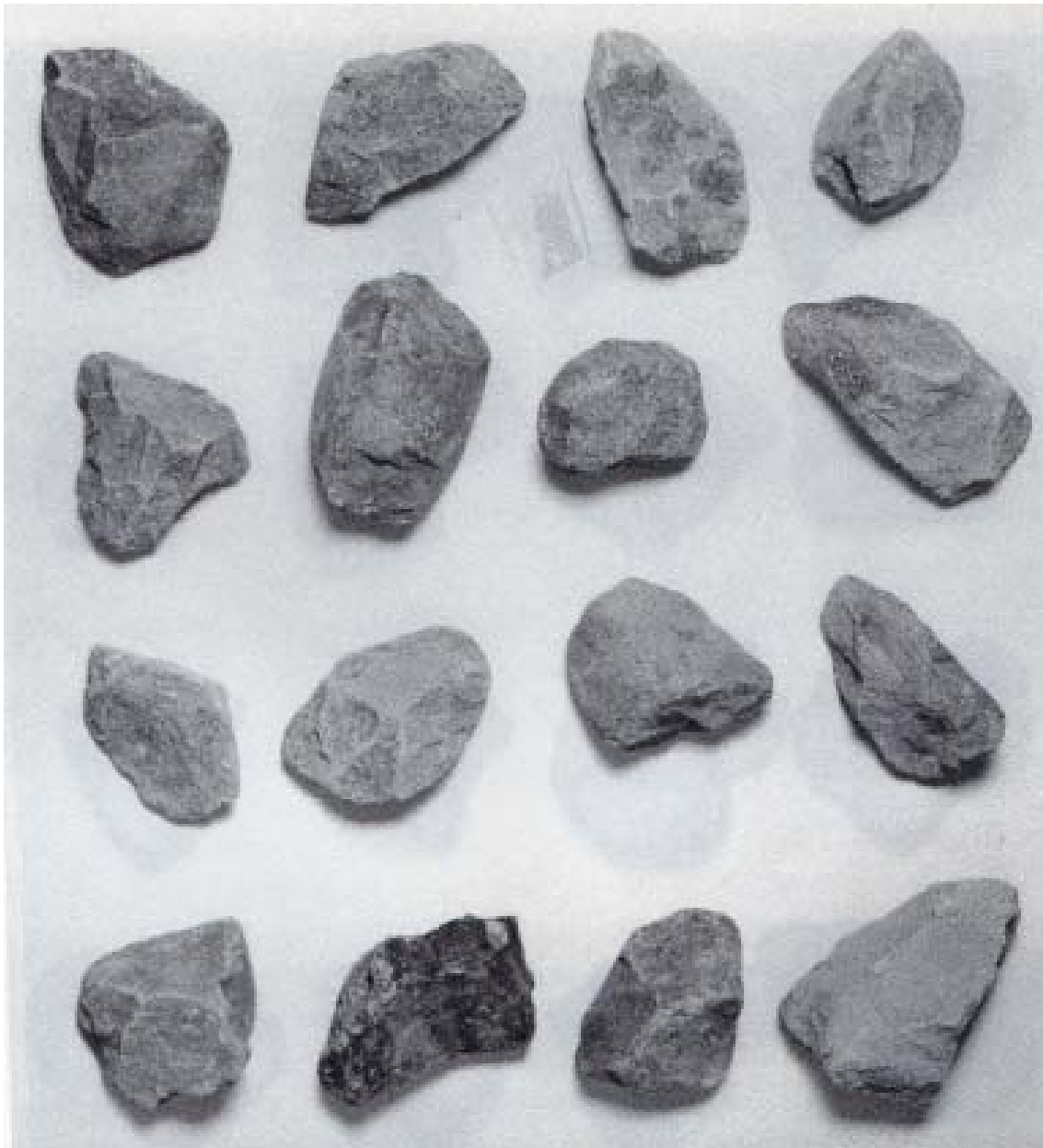
Uniform stone after 41 tests, not painted
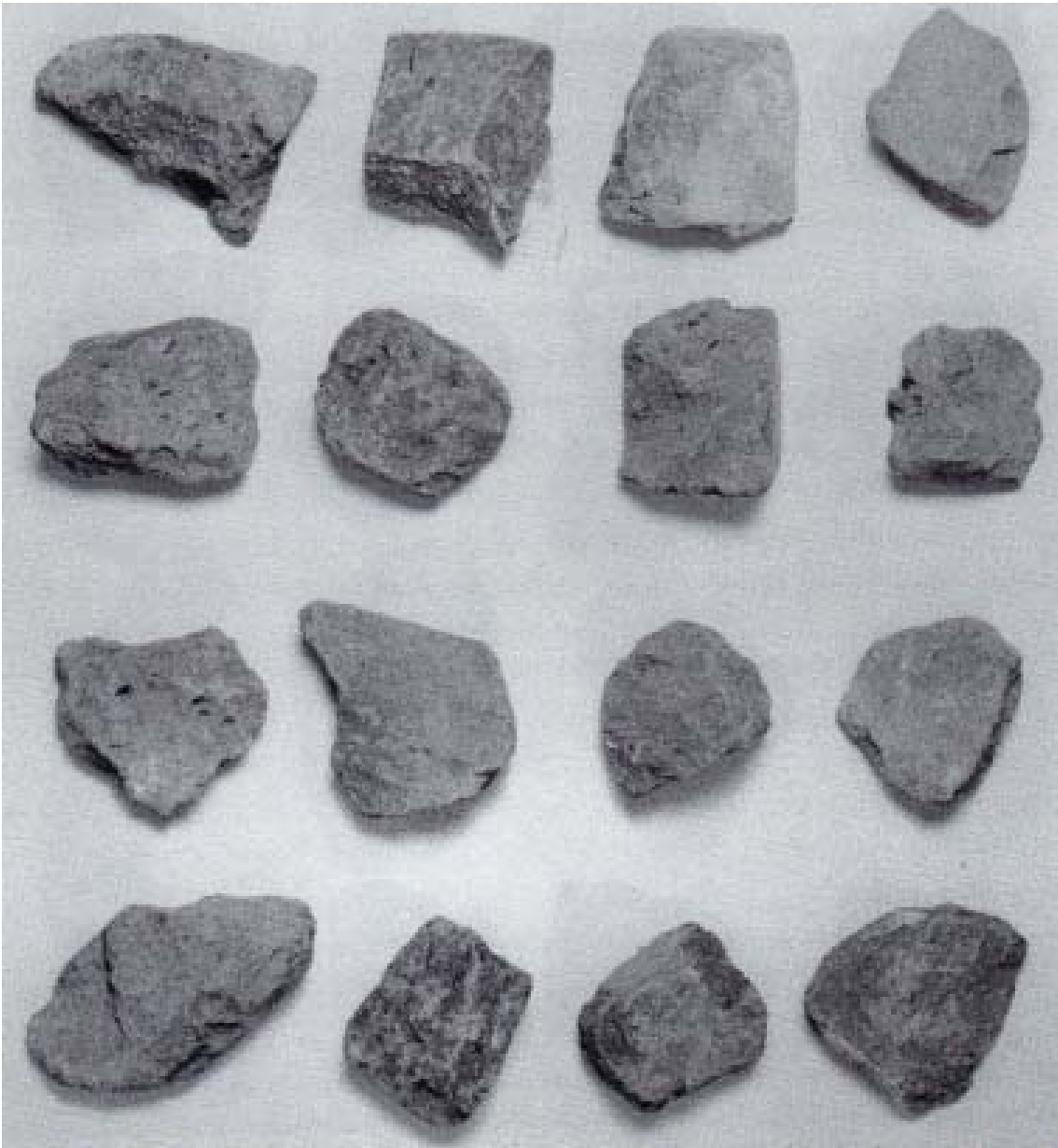
Quarry run after 10 tests, not painted
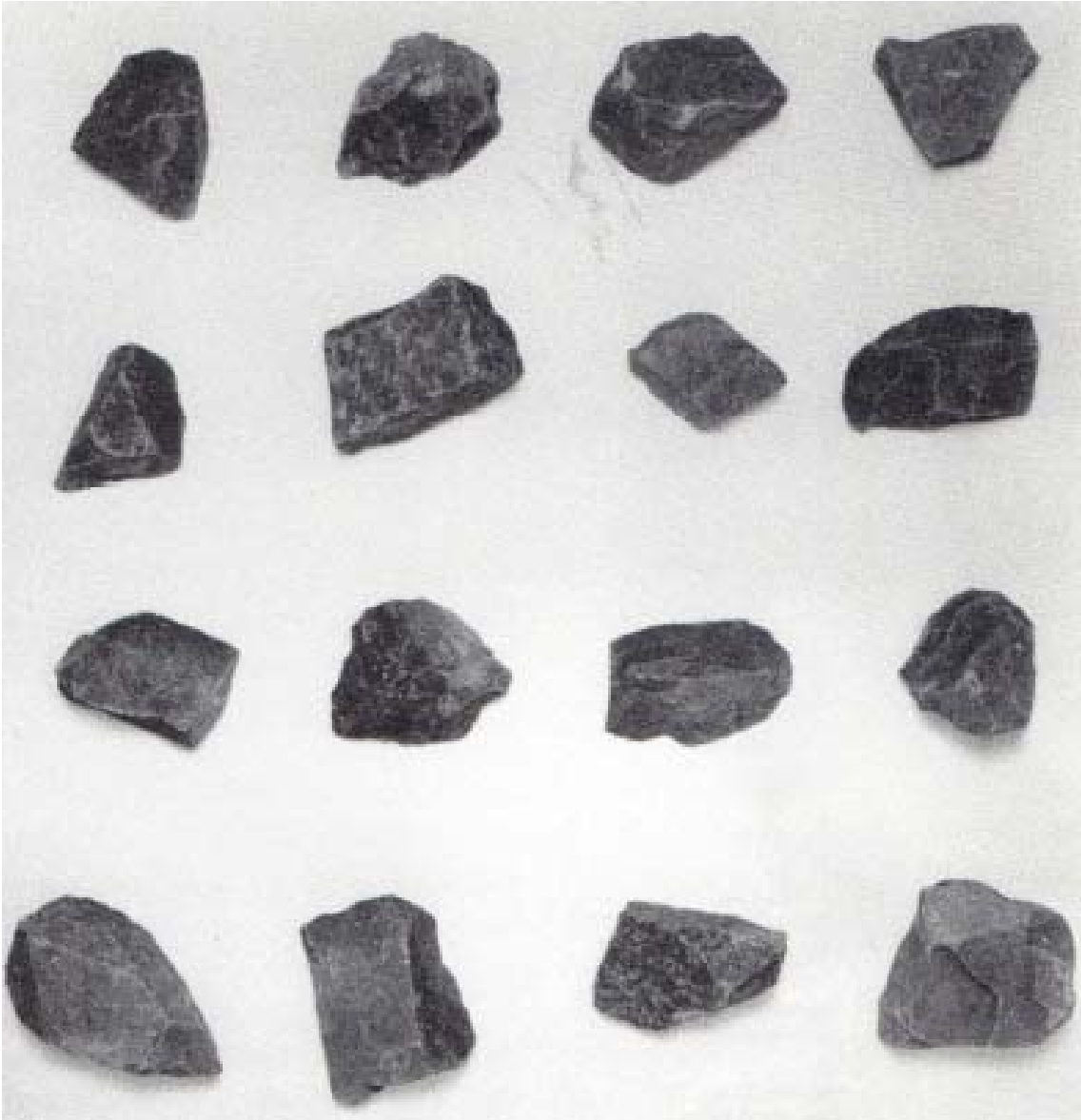
Basalt after 10 tests, not painted

APPENDIX D   LEGEND GRAPHS VAN DER MEER

- Impermeable cota=3 ; N=3000

- Impermeable cota=4 ; N=3000

- Impermeable cota=6 ; N=3000

- Spectrum Narrow ; N=3000

- Spectrum Wide ; N=3000

- Permeable cota=3 ; N=3000

- Permeable cota=2 ; N=3000

- Permeable cota=1,5 ; N=3000

- Homogenous ; N=3000

- Depth 0,4m ; N=3000

- Depth 0,2m ; N=3000

- Delta 0,92 ; N=3000

- Delta 2,05 ; N=3000

- Large scale ; N=3000

- Impermeable cota=3 ; N=1000

- Impermeable cota=4 ; N=1000

- Impermeable cota=6 ; N=1000

- Spectrum Narrow ; N=1000

- Spectrum Wide ; N=1000

- Permeable cota=3 ; N=1000

- Permeable cota=2 ; N=1000

- Permeable cota=1,5 ; N=1000

- Homogenous N=1000

- Depth 0,4m ; N=1000

- Depth 0,2m ; N=1000

- Delta 0,92 ; N=1000

- Delta 2,05 ; N=1000

- Large scale ; N=1000

APPENDIX E   DETAILED GRAPHS
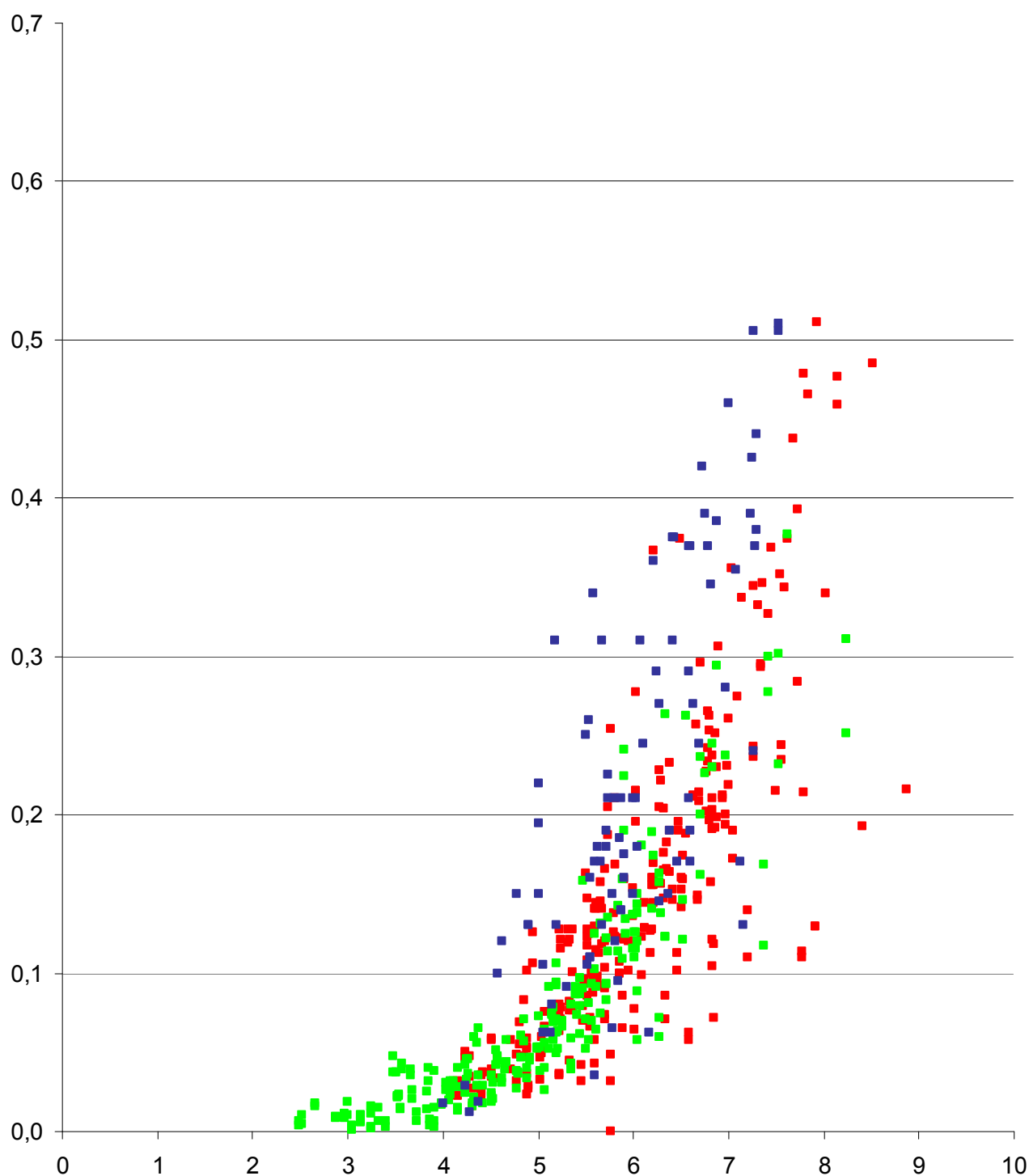
FigureA.6: Plunging waves with maximum accepted damage levels: THOMPSON & SHUTTLER [1975] (green), VAN DER MEER [1988] (red), VAN GENT ET AL. [2003] (blue)
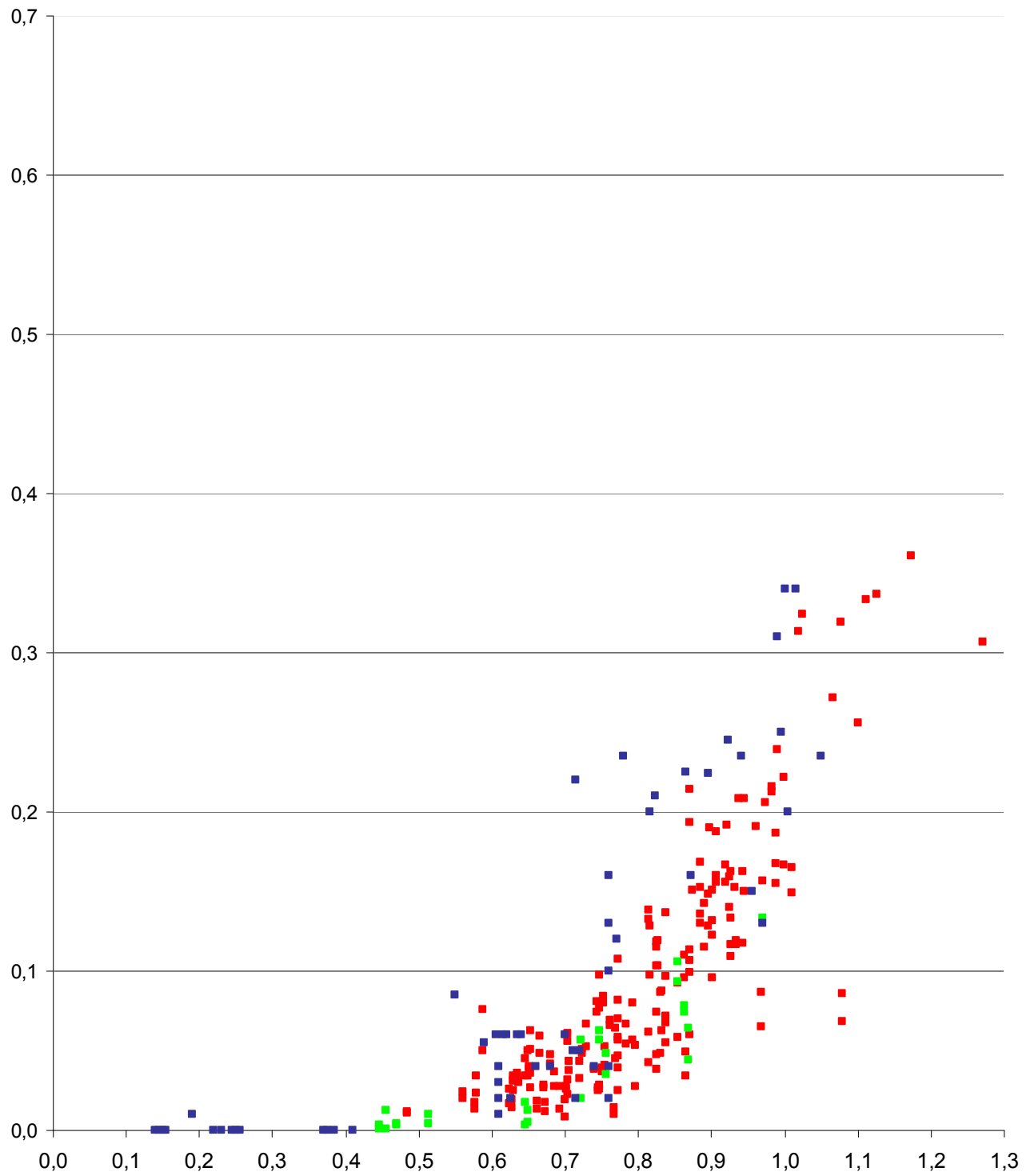
FigureA.7: Surging waves with maximum accepted damage levels: Thompson & Shuttler [1975] (green), Van der Meer [1988] (red), Van Gent Et Al. [2003] (blue)